Carbonate mounds of Morocco

An IGCP Project 380 Field Workshop

Leaders

Pierre-André Bourque
Driss Mounji
Fritz Neuweiler
Joachim Reitner
Otto Heinrich Walliser

October 1999

Carbonate Mounds of Morocco

IGCP 380 Field Workshop

October 24 - November 1, 1999

Leaders : **Pierre-André Bourque**
Géologie et Génie géologique
Université Laval,
Québec, Canada G1K 7P4
bourque@ggl.ulaval.ca

Driss Mounji
SMI – Foyer des Cadres
Cité minière Taouazaakt
Tinerhir 47800, Maroc

Fritz Neuweiler
Joachim Reitner
Otto Walliser
IMGP, Univ. Goettingen
Goldschmidtstrasse 3
D-37077 Goettingen
Germany
fneuwei@gwdg.de
jreitne@gwdg.de

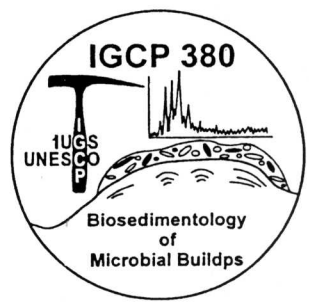

Cover photo : steep flanked kess-kess mud mound at Hamar Laghdad, Tafilalt, Morocco. Photo by P.-A. Bourque, 1996

Foreword

This field workshop is concerned with mound-shaped rock bodies composed mainly of finely crystalline carbonates. These bodies were primarily carbonate mounds defined as structures whose accretion was controlled by small, commonly delicate and/or solitary elements (biogenic mounds) or by inorganic accumulation of mud with variable amount of fossils (mud mounds, *sensu strictu*), in contrast with reefs that are structures constructed by large, usually clonal elements, and capable of thriving in energetic environments (James and Bourque, 1992). Because a large part of their volume is made up of finely crystalline material, they are often collectively called mudmounds (or mud-mounds, or mud mounds), despite many of them are not mud mounds (*sensu strictu*) since their accretion was not controlled by accumulation of loose lime mud alone, but controlled by organisms trapping and/or binding lime mud, or mediating finely crystalline carbonate precipitation. However, since it came into current use to designate all mud-rich mounds as mudmounds, we unfortunately have to live with this terminological ambiguity!

Despite they have been the subject of numerous studies, the « mudmounds » remain enigmatic on several aspects. For those workers concerned with the understanding of life evolution and biological community structure in the past, their study is as much rewarding as is the study of reefs. Prior to any attempt to propose community evolution or ecological zonation in carbonate mounds, one of the challenges is to recognize the primary biological communities responsible for mound accretion, communities which are often cryptic and even destroyed by early diagenesis.

During the last decades, many studies have insisted on and demonstrated the role of microbial communities in several mound accretion. It was also demonstrated, in other mounds, the preponderant role (with or without microbes) of skeletal organisms such as sponges, delicate corals, bryozoans, etc. Today, the multi-spectrum origin of carbonate mounds is well recognized, hence the three pole mound classification of James and Bourque, 1992 : microbial mounds, skeletal mounds, and mud mounds *sensu strictu*.

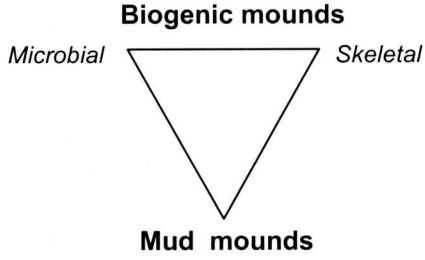

There is therefore a natural and strong link between the theme of IGCP Project 380, Biosedimentology of microbial buildups, and the « mudmound » question. This is why IGCP Project 380 is holding this Morocco 1999 field workshop.

This field workshop is divided into two parts : a six day field trip where superbly exposed outstanding examples of carbonate mounds will be examined, and a one day oral

session presenting the last research results of the participants on modern and ancient carbonate mounds.

Morocco offers first hand examples of the carbonate mound spectrum, among which the ones we will visit during this field workshop :

- the Liassic sponge mounds of the central High-Atlas;
- the famous Devonian kess-kess mud mounds (*sensu strictu*) of the Tafilalt province, interpreted as hydrothermal in origin;
- the puzzling Devonian skeletal mounds of the Maïder province.

IGCP is a UNESCO program, and it is perfectly normal that a project activity like this field workshop involves a part devoted to the knowledge of local cultures. For instance, our stay and travel in the High-Atlas and the Anti-Atlas will give us the opportunity to get in contact with the Berber culture, in particular with the people and villages of remote areas while we will travel to Aferdou el Mrakib mound, and with the splendid *kasbas* of the Berber villages (*ksour*) all along the route between Erfoud and Ouarzazate. In Ouarzazate, if time permits, we may visit the beautiful Taourirt Kasba and the surrounding old village. One of your leaders is a proud native Berber and will be a first hand (inexhaustible) source of information on his cultural heritage. The royal dynastie of the Alaouites that governs Morocco today, originates from the Tafilalt. The Arabian Alaouites *chorfa* (sage person), descendants of the Prophet Mahomet, came into the area in the 13th century. It is in the middle of the 17th Century that the Arabian culture spread through the entire country. The colourful and animated Marrakech whose the Berber origin goes back to the 11th Century and that we will visit on the last day, is a UNESCO World Heritage city.

Pierre-André Bourque
October 1999

Acknowledgements

Financial support from the IUGS through the IGCP secretariat in Paris, and permission to use the Département de géologie et de génie géologique de l'Université Laval, Québec, computer facilities to produce this guidebook are warmly acknowledged.

Table of content

Field Trip

Overview of Moroccan Geology
and
Itinerary

Morocco is comprised of three structural domains : the Rif, Atlas and Anti-Atlas domains (Fig. 1). The Phanerozoic cover above the Precambrian shield has been deformed by two major orogenies, the Hercynian and the Alpine orogenies.

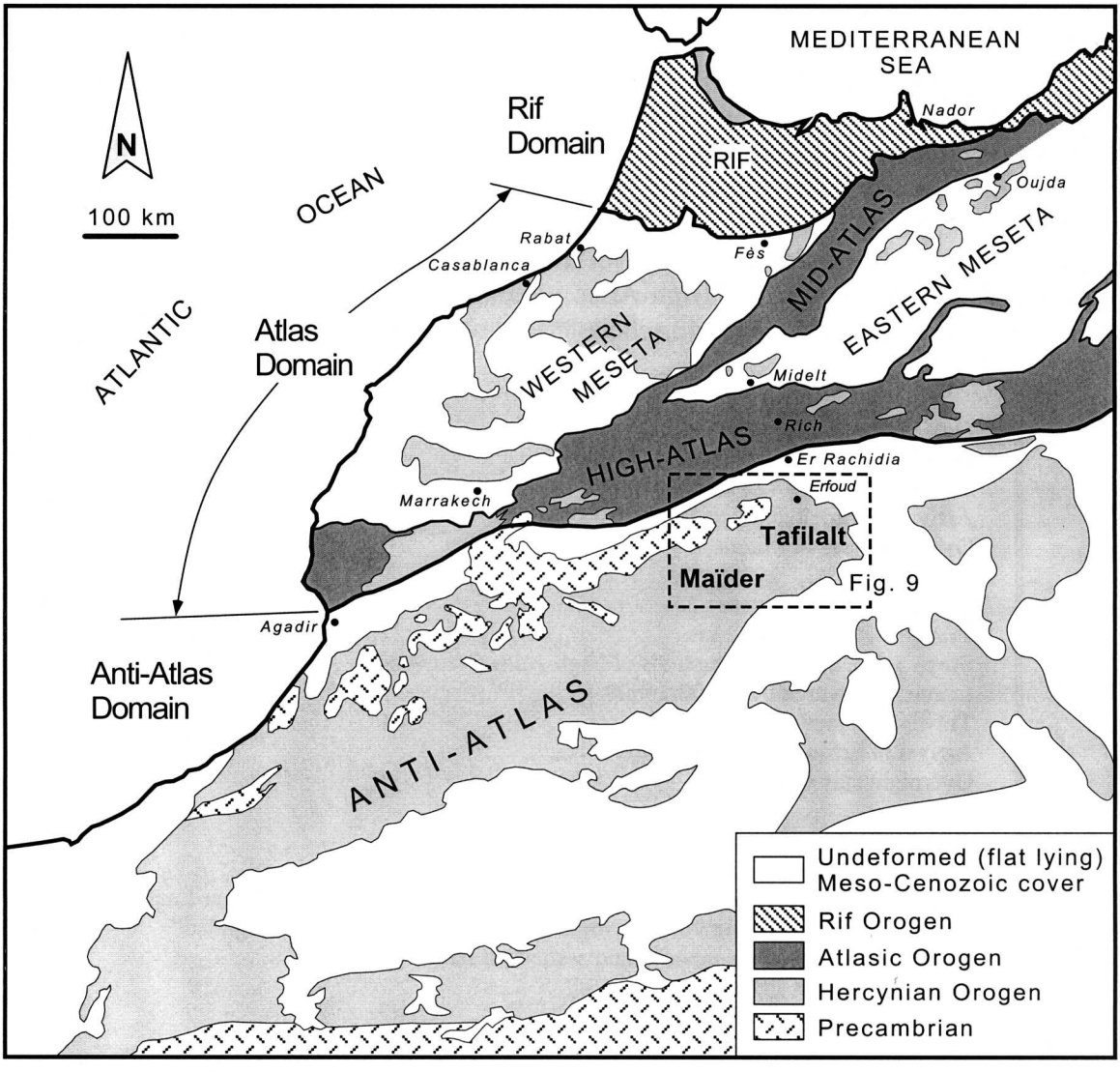

Figure 1 – Structural domains of Morocco. *From Piqué and Michard (1989).*

In the **Anti-Atlas domain**, the Hercynian orogeny has only slightly deformed the Paleozoic rocks that unconformably overlie the Precambrian basement, so that, at the outcrop level, the beds are essentially flat-lying. The Alpine orogeny had no effect in this

domain. The Atlas and Anti-Atlas domains are separated by a major fault corridor, the « accident sud-atlasique », thought to have played as a strike-slip fault at least during the Hercynian orogeny. The **Atlas domain** is divided into two sub-domains : the Atlas Range itself (High and Mid-Atlas) and the Meseta. The Atlas Range is mainly composed of Mesozoic rocks with subsidiary Paleozoic and Cenozoic rocks. The Mesozoic overlie a peneplanated Hercynian-deformed Paleozoic basement. All rocks has been deformed by the Alpine orogeny. In the Meseta, the Alpine orogeny was much less severe than in the Atlas Range. The peneplanated Hercynian-deformed Paleozoic rocks underlie an essentially flat-lying Mesozoic-Cenozoic cover. The Phanerozoic rocks of the **Rif domain** have been strongly deformed and transported as several nappes during the Alpine orogeny.

On day 1 we will travel, from Casablanca to Midelt, mainly in the Meseta, and most of the time on Paleozoic rocks, although we will cross the Mid-Atlas before arriving in Midelt. On day 2, we will enter the magnificent High-Atlas and, after two geological stops while crossing the High-Atlas, we will enter the Anti-Atlas, the door of the desert, by the end of the day. Days 3 to 6 will be spent in the Anti-Atlas for field observation and oral session. On day 7, we will travel in the Berber country, from Erfoud to Ouarzazate, still in the Anti-Atlas. On day 8, our travel from Ouarzazate to Marrakesh will give us the opportunity to cross again the High-Atlas mountains, one of the most scenic road of Morocco. The detailed itinerary and schedule follow.

Day 1 - Sunday, October 24
Departure from Casablanca, at about 12h00
Travel to Midelt - 422 km
Arrival in Midelt at about 18h00
Overnight stay in Midelt

Day 2 - Monday, October 25
Travel to Rich area - 82 km
Stops 1.1-1.2 : Jurassic mounds of High-Atlas (Neuweiler)
Leaving Rich area by 15h00-16h00
Travel to Erfoud - 77 km
Arrival in Erfoud by 17h00-18h00
Overnight stay in Erfoud

Day 3 - Tuesday, October 26
Kess-kess mounds of Hamar Laghdad - part 1 (Bourque and Mounji)
Stop 2.1 : quick stop on Boutchrafine section (lateral equivalent of Hamar Laghdad)
Stop 2.2 : the underlying volcanic rocks and crinoid sole at Hamar Laghdad
Stop 2.3 : the kess-kess mounds and associated facies
Overnight stay in Erfoud

Day 4 - Wednesday, October 27
Stop 2.3 (cont') : Kess-kess mounds of Hamar Laghdad - part 2 (Bourque and Mounji)
Stop 2.4 : Hollard mound of Hamar Laghdad (Bourque, Mounji, Reitner and Walliser)
Overnight stay in Erfoud

Day 5 - Thursday, October 28
Scientific session in Erfoud (oral communications and plenary session)
Overnight stay in Erfoud

Day 6 - Friday, October 29
Stop 2.5 : Aferdou el Mrakib mound, Maïder area (Bourque and Mounji) - a long day
Overnight stay in Erfoud

Day 7 - Saturday, October 30
Travel to Ouarzazate, via Tazzarine - Zagora - 440 km
Optional stop : Givetian coral-stromatoporoid breccia, Tamjout n'Ouihlane
Arrival in Ouarzazate by 17h00-18h00
Cultural stop : visit of the Casbah, if time permits
Overnight stay in Ouarzazate

Day 8 - Sunday, October 31
Travel to Marrakech - 204 km
Arrival in Marrakech by noon
Cultural Stop : visit of Marrakech medina in afternoon
Plenary session : wrap up, discussion, future plans
Farewell dinner and overnight stay in Marrakech

Day 9 - Monday, November 1
Travel to Casablanca - 238 km
Arrival in Casablanca in early afternoon
End of trip

Itinerary map 1 - Midelt to Er Rachidia

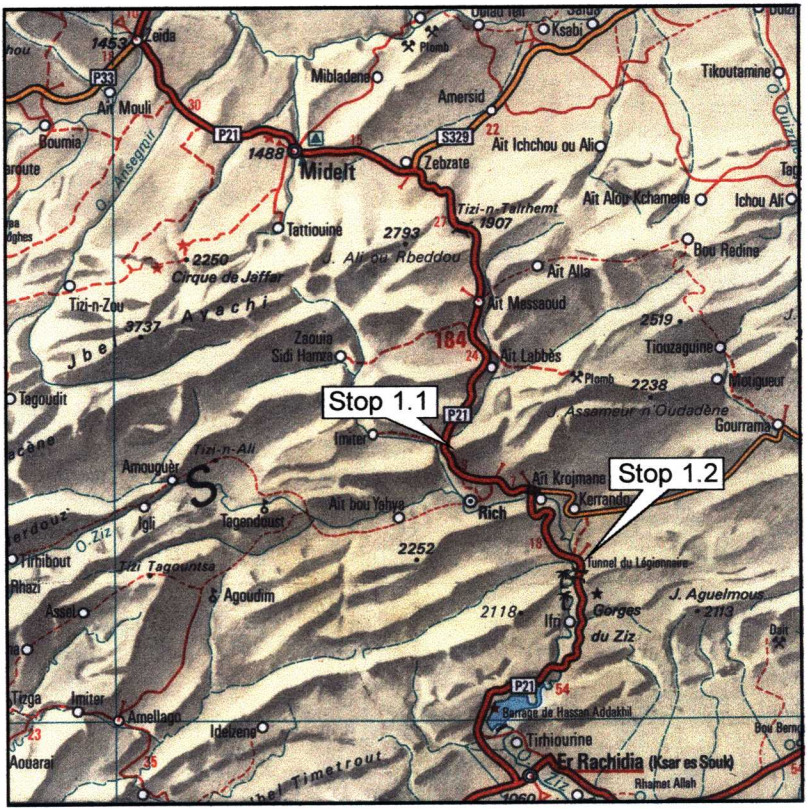

Stop 1.1 *: Foum Tillicht; Liassic sponge mounds*

Photostop A *: Aalenian marls and Bajocian coral bioherms*

Stop 1.2 *: Tunnel du Légionnaire; stratigraphic equivalent of mounds*

Photostop B *: Liassic "reef tract" with scleractinian corals and lithiotid bivalves*

Itinerary map 2 - Er Rachidia to Erfoud

Stop 2.1 *: Boutchrafine section, SE Erfoud, Tafilalt*

Stops 2.2-2.4 *: Hamar Laghdad massif, SE Erfoud, Tafilalt*

Stop 2.5 *: Aferdou el Mrakib, Maïder*

Itinerary map 3 - Erfoud to Ouarzazate

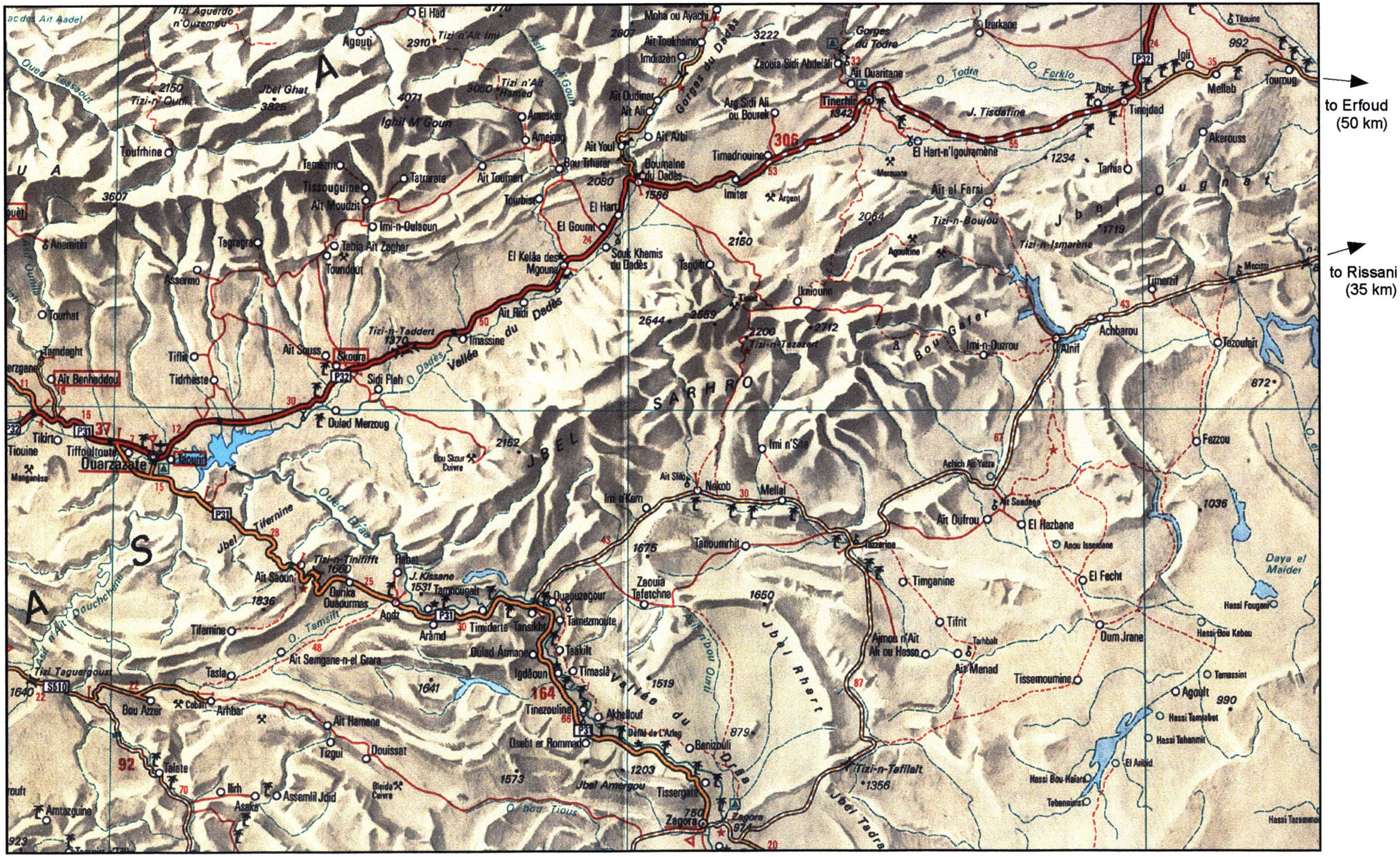

Scale 1:1 000 000

0 10 20 30 40 50 km

0 10 20 30 miles

Itinerary map 4 - Ouarzazate to Marrakech

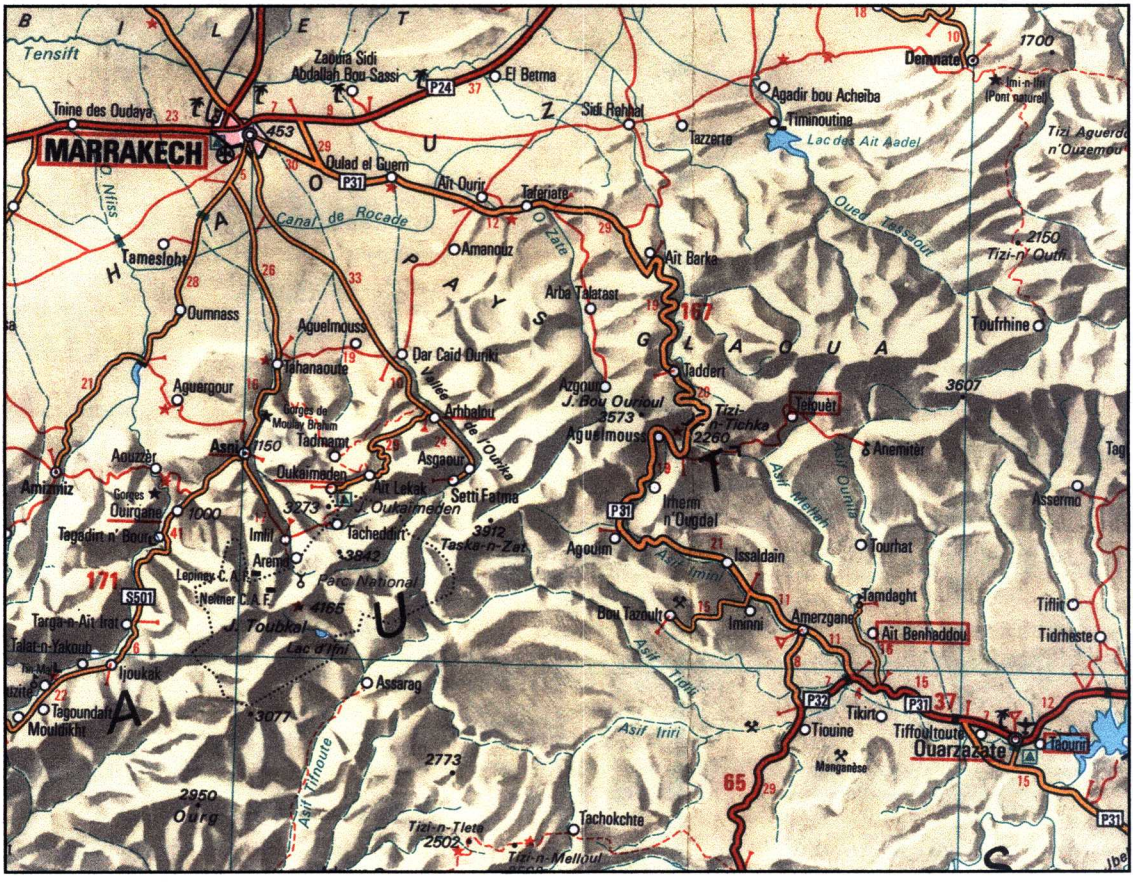

Part 1

Liassic Sponge Mud Mounds of the Central High-Atlas Mountains, Morocco

By Fritz Neuweiler (Université de Liège, and Universität Göttingen),

in cooperation with Mohammed Mehdi (Oujda)

Aknowledgement
Fritz Neuweiler acknowledges the financial support from the German Research Foundation (MAR 111/6/98; Ne 652-3) and the FNRS (Bruxelles, Alexander-von-Humboldt Stiftung).

Introduction

Within the Moroccan High Atlas Mountains (Fig. 1) there are two Mesozoic basins containing Jurassic sedimentary deposits (Figs. 1 and 2). The relatively small Essaouira Basin (or Haha Basin) of the western High Atlas represents marginal marine deposits of the early mid-Atlantic seaway. In the Essaouira Basin Jurassic shallow marine carbonates are replaced by sandstones and terrigenous conglomerates towards the eastern landbridge of the « Massif Ancien » a late Paleozoic granitic intrusion (Michard, 1976; Jacobshagen *et al.*, 1988). East of the 'Massif Ancien' the Atlas Gulf formed a large marine embayment. It includes shallow marine platform environments, *e.g.* directly east of the Massif Ancien (*e.g.* Burgess & Lee, 1978; Septfontaine, 1986) or south of the Rif Mountains (Mehdi, 1995), and the two more rapidly subsiding sub-basins of the Central-Eastern High Atlas and of the Mid-Atlas, respectively. The Mid-Atlas sub-basin reveals a SW-NE trend (*i.e.* Atlantic trend), the Central to Eastern High Atlas sub-basin shows an E-W (Tethyan) trend and therefore shows both correlations as related to transcurrent fault system of the mid-Atlantic and the westward migration of the Tethys (Manspeizer *et al.*, 1978; Manspeizer, 1988). These rift-related sub-basins are surrounded by a craton such as the Saharan platform (or African Craton) in the south, or smaller terranes like the Western Meseta in the northwest and the Eastern (Oran) Meseta (Hauts Plateaux) in the east. The latter contains a widespread but thin cover of marine Jurassic deposits (Fig.2).

Pliensbachian sponge mud mounds were described from both sub-basins of the Atlas Gulf, either as sponge bioherms or lithoherms (Dresnay, 1988; Evans *et al.*, 1974; Evans and Kendall, 1977) or as sponge-algal buildups and mudmounds, respectively (Warme, 1988, 1989). We will visit Pliensbachian sponge mud mounds and related sedimentary sequences of the Central High Atlas along a road transect between Midelt and Errachidia (Itinerary map 1).

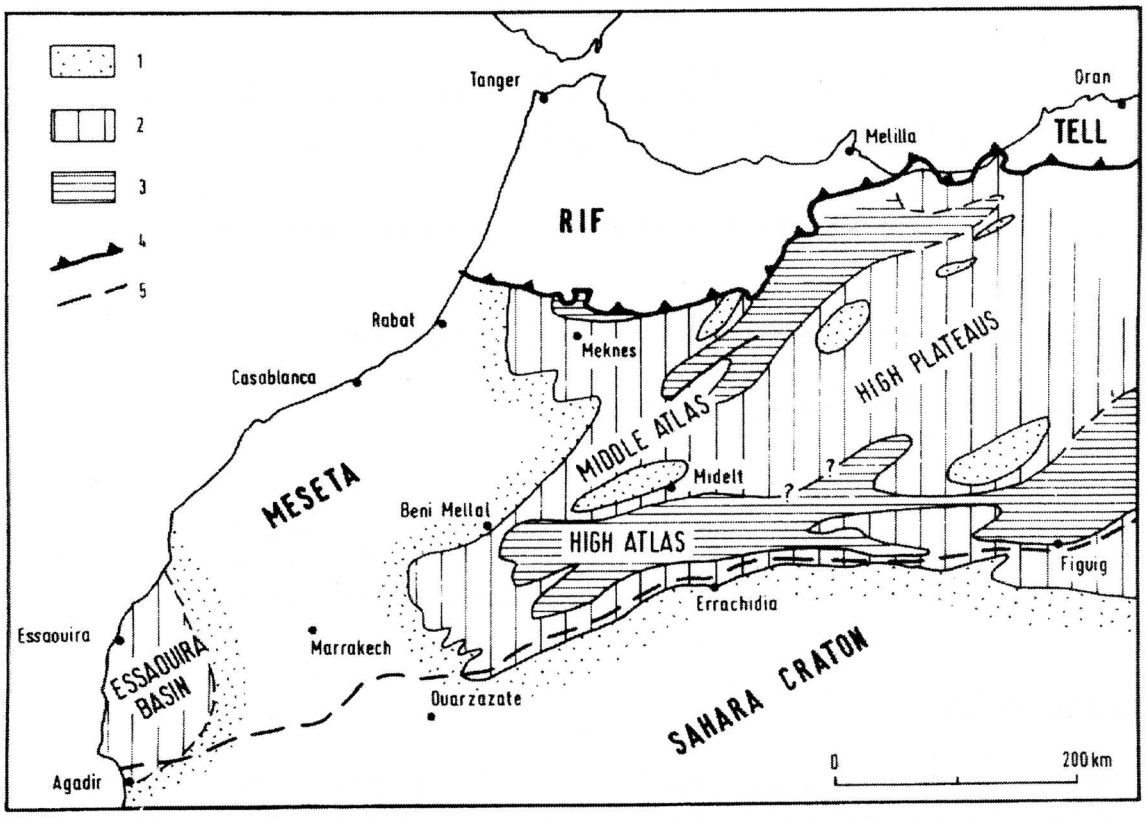

Figure 2 - Middle Liassic palaeogeography showing the Essaouira Basin in the W, the landbridge of the Massif Ancien, and the large Tethys embayment of the Atlas Gulf. *Note the two sub-basins of the Atlas Gulf exhibiting SW-NE (Atlantic) and W-E (Tethyan) trends. High Plateaus correspond to the Eastern Meseta (Oran terrane). According to Dresnay (1971) in Jacobshagen et al. (1988).*

Tectono-sedimentary History of the High Atlas Sub-basin

Variscan basement rocks are Carboniferous slightly metamorphic sandstones and mudstones. Rifting started during the Triassic and lasted until the Early Jurassic (Warme, 1988). Syn-rift deposits are fault-block related sequences of redbeds, evaporites and basalts (cf. Mattis, 1977). Lower Liassic, Hettangian(?) to Sinemurian carbonate sediments (Fig. 3) represent marine flooding (dolomites, oyster beds). Upsection there follows a ramp-like Sinemurian to Pliensbachian sequence dominated by bahamites, *i.e.* ooids, coated grains, micritized grains, faecal pellets, and minor calcareous algae. According to Warme (1988) synsedimentary block-faulting lead to the formation of tectonically controlled platforms which were covered or bordered by Pliensbachian sponge mud mounds (Fig. 4). The Pliensbachian/Toarcian boundary interval appears as a platform drowning interval. Here, deep-water rhythmites and turbidites cover the Pliensbachian sponge mounds. Early Dogger (Aalenian) deposits are represented by marly limestones and marls, which pass vertically into Bajocian coral biostromes and bioherms (Fig. 3). The succeeding sedimentary fill of the basin resulted in the end of marine conditions during the Dogger. The transgressive-regressive sedimentary cycle was completed by middle to late Jurassic continental redbeds.

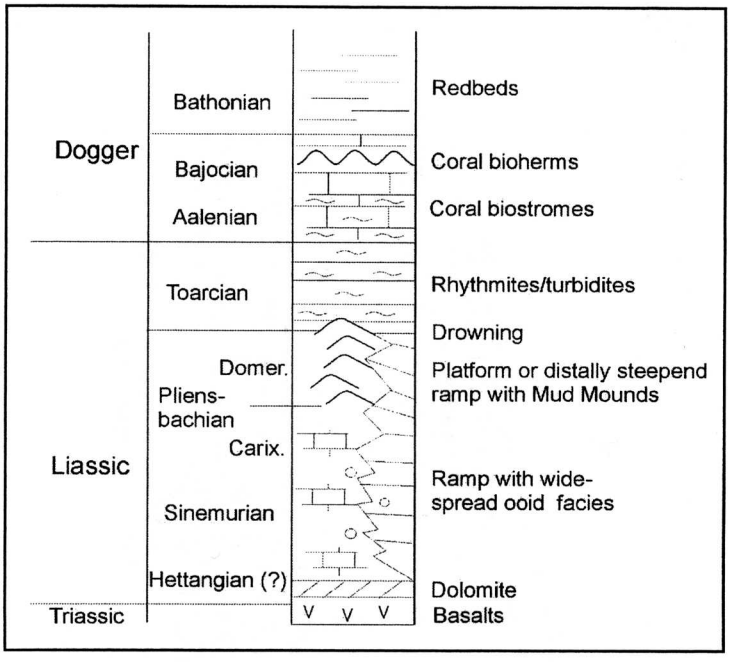

Figure 3 - Generalized stratigraphic section of the Jurassic of the Central High Atlas. *From various sources and own results*

After mild uplift and erosion, Cretaceous and Paleogene shallow marine sediments were deposited. Alpine (*i.e.* Oligo-/Miocene) deformation resulted in an inversion of the basin along reactivated faults including en echelon folding and upthrusting (Fig.6). This style of mild deformation (i.e. inverted blocks, flower structure) is geomorphologically well-expressed and allows to study fairly complete lateral transects of the High Atlas sub-basin. Ridges represent narrow anticlines with upthrusts and occassional box folds (Triassic/Liassic sequence) whereas broad valleys represent synclines of Toarcian and younger sediments.

Stops 1.1 and 1.2 Liassic sponge mounds

Between Midelt and Errachidia, the main road P21 provides excellent access to the Central High Atlas geology (Itinerary map 1; Fig. 1 and 2). Much work the palaeontology, stratigraphy, and sedimentary facies has been done in this area (*e.g.* Dubar, 1948, Dresnay, 1971,1977; Evans *et al.*, 1974, 1977; Evans and Kendall, 1977; Warme, 1988, 1989). However, our understanding of the compositions of sponge mud mounds, as well as their space and facies sequence relationships, is very limited. In October 1998, Prof. M. Mehdi (Université d'Oujda) and the author surveyed this area in order to prepare a research project on the biosedimentology of Liassic sponge mud mounds. This first survey was funded by the Conseil National de Recherches (CNR) du Maroc and the German Research Foundation (GZ: 445 MAR 111/6/98) with additional logistic support by the Service géologique du Ministère de l'Énergie et des Mines, Centre Régional de la Géologie d'Errachidia, and ONAREP. All data presented below refer to this very first approach (Neuweiler and Mehdi, in prep.).

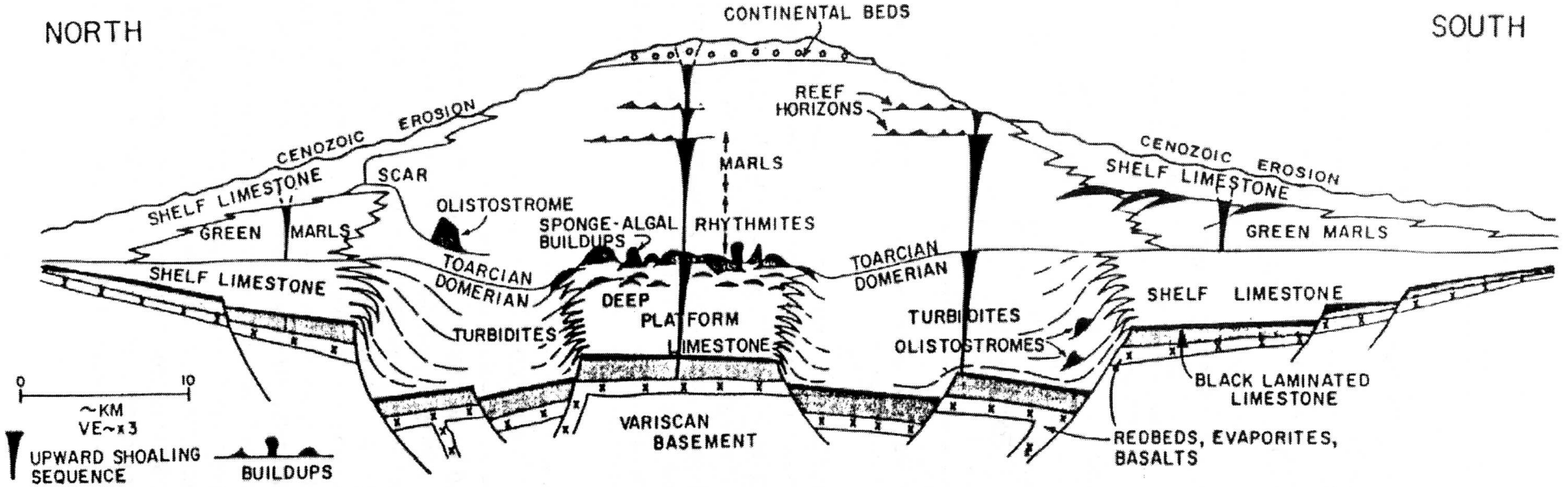

Figure 4 - Diagrammatic cross section across the Central High Atlas. *From Warme (1988, 1989).*

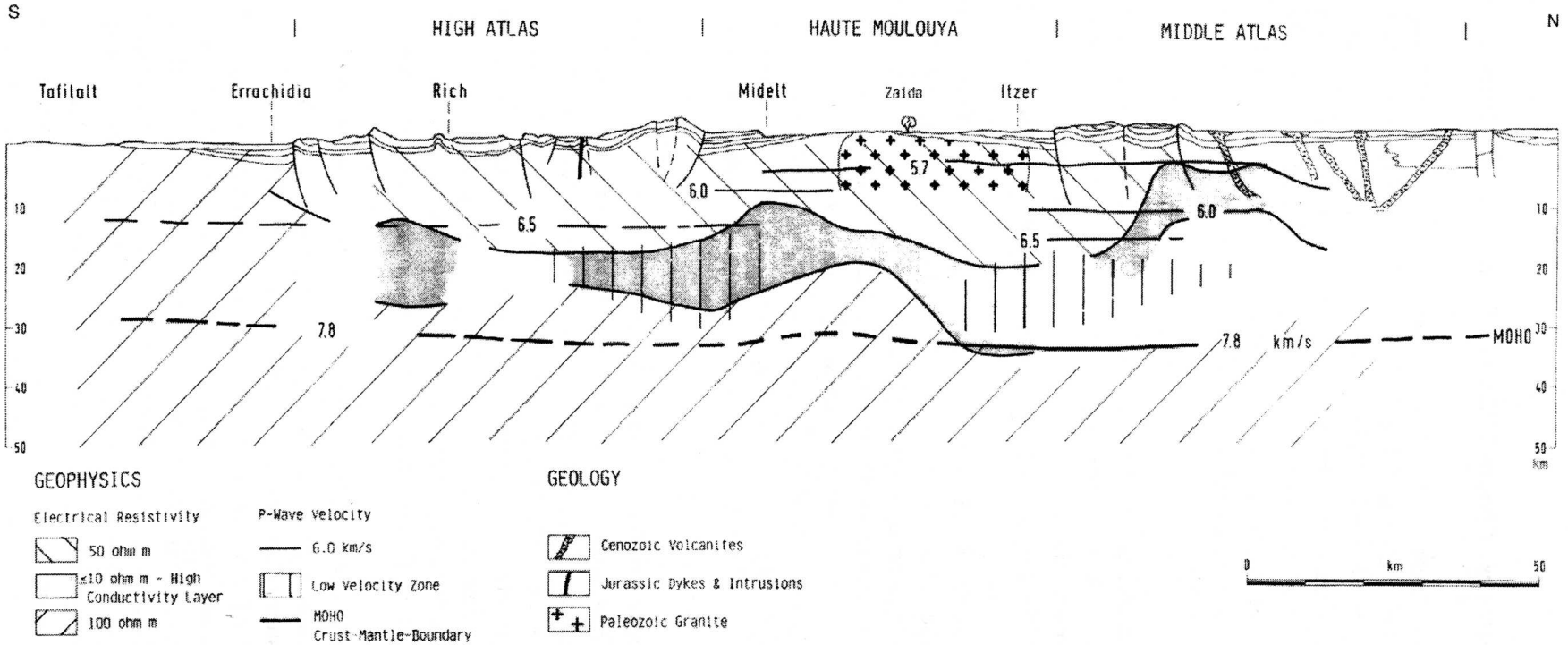

Figure 5 - Crustal section through the inverted v'basins of the High and Middle Atlas. *High conductivity layer and seismic velocity zone indicate zone of partial melt. From Schwarz and Wigger (1988).*

Facies and Sequences at Foum Tillicht and Tunnel du Légionnaire

In general, the Liassic carbonate sediments show only little variation of litho- and microfacies (summarized in Table 1, Fig. 7). Most of these sediments are well-bedded and accumulated from non-skeletal grains such as faecal pellets (*Favreina*, a.o.), ooids and detrital carbonate mud. The few exceptions from this are oyster-sponge clusters in the lower part of the sequence, and sponge mud mounds with adjacent lumachelle beds (bivalves and brachiopods). High-diversity assemblages of scleractinian corals and lithiotid bivalves are restricted to a 'reef tract' (Dubar, 1948) further south in the Central High Atlas (photostop B).

Sections taken at Foum Tillicht (Stop 1.1) and Tunnel du Légionnaire (Stop 1.2) are illustrated in Figure 6. Albeit we are not able to look at the very details of these sections due to time constraints, these two sections demonstrate well the overall lithofacies characteristics of the Liassic sequence of the Central High Atlas sub-basin.

From observations during our first field work and from thin-sections, Liassic sponge mounds reveal the following characteristic features. Mounds are aligned along the strike of the basin axis, and accumulated to form composite structures with synoptic relief in the 20 to 50 m range. The mounds are stratigraphically related to transgressive system tracts within the Pliensbachian, and got covered by deep-water rhythmites during the Toarcian relative rise of sea-level. This Toarcian drowning event may well correlate with the Toarcian anoxic event of western Europe (cf. Hallam, 1986, 1988, 1996; Jenkyns, 1988; Little and Benton, 1995), but the stratigraphic and geochemical details of this have still to be worked out.

Skeletal metazoans of these mounds include various types of lithistid and non-rigid demosponges, lyssakine and hexactinose Hexactinellids, and at certain levels also pharetronid sponges. These sponges show overgrowths by bryozoans, serpulid and terebellid worm tubes, encrusting foraminifera and may include various types of borings. Associated are terebratulid brachiopods and occassionally high amounts of crinoidal debris. Towards the drowning-level there is an apparent change towards a simply composed facies consisting of hexactinellid sponges embedded within wackestones with sponge spicules and calcified radiolarians (deepening-upward trend).

The 'matrix' between skeletal metazoans is far from being uniformly composed. It shows three main types: A) the most conspiceous type is that of thrombolites, occassionally occupying several square meters. In thin-section the thrombolites form 'nodular heads' of peloidal carbonate mud, sometimes grading laterally into skeletal remains of siliceous sponges. Some nodules accrete upon sponges, some are themselves colonized by encrusting foraminifera. Between the nodules there is an argillaceous wackestone with spicules, microbioclasts and nodosarid foraminifera. B) volumetrically most important is a polymud fabric consisting of authigenic micrites (automicrites) and geopetal, microcrystalline sediment (allomicrite). Automicrite shows borings and therefore seems to be the site of early induration and active vertical accretion. Allomicrite shows a mottled fabric, sometimes with evidence of a burrowing and deposit feeding

endofauna. C) rather exceptional is a 'matrix' of a microbioclastic wackestone with radiolarians filling the space between micritic crusts accreting upon hexactinellid sponges (beginning of Toarcian drowning sequence).

Small stromatactoid cavities mostly occur as early shrinkage features related to sponge soft tissue diagenesis. Larger collapse features may grade into the early phases of autobrecciation. The mounds contributed to narrow off-mound areas by lithoclasts and sponge debris. Total organic carbon content is in the range of 0.3 %.

	Lithology	Microfacies
1	dark limest., marlst., marls; thinly bedded	microbioclastic mud-/wackestones, only late *Chondrites* burrows. *Favreina* (faecal pellets of decapod crustaceans); microsparitisation. Dysoxic soft bottom conditions.
2	rhythmic lime-/marlstones intercalations with chert nodules	densly packed *Favreina*-'packstone' with small amounts of microbioclasts, pellets and micritised ooids. Oxic soft bottom conditions.
3	oyster banks of the lower Sinemurian sequence	boundstones of *Exogyra/Nanogyra*, siliceous sponges and automicrite. Fragments of scleractinian corals. Hexactinellids, lithistid and non-rigid demosponges, calcareous sponges. Lithophagous bivalves (condensed facies).
4	marly lumachelle limestones	reworked and concentrated shells of bivalves and brachiopods. Partially imbricated and with vertical orientation. Some lithoclasts of siliceous sponges. Geopetal, interparticle mud (shelter porosity). Evidence for strom wave action (tempestites).
5	sponge mud mounds	siliceous sponge/automicrite boundst.. Hexactinellids and lithistid demosponges. Calcareous and agglutinated polychaetes (*Serpula*- and *Terebella* type). Crinoidal debris, ubiquitious cryptic ostracods. Organic carbon = 0.3 %. TST deposits
6	intraformational conglomerates	'textural inversion', e.g. intraclasts with radiolarians embedded in ooid/onkoid grainstones. Some calcareous algae (dasycladaceans). Sequence boundaries.
7	limestones with ooids and oncoids	partialy marine cemented grainstones; single, normal and composite ooids. Oncoids with filamentous microfabrics and encrusting forams. Fragments of calcareous algae (dasyclads, solenoporids, and 'cyanophyceans'. Organic carbon = 0.35 %. HST
8	marly limestones	packstones with peloids, fragments of molluscs and crinoids. Large dasycladaceans
9	marl-/limestone rhythmites	sponge spicule bearing wackestones with *Chondrites* and *Planolites*. Minor radiolarians, peloids and microbioclasts. Ocassionally automicritic crusts. Toarcian drowning interval.

Table 1 - *Summary of lithologies and microfacies characteristics observed with the Liassic carbonate sequences at 'Foum Tillicht' and 'Tunnel du Légionnaire' (Neuweiler and Mehdi, in prep.). See Figure 6 for illustrations.*

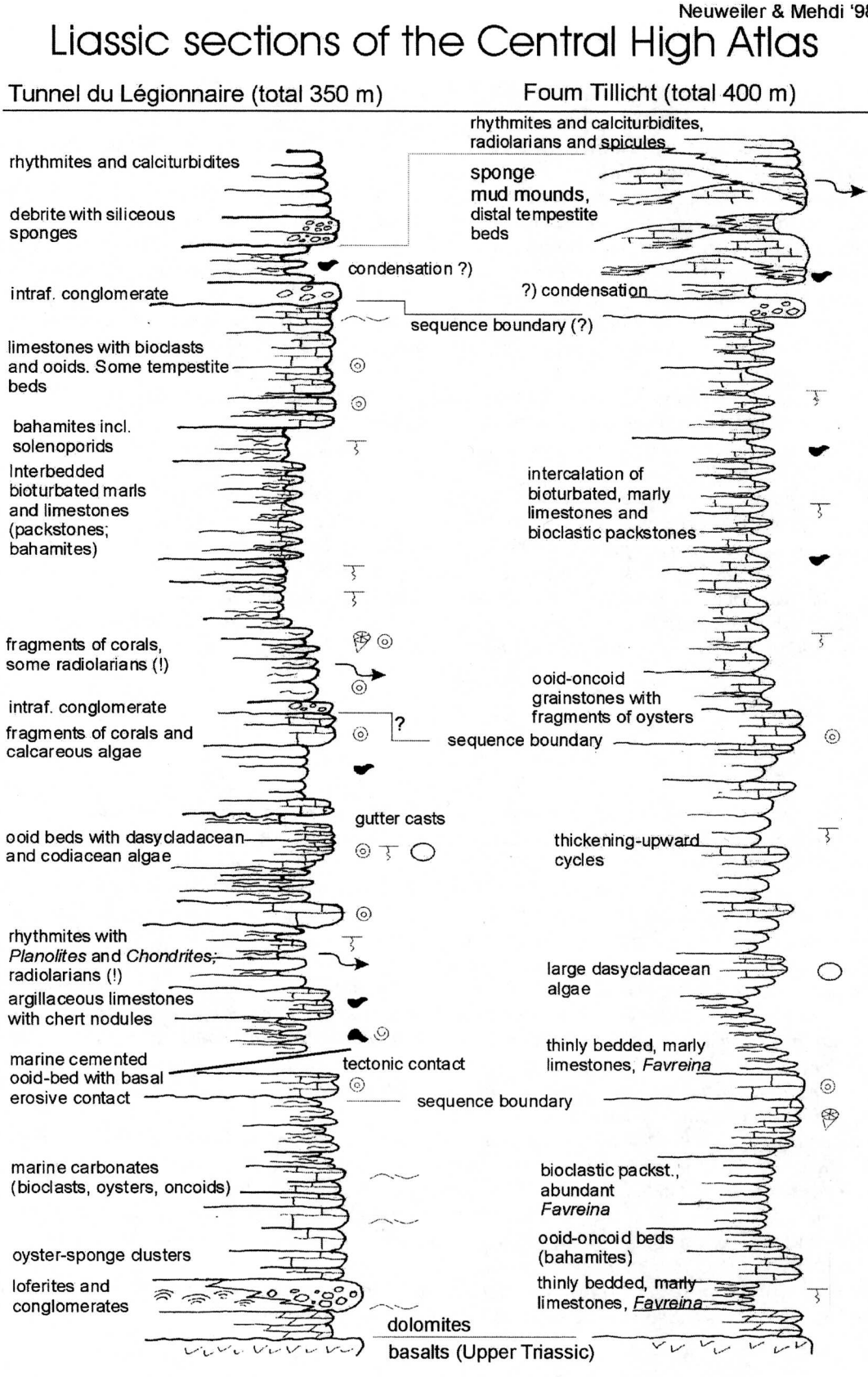

Figure 6 - Sections of Sinemurian to Pliensbachian carbonate sediments taken at Foum Tillicht (Stop 1.1) and Tunnel du Légionnaire (Stop 1.2).

→

Figure 7 - Microfacies variation of Liassic carbonate sediments. Foum Tillicht and Tunnel du Légionnaire, Central High Atlas.

a) *Oyster-sponge boundstone with secondary frame of automicritic crusts and allochthonous mud (polymud fabric). From lower parts of the Liassic carbonate sequence at Tunnel de Légionnaire.*

b) *Marine-cemented grainstones with ooids, oncoids, and cortoids representing potential sequence boundaries within the lower part of the Liassic sequence at Tunnel du Légionnaire. Nuclei correspond to fragments of gastropods, bivalves, and echinoids.*

c) *Prograding late highstand deposits typically consisting of an incrasing volume of bahamite sands shed over microbioclastic spicule bearing wacketones. From marly limestone-limestone intercalations at Tunnel du Légionnaire.*

d) *Dolomitised ooid packstone with large dasycladacean algae. Tunnel du Legionnaire.*

e) *Well-sorted bahamite grainstone. Tunnel du Légionnaire*

f) *Bahamite grainstone with calcareous algae (Cayeuxia-Orthonella type) and small, aggutinated foraminifera. Tunnel du Légionnaire.*

g) *Favreina, crustacean faecal pellets within a recrystallized matrix of microbioclastic wackestone. Lower parts of Foum Tillicht section.*

h) *Poorly sorted ooid-oncoid packstone. Nuclei are molluscan debris and Favreina. Foum Tillicht.*

i) *Concentrated shell fragments of bivalves and terebratulid brachiopods, the dominant feature of tempestite beds coeval to Pliensbachian sponge mud mounds. Foum Tillicht.*

k) *Wackestone with calcified radiolarians and sponge spicules representing the complete drowning of Pliensbachian sponge mud mounds. Upper parts of Foum Tillicht section.*

→

Page 27

Figure 8 - Microfacies of Liassic sponge mud mounds. Foum Tillicht, Central High Atlas.

a) *Our first results indicate that pharetronid sponges are fairly common within, but restricted to the lower parts, of sponge mud mounds*

b) *Hexactinose sponges are common all over but begin to dominate in the uppermost parts of sponge mud mounds. Note borings indicating early calcification of the spicular skeleton as well as the early authigenic formation of relatively dark peloidal automicrite within the sponge.*

c) *Poorly preserved hextactinellid sponge grading into thrombolithic fabric.*

d) *In thin section thrombolites form nodules with relative high amounts of internal spar cement. Some of these open space structures can be related to shrinkage, some may be due to calcification of spicules or cementation of spicular moulds. Dense microbioclastic wackestone accumulated between the individual thromboids.*

e) *Non-rigid demosponge presverved in place. Note early collapse features related to differential compaction acting within the mound.*

f) *Lithistid sponge with internal micropeloids overgrown by encrusting bryozoans and calcareous worm tubes. Note thromboid in upper left part of micrograph and microbioclastic sediment fill inbetween.*

g) *Heavily bored hexactinellid sponge with abundant terebellid worm tubes.*

h) *Polymud fabric developed within hexactinellid sponge. Sponge soft tissue calcification is followed by borings and infill of secondary geopetal mud. This type of microfabric represent the volumetrically most important part of Liassic sponge mud mounds..*

i) *Primary host of spicular micrite, bored and infilled by secondary geopetal mud. This type of microfabric represents the volumetrically most important part of sponge mud mounds.*

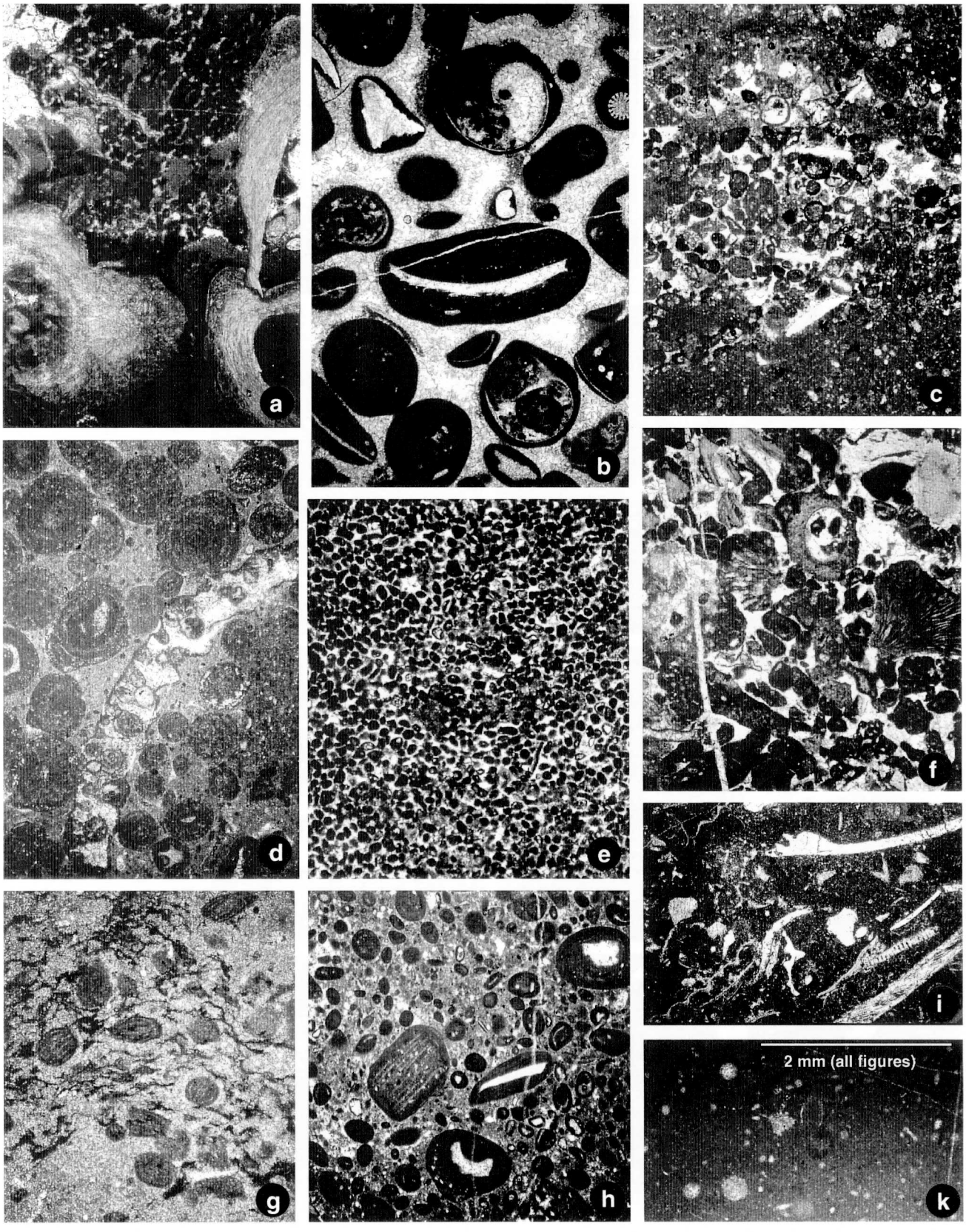
a
b
c
d
e
f
g
h
i
2 mm (all figures)
k

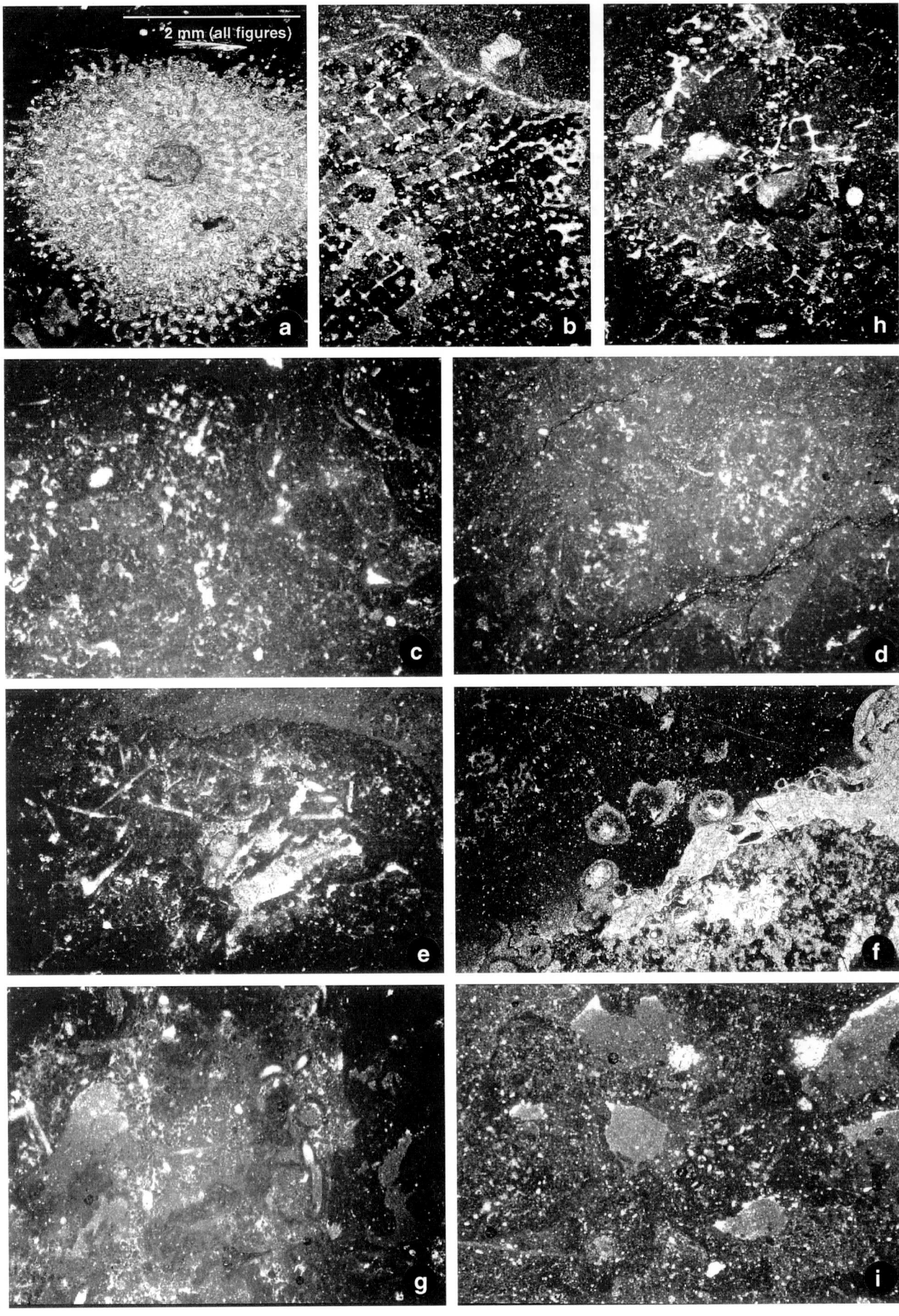
2 mm (all figures)
a
b
h
c
d
e
f
g
i

Discussion Topics

a) Origin and significance of the peculiar thrombolite texture within Liassic mounds.
b) Are sponges mound dwellers or active mound builders?
c) Is there any significance of seepage or other influences of ascending fluids?
d) Did these mounds form upon an isolated platform or on a distally steepening ramp?
e) What is the time-specific ‚Liassic imprint' on these mounds?
f) What is the role of the early Jurassic mass extinction?
g) What are the common and distinguishing features of Liassic sponge mounds?

Part 2

Devonian mounds of the Tafilalt-Maïder

By P.-A. Bourque and Driss Mounji (Université Laval, Québec),

with contributions from Jörn Peckmann, Otto Heinrich Walliser, Walter Riegel and Joachim Reitner (Universität Göttingen), and Martine M. Savard (Geological Survey of Canada, Québec) for the Hollard mound, Tafilalt;
and Otto Heinrich Walliser for chart of Figure 15.

Acknowledgement
Pierre-André Bourque acknowledges the financial support from the Natural Sciences and Engineering Research Council of Canada, and both P.-A. Bourque and Driss Mounji acknowledge logistical support for field work from the Office Nationale de Recherches et d'Explorations Pétrolières du Maroc (ONAREP).

Inroduction

A particularly well-developed and well-exposed Devonian sequence is found in the Tafilalt and Maïder geological provinces of the Moroccan Anti-Atlas (Fig. 1). The rocks were only very slightly deformed during the Late Paleozoic Hercynian Orogeny, and outcrop areas, often in the form of long cuestas, are extensive and offer first hand sections (Fig. 9). It is not surprising though that several geological studies were carried on the Devonian sequence:

- mapping and stratigraphy by Menchikoff (1933, 1936) Roch (1934), Clariond (1934, 1935), Clariond and Hendermeyer (1952), LeMaître (1947a, 1947b), Choubert (1948, 1952), Choubert *et al.* (1952), and particularly by Hollard (1958, 1960, 1961, 1962, 1963, 1965, 1967, 1974, 1977, 1981) and Massa (1965);
- bio- and chronostratigraphy using conodonts and/or goniatites by Bensaid (1974), Bultynk and Hollard (1980), Bultynk and Jacobs (1981), Bultynk (1985, 1987, 1989), Bensaid *et al.* (1985), Becker and House (1991, 1994), Walliser (1991), Walliser *et al.* (1995), Belka *et al.* (1997);
- sedimentology of more specific facies such as the Kellwasser facies by Wendt and Belka (1991), the cephalopod limestones by Wendt *et al.* (1984) and Wendt and Aigner (1985), the Tafilalt mounds by Roch (1934), Menchikoff (1936), Alem and Gendrot (1968), Elloy, 1972, Gendrot (1973), Brachert *et al.* (1992), Hopkins and Aitken (1993), Mounji (1995, 1999), Mounji *et al.* (1996, 1998), Belka (1998) and

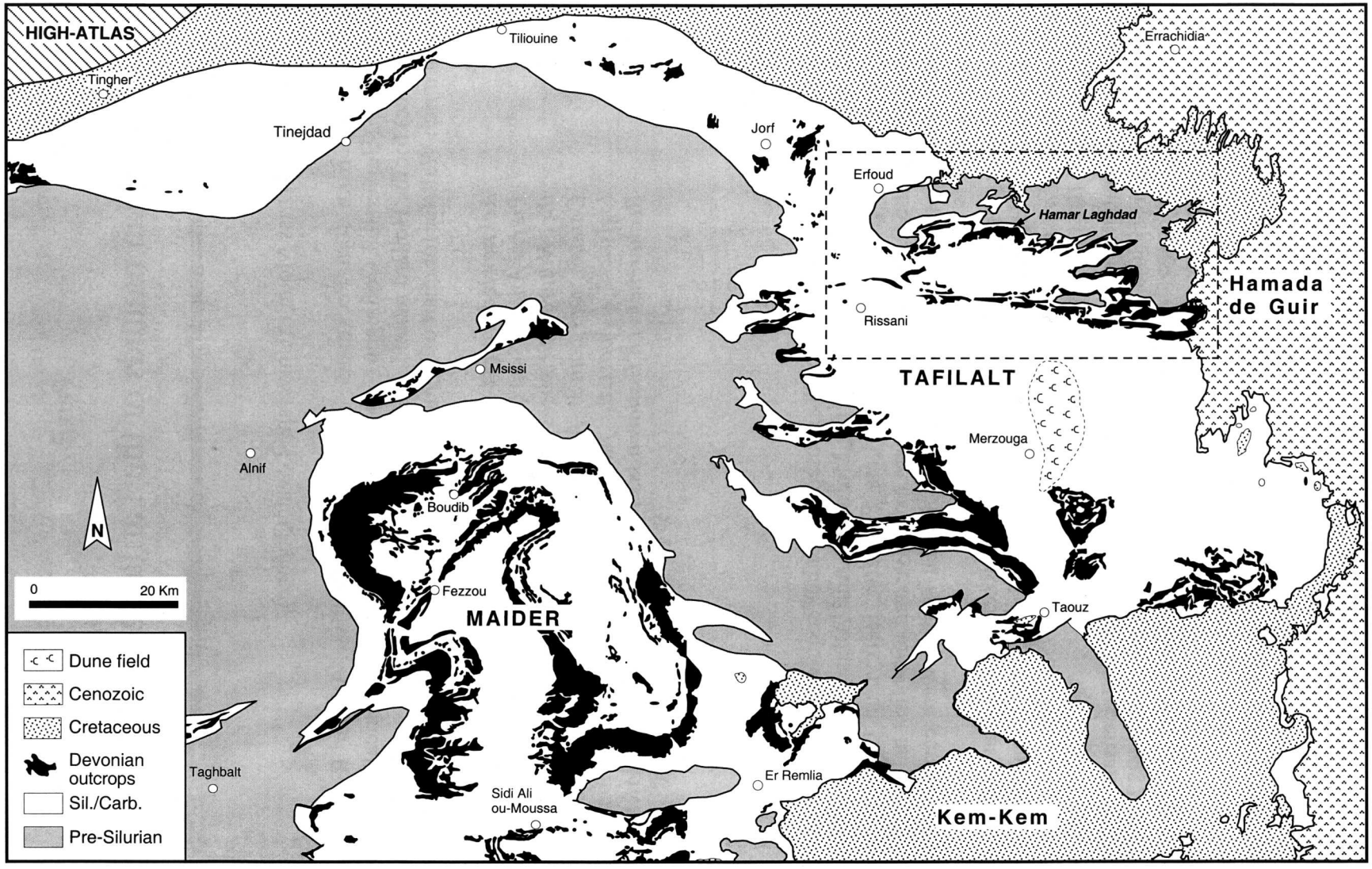

Figure 9 - Generalized geological map of the Tafilalt-Maïder basin and distribution of Devonian outcop areas. *See Figure 1 for location. HL is Hamar Laghdad massif. From Massa (1965) and Walliser (1991).*

Peckmann *et al.* (1999), and the Maïder mounds by Hollard (1974), Wendt (1993), Kaufmann (1996, 1997, 1998) and Mounji (1999);

- oil potential by Hopkins and Aitken (1993), Robertson Res. (1993), ONAREP (1998) and Mounji (1999).

The Devonian sequence of the Tafilalt is by far dominated by relatively deep water hemipelagic and pelagic fine-grained facies represented by shales and fine-grained tentaculitid and bioclastic limestones (Fig. 11, location of columnar sections on Fig. 10), with local crinoidal limestones, stromatoporoid-coral breccias and *Zoophycos*-bearing dark limestones, and a few sandstones. The Lower Devonian part of the Hamar Laghdad section is atypical of the sequence because of the occurrence of volcanic rocks at its base (see further). In the Maïder, the fine-grained deep water facies are proportionnally less important with respect to the crinoidal limestones, the stromatoporoid-coral breccias and the *Zoophycos* limestones.

During the Lochkovian to Emsian time, the regime of sedimentation in the Tafilat and the Maïder was rather uniform, being dominated by shale and tentaculitid limestone facies, except for the Hamar Laghdad sector. The same regime of sedimentation went on during the Eifelian time, except for the development of crinoidal limestones and sponge-coral mounds in the Maïder, pointing to local slightly shallower water depth conditions. The Givetian time was a time of stromatoporoid-coral reef or bank construction, apparently somewhere outside the Tafilalt-Maider area, since only breccias, associated with dark *Zoophycos* limestones, are known (see below). During the Frasnian time, the fine-grained hemipelagic and pelagic sedimentation persisted with local remains of crinoidal limestones. The Frasnian-Famennian boundary is marked by the Kellwasser facies.

Previous studies have concluded that the stromatoporoid-coral beds we observe in the Tafilat and the Maïder were reefs (LeMaître, 1947; Massa, 1965; Gendrot, 1973; Hollard, 1974, 1981), subsequently used as shallow water depth indicators in paleogeographical reconstructions (Massa, 1965; Wendt, 1988b, 1993). We have observed these stromatoporoid-coral units at several localities and on numerous beds (Fig. 11). The units are tabular or lenticular bodies, a few centimeter up to 50 meter-thick, more commonly in the range of 10's of cm to a few meters, interbedded with well-bedded fine-grained limestones. They share the following features :

- the stromatoporoid coenestea and coral colonies are usually chaotically oriented with respect to their growth position and they are broken most of the time;
- the beds often show a vertical graded-bedding, with large (cm to 10's of cm) fossil fragments at base, decreasing in size upward, and commonly capped with parallel-laminated sand-sized bioclastic limestone;
- the base of the beds is often erosive;
- the texture is mostly floatstone rather than rudstone, with a fine to medium-grained bioclastic limestone as supporting matrix;
- the stromatoporoid-coral units are interbedded with a dark fine-grained limestone locally rich in the trace fossil *Zoophycos* which is commonly, although not exclusively, indicative of relatively deep water settings;

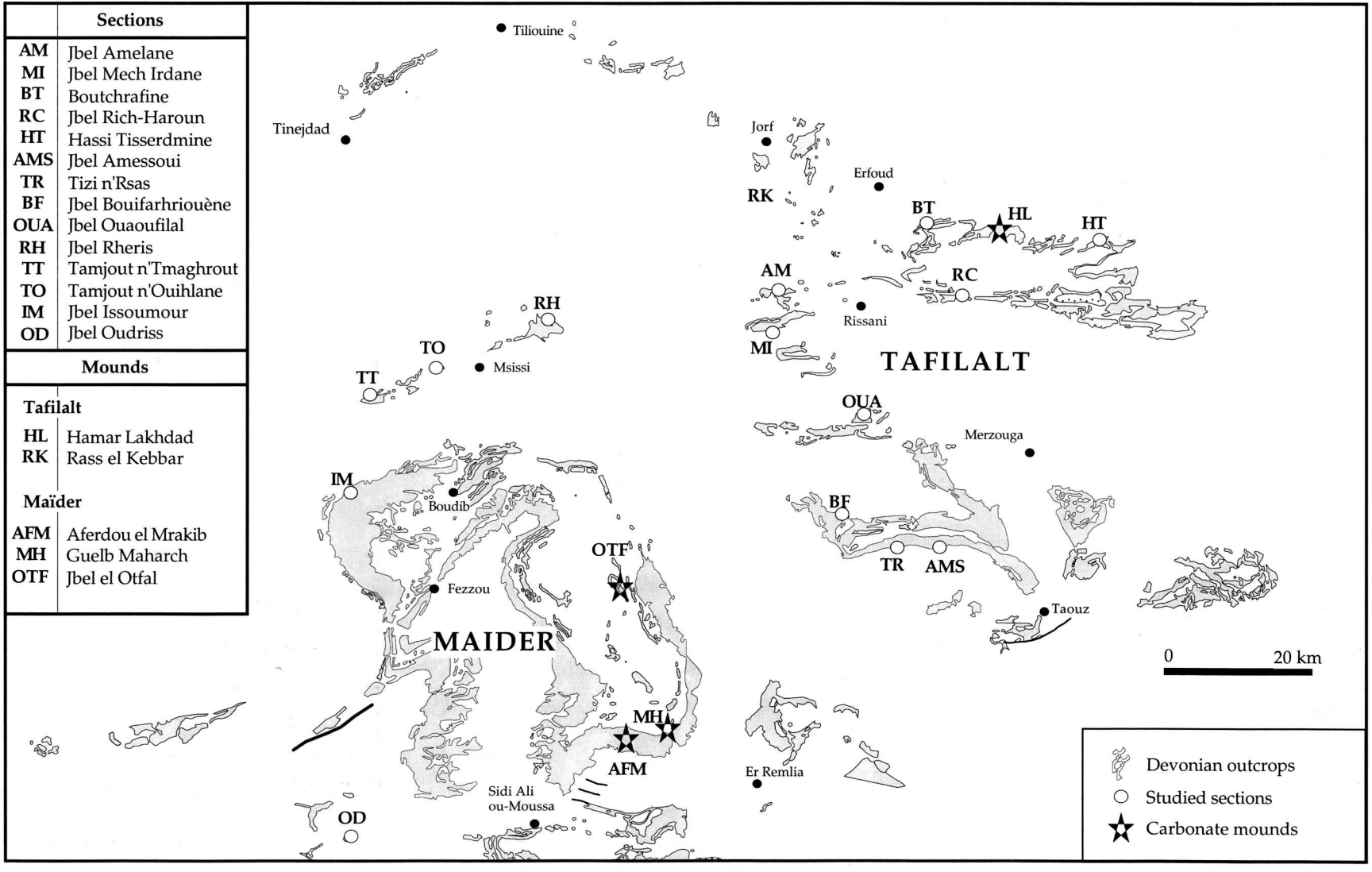

Figure 10 - Devonian outcrop areas in the Tafilalt-Maïder basin and location of representative sections shown on Figure 11. *From Mounji (1999)*

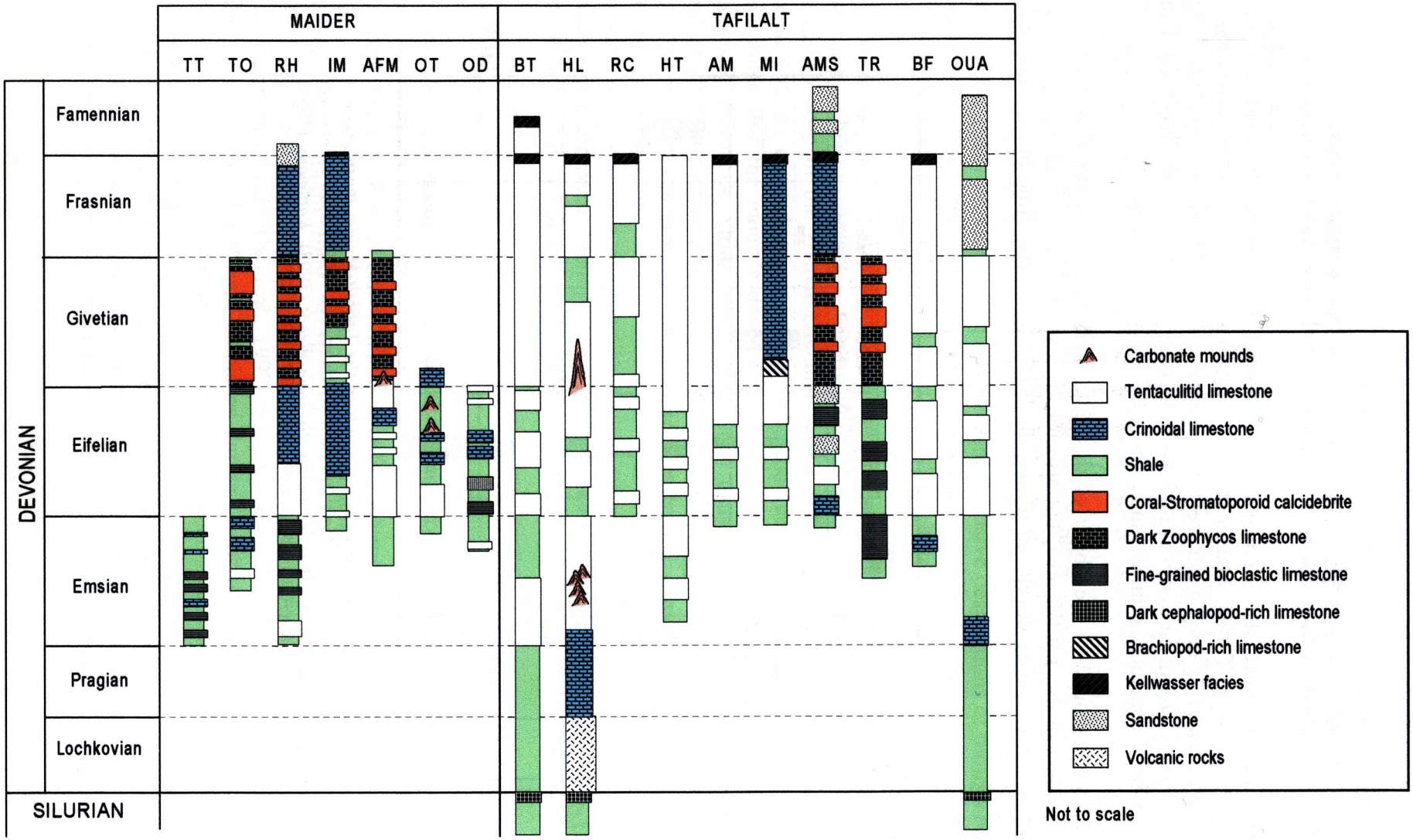

Figure 11 - Representative columnar sections showing facies distribution with respect to time in the Tafilalt-Maïder basin. *Section measurement and description, and facies definition by Mounji (1999). Location of sections on Figure 10. Ages are from Massa (1965), Hollard (1967, 1974, 1977, 1981), Bensaid (1974), Bultynck and Hollard (1980), Bultynck and Jacobs (1981), Bultynck (1985, 1987, 1989), Bensaid etal. (1985), Becker and House (1991, 1994a), Walliser (1991), Walliser et al. (1995), and Belka et al. (1997).*

- the units are seldom associated with slumping.

Taken all together, these features suggest that the stromatoporoid-coral units are gravity deposits in a relatively deep water setting, rather than shallow water constructions.

All in all therefore, the sedimentary environments were poorly differentiated during the Devonian in the Tafilalt-Maïder basin. It seems that the basin floor remained most of the time in relatively deep water, below the photic zone and the storm wave base. Algae are strickingly absent and no wave-driven sedimenatry structures were recorded. Fauna (tentaculitids, goniatites, crinoids) indicates open marine conditions.

Carbonate mounds – the object of this field workshop – developed mainly during Emsian time in the Tafilalt area, but also for at least one example during the Eifelian-Givetian, whereas they developed during the Eifelian-Givetian time in the Maïder area (Fig. 12).

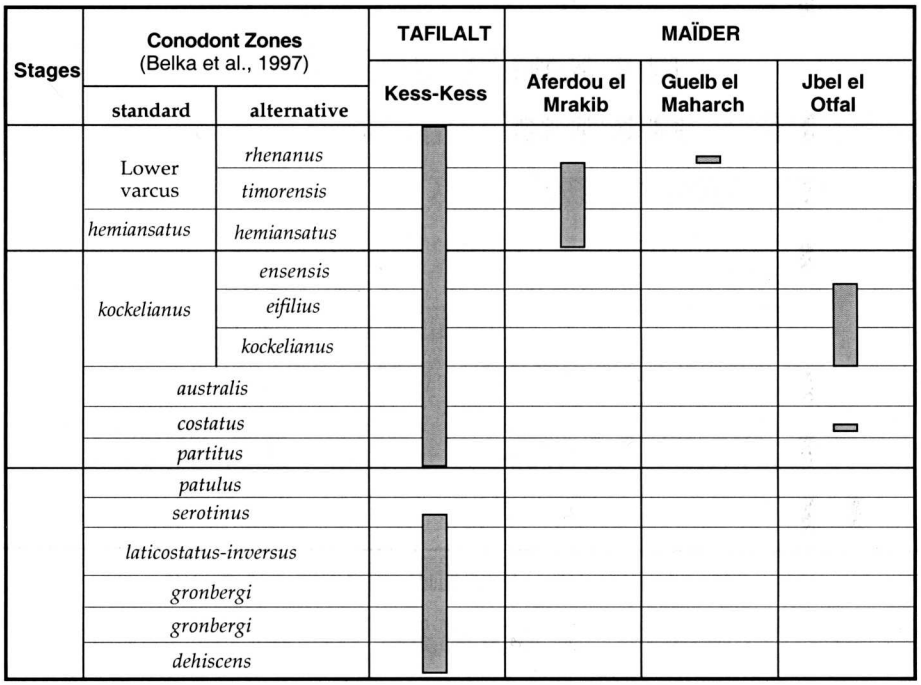

Figure 12 – Ages of the carbonate mounds in the Tafilalt-Maïder basin. *Ages of Hamar Laghdad mounds (Tafilalt) are from Brachert et al. (1992) and Peckmann et al. (1999). Ages of the Maïder mounds are from Wendt (1993), Kaufmann (1996) and Belka et al. (1997).*

The Emsian Kess-Kess of Hamar Laghdad (Tafilalt)

Previous work

The enigmatic cone-shaped Kess-Kess structures of Hamar Laghdad, named by local people after the cups (inverted) used to cook the national Moroccan dish, the couscous, have puzzled geologists for decades, and still today. Despite recent modern investigations, several questions remain to be answered. Menchikoff (1933) was the first to claim that they were reefs, but had very few echos to his proposal. Roch (1934) described them as « phénomènes remarquables » without actually proposing an origin, and Clariond (1935) described them as volcanic « tumuli ». Choubert *et al.* (1952) viewed them as reefs. Subsequent work by Alem and Gendrot (1968), and Hollard (1963, 1967, 1974, 1981) provided more or less comprehensive descriptions of those « reefs ». Gendrot (1973) was the first to recognized the « mud mound » nature of the Kess-Kess, whereas Michard (1976) compared them to modern pinnacle reefs.

The most comprehensive lithological and paleontological description of these Tafilalt conical mounds to date was given by Brachert *et al.*, (1992) who provided a reliable geological map of the Hamar Laghdad massif with actual mound distribution, and a sound account on rock types, microfacies, and faunal content and distribution. They interpreted that the mounds developed as « accumulations of more parautochthonous bioclastic sediments within the mounds, (...) caused by a self-sustaining system of hydrologic piling of sediment triggered by storms, preferred settlement of organisms upon these piles, producing bioclastic sediments and coeval biocementation of the growing mound flanks ». More recently, Montenat *et al.* (1996) proposed that the mounds developed in a grabben-like setting rather than on a volcanic high. Using a geochemical approach, Mounji *et al.* (1998), Belka (1998), and Peckmann *et al.* (1999) concluded that the mounds were formed by hydrothermal venting on sea floor.

Setting

The carbonate mounds of the Tafilalt are mainly confined to the Hamar Laghdad massif, a small mountain range 15 km southeast of Erfoud (Figs. 9 and 10). Mounds are also reported from Rass el Kebar, a locality a few kilometers south of Jorf (Fig. 10), but, there, the massive limestone bodies of mound lithology are demonstrably olistolites (Wendt, 1993; Mounji, 1999). At Hamar Laghdad, the carbonate mounds are confined to a 0.5 by 3.5 km area, above a volcanic high where as many as 48 individual mounds were recorded (Brachert's *et al.*, 1992, mapping; Fig. 13 herein). The 100 meter-thick pile of calc-alkaline basalt was emplaced during Lochkovian time (earliest Devonian) above a very thick shale-dominated Ordovician-Silurian succession. The upper surface of the volcanic succession was first colonized during Pragian to early Emsian time by crinoids that left a thick cover (up to 180 m in places) of crinoid sands and gravels (Fig. 14). The mounds and the intermound fine-grained limestones developed on top of the crinoid beds, during Emsian time, and were buried by Emsian siliciclastic-rich mud.

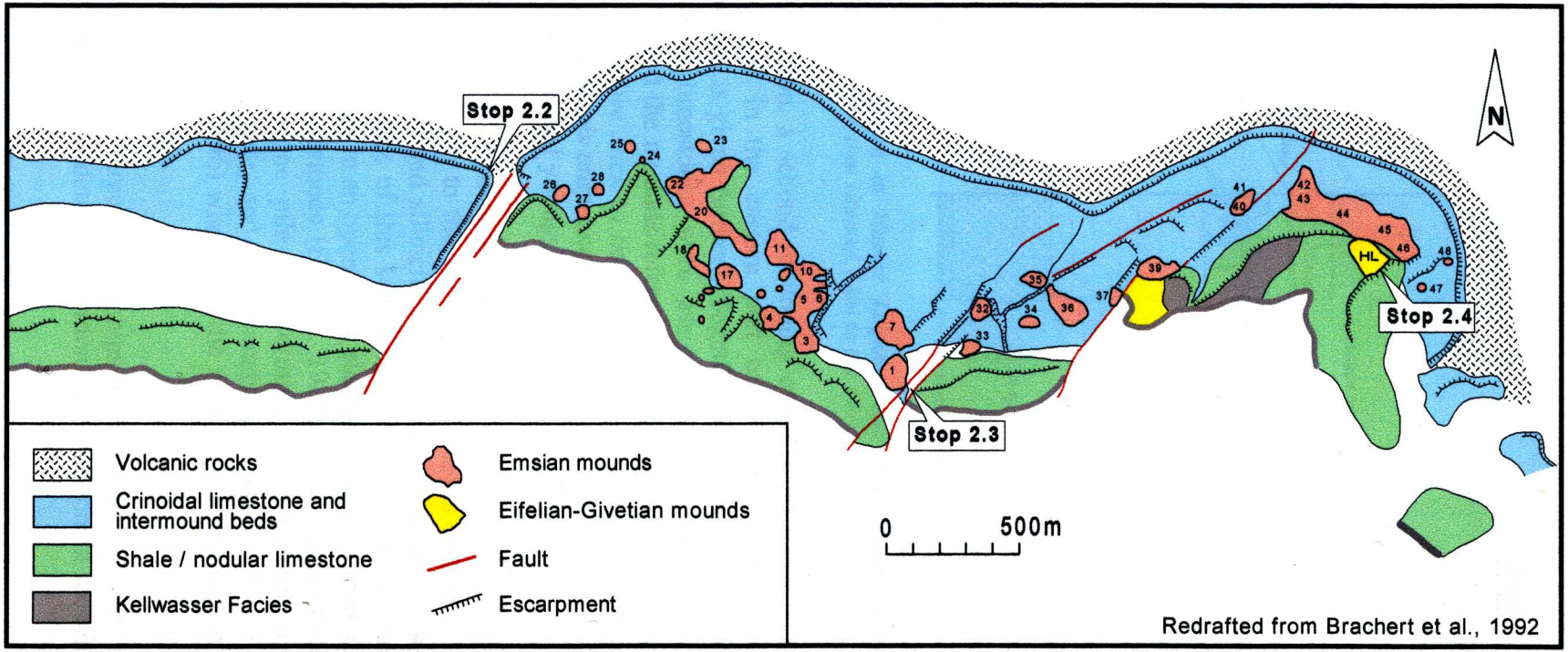

Figure 13 - Map of Hamar Laghdad massif showing mound distribution. *From T.C. Brachert and M.M. Joachimsky in Brachert et al. (1992). Mound numbers are those of Brachert et al. (1992). HL is Hollard mound.*

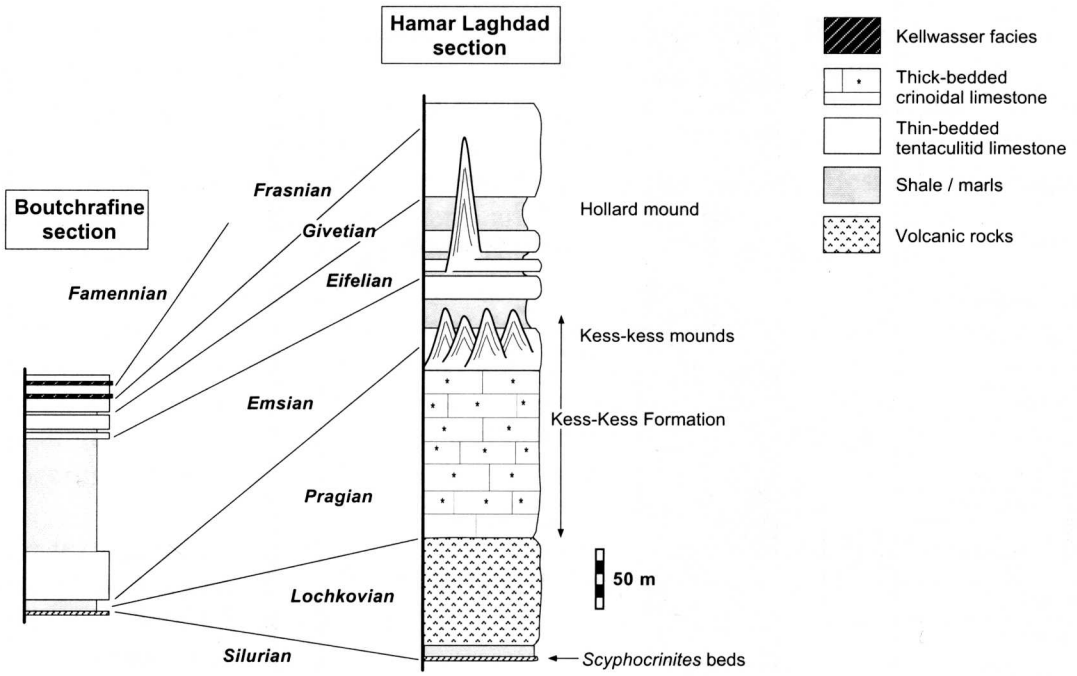

Figure 14 - Facies succession at Hamar Laghdad massif and correlation with the neighbouring Boutchrafine section situated 7 km to the west.

Higher in the succession, a second mounding event is represented by the Eifelian-Givetian Hollard mound in the eastern part of Hamar Laghdad (description and discussion of that mound is given further). Together, the crinoid sole and the overlying mound and intermound limestones were assigned to the Kess-Kess Formation by Brachert *et al.* (1992), and the mounds referred to as the kess-kess mounds (Fig. 14). *In order to avoid confusion, we stick to this practice here, and keep the term Kess-Kess mounds for the Emsian mounds only*, excluding for instance the Hollard mound which is composed of basal kess-kess and younger beds.

The coeval neighboring Lochkovian-Emsian sedimentary pile, as represented by the Boutchrafine section some 7 km to the west, is a continuous sequence of well-bedded mixed fine-grained limestones and siliciclastics that lacks volcanic rocks, crinoid beds and mounds (Fig. 14). Biofacies of this sequence is characterized by tentaculitids and goniatites indicating deposition in an open outer platformal environment deeper than that of the crinoid and mound limestones (Hollard, 1981), which suggests that the Hamar Laghdad volcanic and limestone pile was forming a topographic high during the development of the crinoid sole, and the mounds and associated coeval limestones, contrary to Montenat *et al.* (1996) who place the mound development in a grabben-like setting.

To help better understand the age relationships in the Tafilalt, Figure 15 prepared by Professor O.H. Walliser presents detailed zonation of the Devonian sequence.

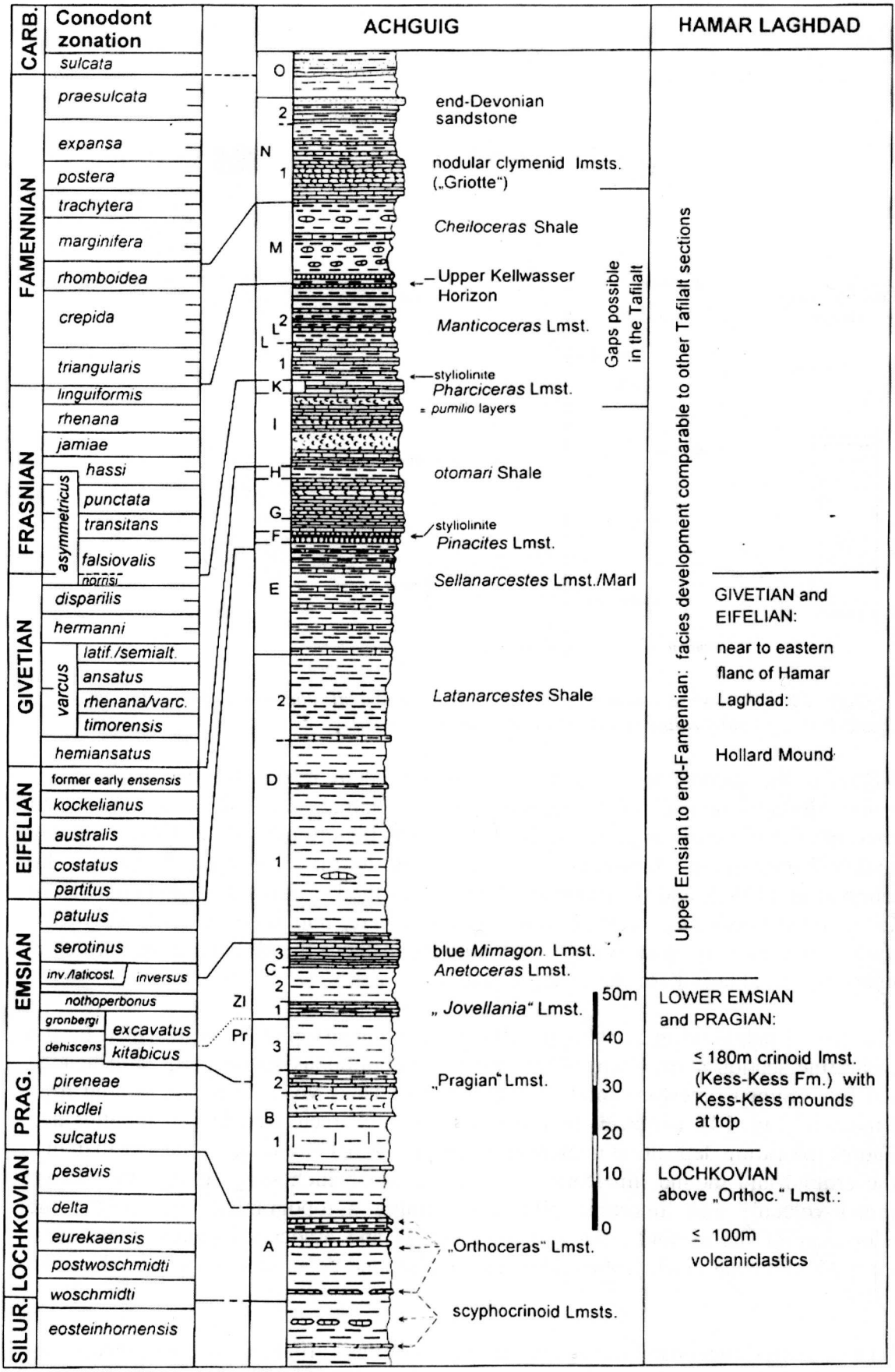

Figure 15 - Devonian sequence zonation of the Tafilalt. *From O.H. Walliser (unpublished).*

Crinoid sole

This unit on top of the volcanic pedestal is composed of medium to thick-bedded crinoid limestone. The lowest limestone beds contain volcanic material in the form of clasts and fine-grained matrix, but a few meters above the base of the unit, it is pure limestone. The bulk of this limestone is composed of sand to fine gravel-sized crinoid ossicles, mostly disarticulated, but locally still forming stems. Besides the dominant crinoid bioclasts, the limestone contents articulated and disarticulated brachiopod shells, trilobite fragments, three types of bryozoans (broken and unbroken fenestrate bryozoans, ramose bryozoans, encrusting bryozoans on brachiopod shells), and coral fragments (Thamnoporids, Favositids). There are also a few beds rich in orthoceratids. In places, these are condensed beds with ferruginous encrustation pointing to periods of marked decrease in sedimentation rate. No algae were observed. Although ubiquitous, tentaculitids are much less abundant than in the mound and intermound facies, except in the uppermost meters where they become abundant.

The texture of the limestone oscillates between grainstone and packstone. The more common lithology is a packstone-grainstone (partly packstone, partly grainstone) formed by infiltration of lime mud into a clean sand or gravel as demonstrated by the numerous geopetal structures.

In short, the crinoid sole is a well-bedded crinoid-brachiopod-bryozoan-trilobite packstone-grainstone very different from the overlying mound and intermound tentaculitid-coral mudstone-wackestone.

Transition beds

Between the crinoid sole unit and the actual mound and intermound unit, there is a few meter-thick well-bedded transition zone composed of interbedded tentaculitid and tiny bioclast mudstone-wackestone with a few coral bioclasts (auloporids, thamnoporids), crinoid wackestone-packstone, and rugose coral and orthoceratid beds. Sheet-crack-like structures (horizontal cracks), filled with isopachous cement crusts and infiltrated mud are common in the muddy limestones of this transition unit.

Mound and intermound assemblage

The mound and intermound facies assemblage makes up the upper part of the Kess-Kess Formation. The following description relies on Brachert *et al.* (1992) and our own investigation.

Architecture

The peculiar cone-shaped kess-kess carbonate mounds set apart all other Paleozoic carbonate mounds, mainly due to their shape and their occurrence in a cluster (Fig. 16A).

This unique architecture constitutes a first constraint in our understanding of the origin of these mounds.

The mounds are cone-shaped, subcircular to sub-elliptical in cross-section, and commonly reach up to 50 meter-high (Fig. 16B). Their flanks are steeply dipping, ranging between 35° and 60°, more commonly *circa* 50° (see Brachert *et al.* 1992, for a comprehensive account on height and slope variations of the cones). The distance between individual mounds varies from 10's meters to a few 100's meters. The mounds are not all at the same level within the mound and intermound unit, but occur at different levels. The intermound limestones are flat lying and well-bedded. The internal structure of the mounds is not readily observed since very few mounds are cross-cut by erosion. On the few examples observed, it appears that the inner core is a massive limestone, whereas the overlying outer layers are bedded parallel to the flank surface (Figs. 17 and 18A). The relationship between mound and intermound beds is of four types, the first situation appearing to be the most frequent:

- the intermound beds are flat lying extension of the steeply dipping mound flank beds (Fig. 18B and 19A);
- the mound beds are downlapping on intermound beds, which implies they are pinching out;
- the intermound beds are onlapping the mound beds (Fig. 17B);
- the more massive thicker mound limestone passes laterally to well-bedded thinner intermound limestones (Fig. 19B).

No current or wave-driven sedimentary structures were recorded in the mound or intermound limestones. The mound outermost surface is smooth (Fig. 19A), and no paleokarst or erosional features were observed on it.

Lithology and fauna

Generally speaking, the mound and intermound facies are compositionally similar: lime mudstone to wackestone, with a scarce coral fauna consisting mainly of auloporid, thamnoporid and favositid corals, and an accessory fauna of crinoids, trilobites, tentaculitids, and brachiopods. The mud between the corals, represented in thin-section by microspar, contains a fine-grained skeletal fraction (up to 30%) of tentaculitids, delicate ostracode shells, gastropods, and other tiny skeletal pieces (echinoderms, ostracodes, tentaculitids) and unidentifiable microbioclasts (see Fig. 21 for typical aspects of mound microfacies). In places, lenses of tentaculitid packstone and trilobite wackestone are observed. The scarcity of potential frame builders (commonly less than 10% corals/rock volume) strongly suggests that there was no skeletal organism involved in mound accretion. In addition, we found no evidence of cryptic binders or builders such as microbes or sponges. There are stromatactis-like spar bodies and spar-filled sheet cracks in both mound and intermound limestones. Several Neptunian dikes, few millimeters to several centimeters wide, filled with isopachous crusts of marine cement and a small amount of infiltrated mud, crosscut the mound and intermound limestones, as well as the underlying crinoidal limestones. They are dated as Emsian to Famennian by conodont content of infiltrated sediments (Brachert *et al.*, 1992; Belka, 1998).

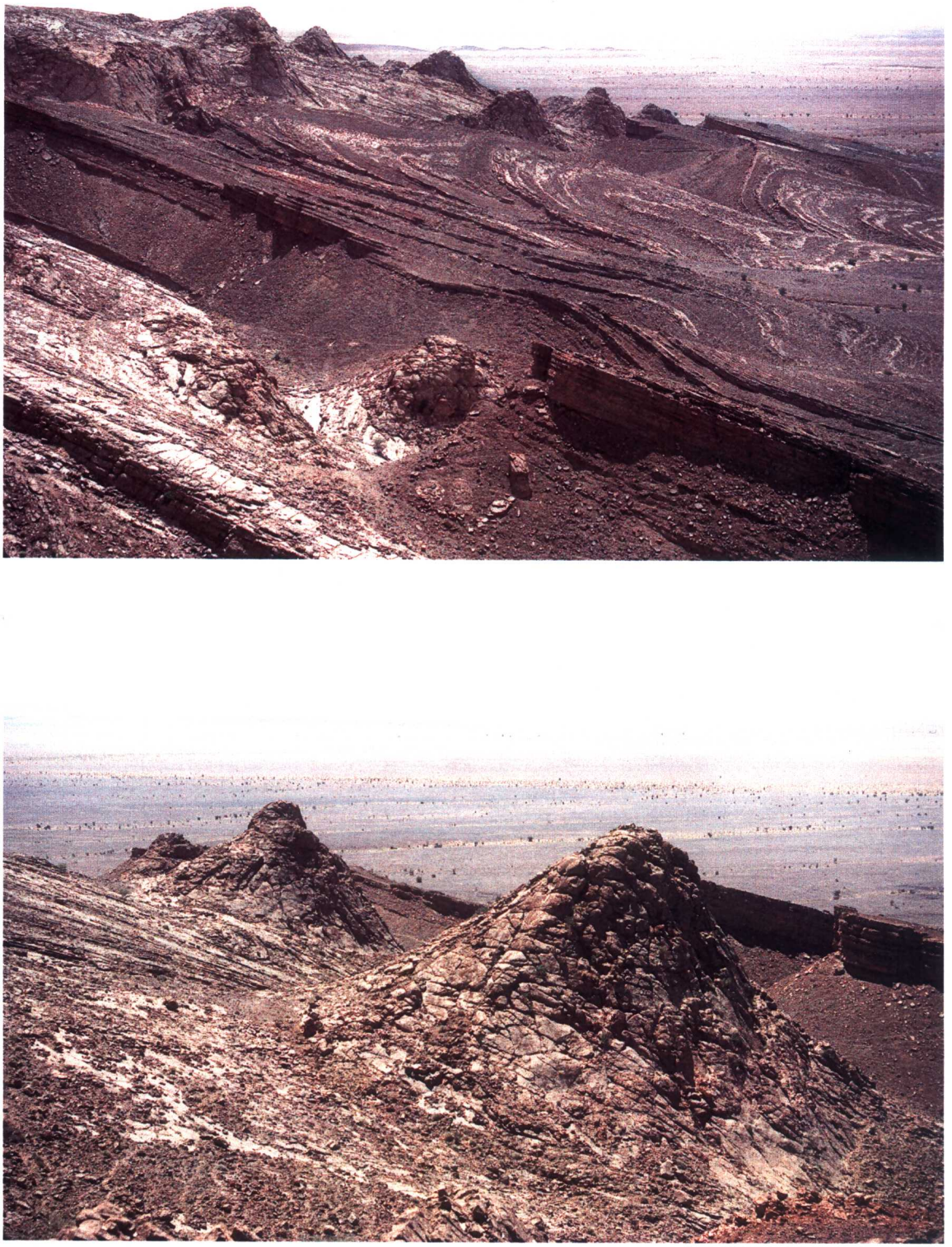

Figure 16 - The kess-kess mounds of Hamar Laghdad. *(A) Viewed from Stop 2.2. Note mounds in the foreground partly buried under Emsian-Eifelian shale and marls; they are at the same stratigraphic level as those in the background. (B) Typical cone-shape of the mounds.*

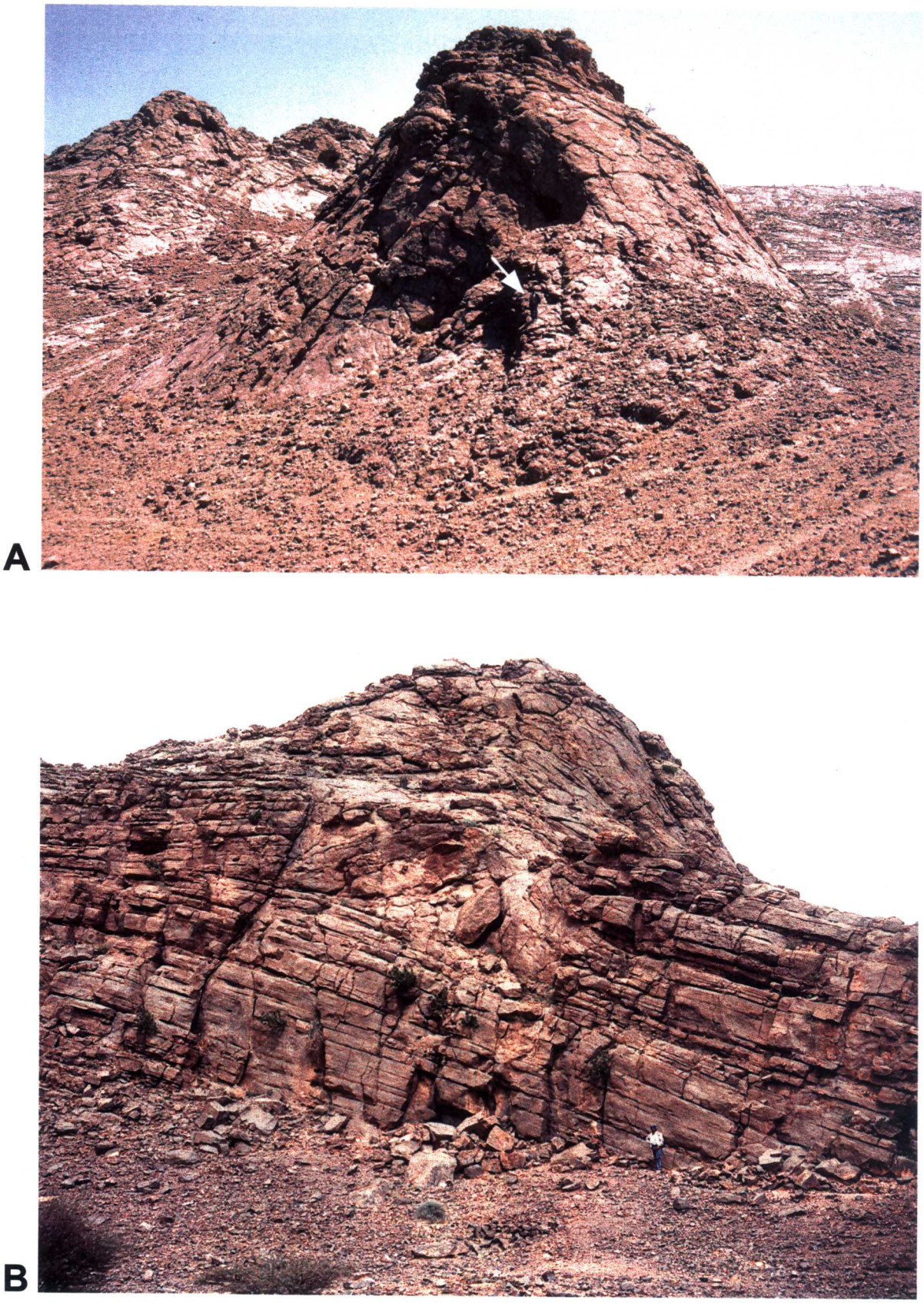

Figure 17 - The kess-kess mounds of Hamar Laghdad. *(A) Mound #3, with partly exposed core. Person for scale (arrow). (B) mound #33 showing intermound beds unlapping mound beds.*

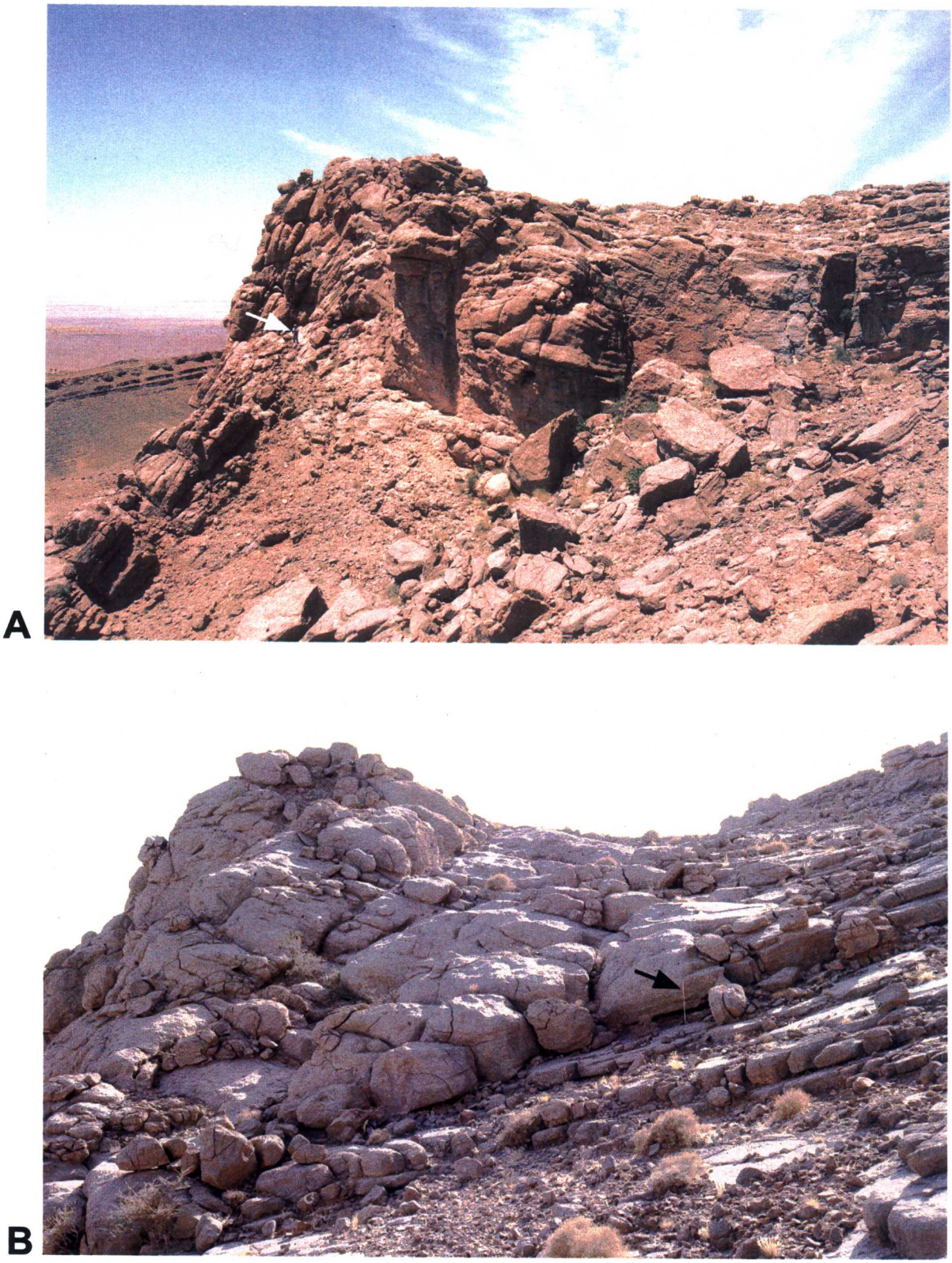

Figure 18 - The kess-kess mounds of Hamar Laghdad. *(A) Mound #36 showing massive inner core compared to well-bedded outer layers. Person for scale (arrow). (B) Mound flanks passing laterally to flat lying intermound beds. One meter scale (arrow).*

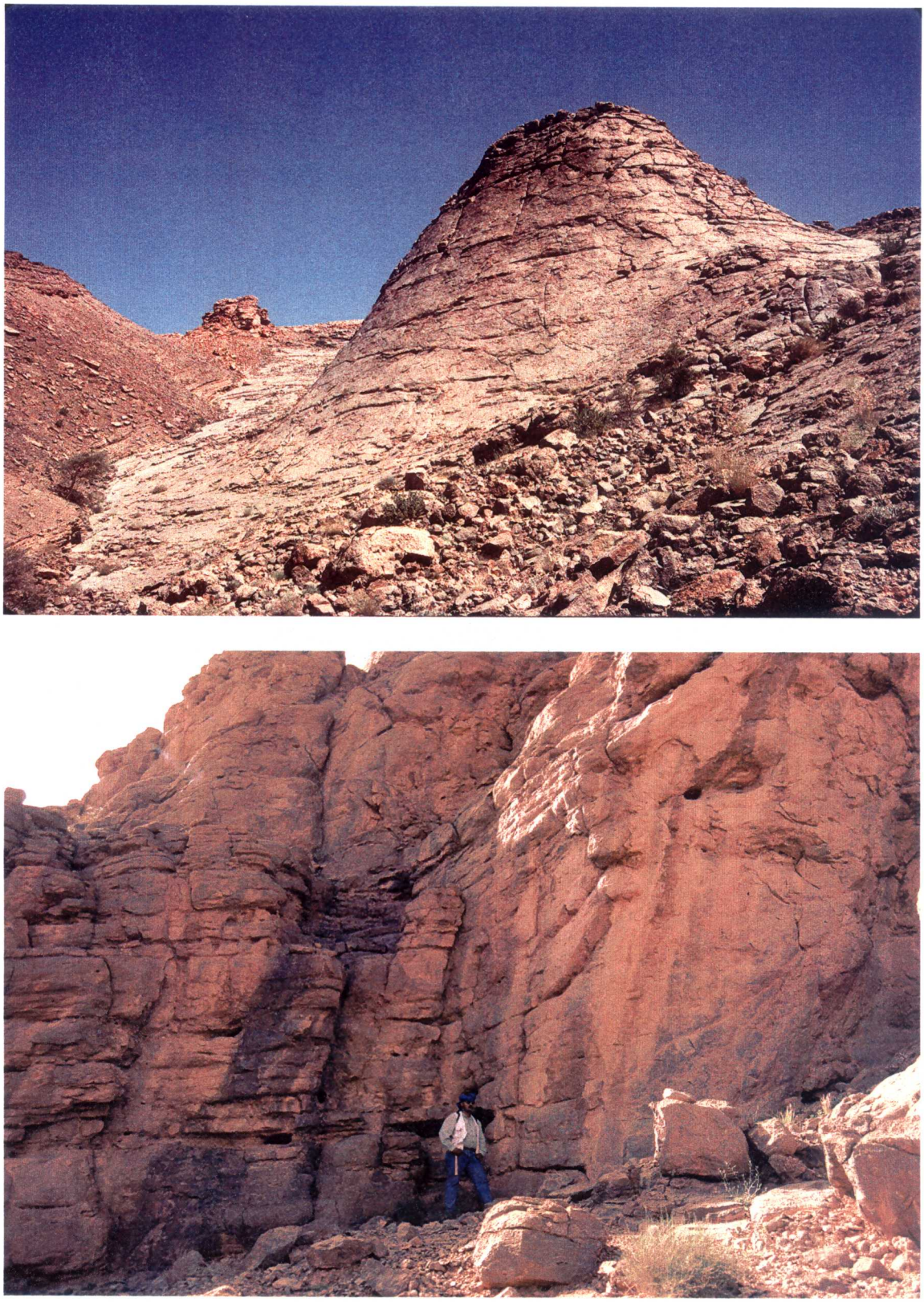

Figure 19 - The kess-kess mounds of Hamar Laghdad. *(A) Mound #22 , with smooth outer surface. (B) Interbedded intermound layers with massive mound core at edge of mound #7.*

Figure 20 – Typical muddy microfacies of the kess-kess mounds of Hamar Laghdad.

(A) Microbioclastic lime mudstone with small-scale stromatactoid cavity filled with isopachous inclusion-rich calcite cement followed by blocky inclusion-poor calcite. Note the polymud nature of the microfacies. Sample 93HL-62, mound #1.

(B) Microbioclastic mudstone with larger crinoid and auloporid bioclasts. Sample 93HL-61, mound #1.

(C) Polymud at base of a stromatactoid cavity with isopachous crust of fibrous-like cement on walls of the cavity and around auloporid skeletons. Sample 93HL-58, mound #1.

(D) Coral and microbioclast mudstone-wackestone at base of a stromatactoid cavity into which the auloporid skeletons are coated with isopachous crusts of fibrous-like cement. Sample 92EF-7, mound #1.

(E) Stromatactoid cavity with patches of clear inclusion-free calcite surrounded by inclusion-rich fibrous-like calcite. Under CL (see Figure 21), this clear calcite is non-luminescent while surrounding cement has a composite dull luminescence. Sample 92EF-8, mound #1.

All figures are scans of thin-sections; (A-C) stained (Dickson's method), (D-E) unstained. Bar scale is 1 cm on all.

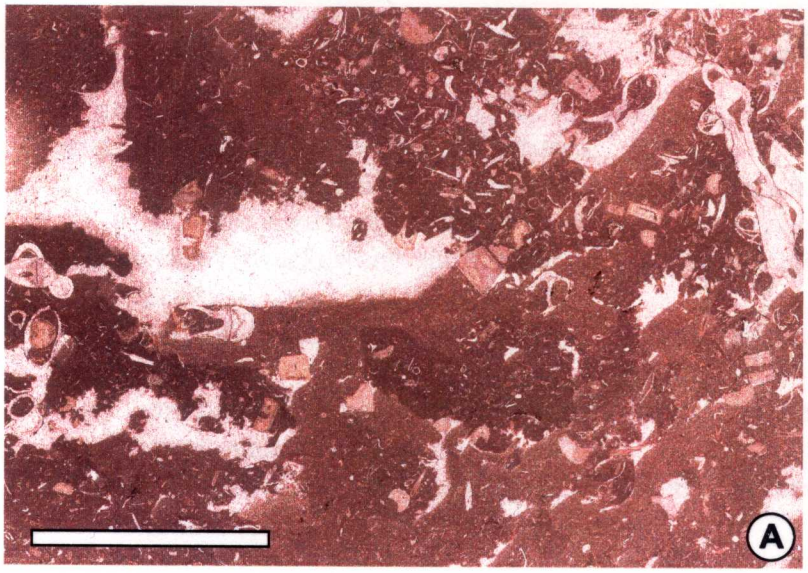
A

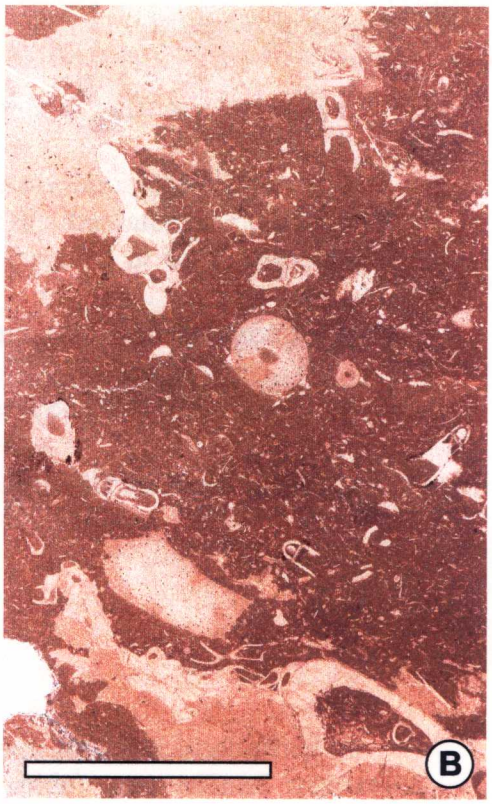
B

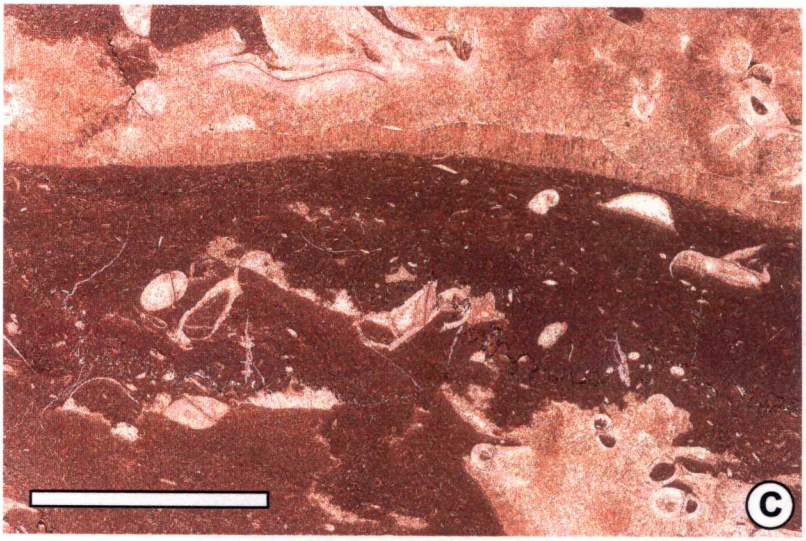
C

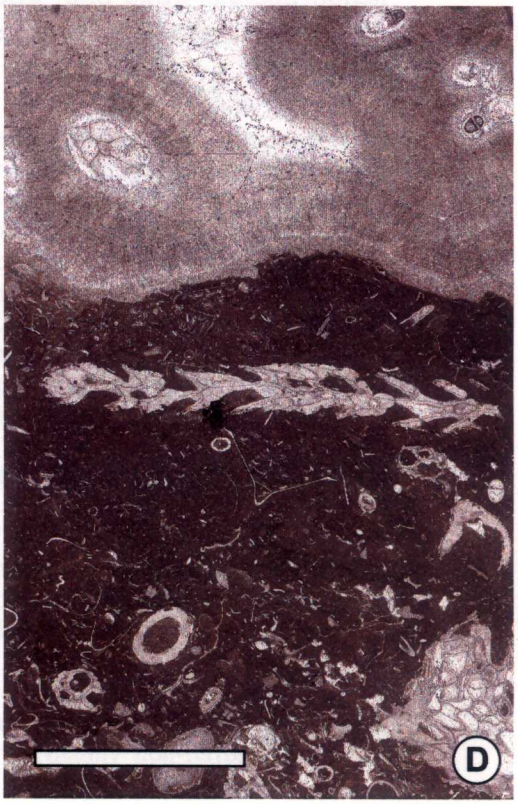
D

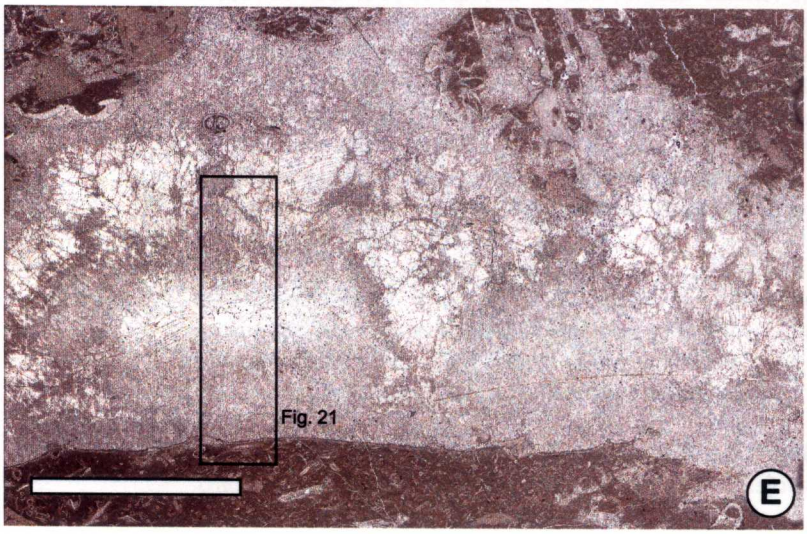
Fig. 21
E

In the finer details, Brachert *et al.* (1992) recorded a number of differences between the mound and the intermound limestones:

- the amount of lime mud is higher in mounds than in the intermound limestones, so that mudstones are frequent in the mounds and rare in the intermound facies, whereas wackestone and packstone textures are more frequent in the intermound facies;
- auloporid corals are distinctly more common in the mound than in the intermound facies;
- horizontal elongated spar-cemented cracks (sheet cracks-like) are mainly an intermound facies feature;
- trilobites (highly diverse), tentaculitids and ostracodes are more frequent in the mound facies.

Diagenesis

Cement stratigraphy

Cement succession for the mound and intermound limestones was first established on stained thin-sections (alizarin red S – potassium ferricyanide) and refined under cathodoluminescence (CL). Except for uncommon dolomitisation localised near the main faults, all cements are low-magnesium calcite (LMC). Three main cement phases were observed in mm- to cm-sized various kinds of cavities : intra- and extra-skeletal pores, stromatactis-like cavities, shelter cavities, Neptunian fissures, horizontal cracks, etc. (Fig. 21).

Cement C1 : 1 to 5 mm-thick isopachous crusts composed of a fine mosaic of composite luminescence more probably resulting from alteration of a non-luminescent fibrous and/or bladed spar cement (cement C1a), ending with scalenohedral non-luminescent crystals. Under plane-polarized light, this cement is inclusion-rich and has a fibrous aspect (Fig. 19D). Staining indicates that it is composed of non-ferroan calcite. It occurs mainly in stromatactoid and shelter cavities, and in Neptunian dikes and sheet-cracks. In places, patches of clear, non-ferroan and inclusion-free cement, occur within the isopachous fibrous-like cement C1a. This clear cement, referred to as C1b (Fig. 21), is non-luminescent and is locally altered by inclusion-rich, composite-luminescent cement. This situation is very similar to that described by Bourque and Raymond (1994) in Silurian stromatactis of Québec. This clear cement was considered to represent unaltered pristine cement.
Based on luminescence of altered zones, it appears that alteration was coeval to precipitation of cements C2 and C3.

Cement C2 : thin layer (<500 µm) of brigh-luminescent spar cement, or of thinly zoned bright-luminescent/non-luminescent cement, on scalenohedral non-luminescent cement of phase C1, observed under CL only. Under plane-polarized light, this is a non-ferroan, inclusion-free calcite, undistinguishable from calcite of cement C3.

Cement C3 : thinly zoned, light and dark dull-luminescent spar cement, filling the remaining pore space. Under plane-polarized light, this cement is inclusion-free, mainly non-ferroan, becoming ferroan toward the very center of cavities (Fig. 21E).

Besides these three cement phases in mm- to cm-sized cavities, there is also cements related to lithification of the mud that formed the bulk of the mound and intermound limestones. This mud is now represented by microspar whose origin is not readily understood. Since the pioneer work of Bathurst (1958, 1975) and Folk (1965) who considered that lime mud was lithified mainly during burial diagenesis by aggrading neomorphism that « digests » primary particles, more and more examples are described where muds were early cemented and where microspar is not the result of aggrading neomorphism (*sensu* Folk, 1965) but of cementation of the primary material (*e.g.*, Lasemi and Sandberg, 1984; Lasemi *et al.*, 1990; Munnecke *et al.*, 1997).

Under plane-polarized light, the kess-kess microspar crystals are in the range of 10-20 µm. When viewed under CL, the microspar is made up of non-luminescent particles, one quarter to half the size of the microspar crystals, embedded in a luminescent cement. The particle distribution with respect to the cement varies from closely to loosely packed. Moreover, SEM observations on slighly etched polished surface (P.-A. Bourque, work in progress) show that the microspar crystals (4-20 µm in size) contain smaller 1-2 µm equant sub-crystals, more likely representing the primary mud particles. We interpret this situation as a representation of the primary mud cemented by early cement, possibly coeval to bright-luminescent cement C2.

Isotope geochemistry and significance

We analyzed 90 samples from the kess-kess mound and intermound limestones for C and O stable isotope ratios; the samples were from cements C1 and C3 (the C2 was too thin to be separated mechanically), the microspar forming the bulk of the mound and intermound finely crystalline limestone, including the internally sedimented lime mud in various types of cavities. Cements C1a and C1b were not considered separately. Results are given on Fig. 22).

After analysis of stable isotopes, we analyzed also splits of 23 samples weighing from 2 to 4 mg for their $^{87}Sr/^{86}Sr$ ratios in both cement C1 and the microspar. Strontium isotopic ratios were determined at the Geological Institute of the Ruhr University-Bochum, Germany, where the data were normalized to $^{86}Sr/^{88}Sr$ of 0.1194. The precision (1σ) for single measurement was always better than 15×10^{-6}. The NBS 987 standard gave average values of 0.71023 ± 13 (2σ). The $^{87}Sr/^{86}Sr$ values (Fig. 23) for the non luminescent early marine cements (0.707934- 0.709392) are in or near the Devonian marine range (*e.g.*, Burke *et al.*, 1982), whereas the ratios for the finely crystalline material (0.708515-0.709656) indicate a more radiogenic Sr source.

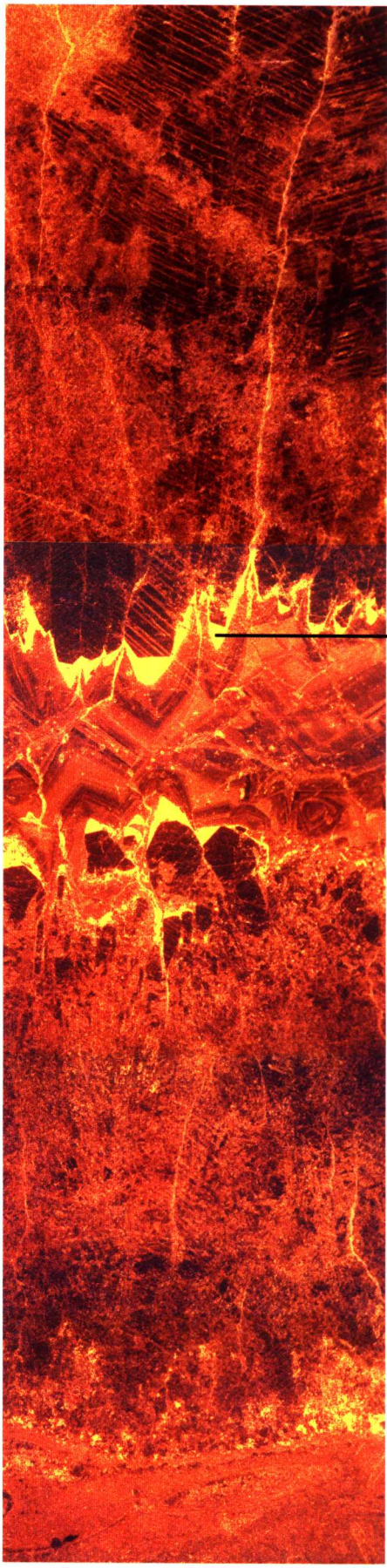

Figure 21 - Cement succession in kess-kess mound limestone cavities as seen under cathodoluminescence. *Position on Figure 20. Sample 92EF-8, mound #1.*

Cement C1b
Non-luminescent bladed spar, partly altered

Cement C2
Thin crust of bright-luminescent cement

Cement C3
Large subequant, thinly zoned dull luminescent spar

Cement C1a
Fine mosaic cement considered to result from alteration of non-luminescent fibrous to bladed spar, ending with scalenohedral crystals

Fossiliferous mound microspar

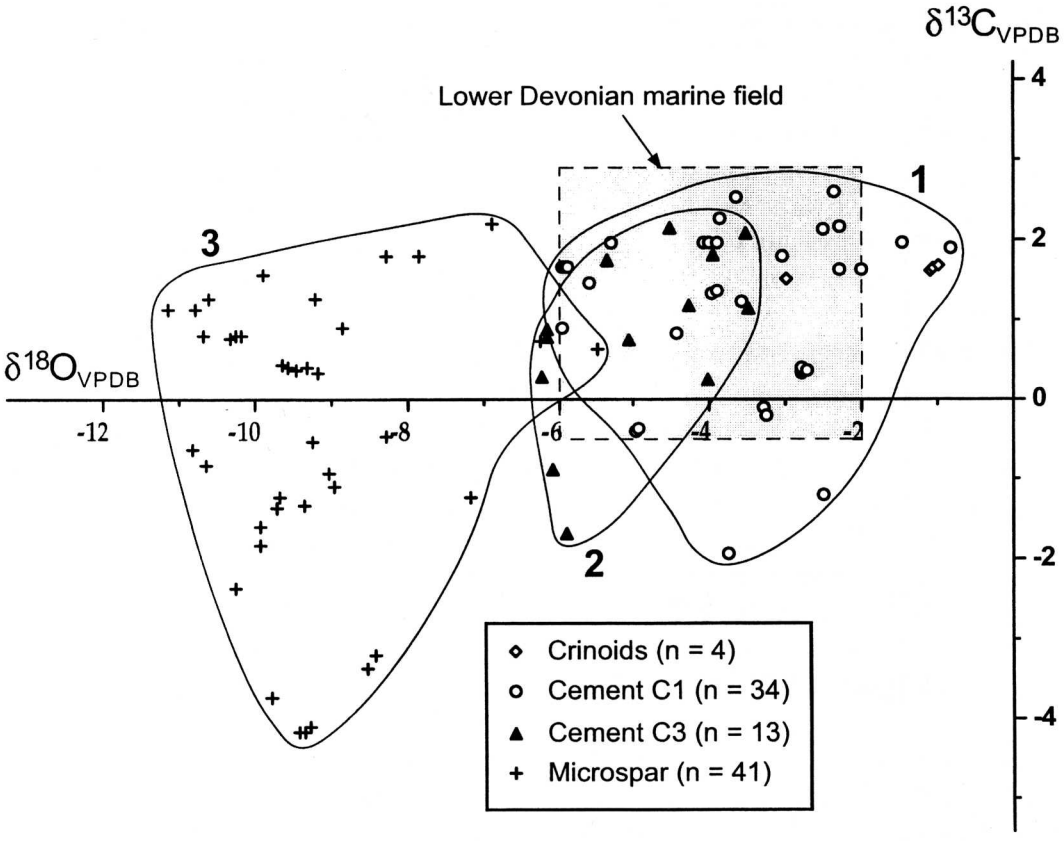

Figure 22 – Cross plot of $\delta^{18}O$ and $\delta^{13}C$ for cement phases C1, C3 and microspar (including finely crystalline material of matrix and mud infiltrated in cavities) of mound and intermound limestones. *Early Devonian seawater field, based on brachiopod shells (Lohmann and Walker, 1989; Popp et al., 1986; Lavoie, 1993 ; Veizer et al., 1997). VPDB is Vienna Peedee belemnite standard.*

Most values of cement C1 (average of $\delta^{18}O_{VPDB}$ = –3.7‰ and $\delta^{13}C_{VPDB}$ = +1,1‰ ; Fig. 21, field 1) are interpreted to indicate marine cementation because the values are in agreement with published values for Lower Devonian carbonates that are thought to have been in equilibrium with their respective seawater (Lohmann and Walker, 1989; Popp *et al.*, 1986; Lavoie, 1993 ; Veizer *et al.*, 1997). Cement C3 field (Fig. 22, field 3) partly overlaps that of cement C1 ; it has similar $\delta^{13}C_{VPDB}$ values (average of +0,8‰), but slightly lower $\delta^{18}O_{VPDB}$ (average of –5,0‰). This means that cement C3 most probably precipitated in the marine to very shallow burial environment (10's of meters). The luminescence of the cement C1 alteration suggests the alteration took place during precipitation of C2 and C3 (see above). This may explain the extension of cement C1 values into C3 field ; that would indicate we analyzed more or less altered marine cements.

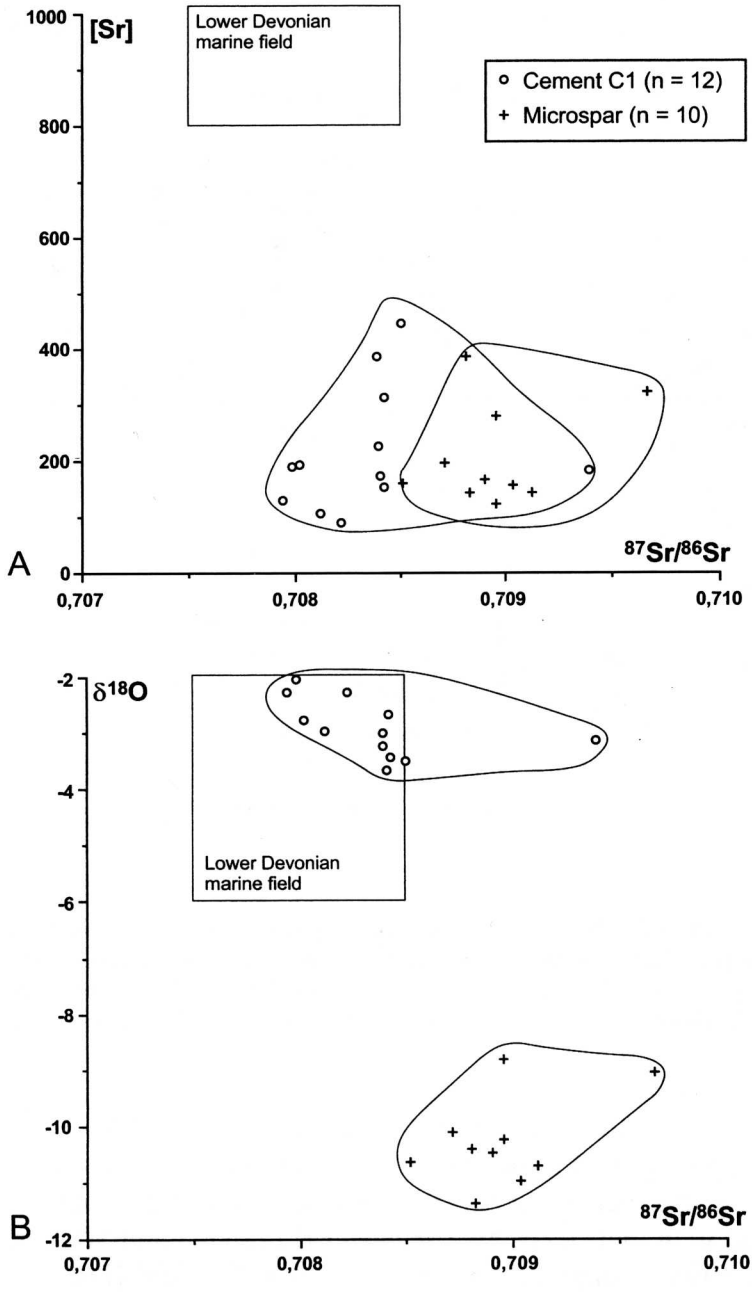

Figure 23 – Cross plot of $^{87}Sr/^{86}Sr$ and $\delta^{18}O$ for cement phase C1 and microspar, from split samples for C and O isotopic analyses, for both Emsian kess-kess mounds and the Hollard mound. *Marine range is from Burke et al. (1982). VPDB is Vienna Peedee belemnite standard. Symbols are same as in Figure 22.*

In contrast, the microspar that makes up the bulk of the mound and intermound limestone, and the internally sedimented mud between crusts of early marine cements have significantly lower $\delta^{18}O_{VPDB}$ values (average of –9,3‰), whereas their $\delta^{13}C_{VPDB}$ values are similar to those of early marine cements (average of –0,5‰).

The low $\delta^{18}O$ values of the microspar and the internally sedimented mud may indicate either a primary signal due to precipitation from hydrothermal waters or a secondary origin due to stabilization of the mud by meteoric waters. However, alteration by meteoric waters is unlikely because the early marine cements that postdate the microspar and the internally sedimented muds are not depleted in ^{18}O or enriched in ^{87}Sr. Moreover, mound accretion and early cementation occurred in a deep-water environment (Brachert *et al.* 1992; and our own interpretation). This excludes the possibility of meteoric alteration because there is no evidence of a drastic sea-level fall following mound accretion or evidence of meteoric diagenesis. We conclude, therefore, that the microspar and the internally sedimented mud were precipitated from hydrothermal fluids.

Carbonates precipitated from hydrothermal fluids composed of a mixture of fluids derived from a deep-seated magma source and seawater, or fluids derived from the interaction of sea water and a young basalt pile, would have yielded a $^{87}Sr/^{86}Sr$ ratio less radiogenic than carbonates precipitated exclusively from seawater. The more radiogenic ratio of the microspar and internally sedimented mud of the kess-kess mounds, as compared to that of the marine cements, suggests that fluids derived mainly from recycled seawater that reacted with the Rb-bearing siliciclastic-limestone sediment pile.

The temperature of the hydrothermal fluid from which the microspar and the internally sedimented mud precipitated can be calculated by using the isotopic equilibrium equation of O'Neil *et al.* (1969), assuming that the parent fluid is heated Devonian seawater. The local $\delta^{18}O$ (SMOW, standard mean ocean water) isotopic signal of the Devonian seawater is estimated to range from -5.0‰ to -3.4‰, on the basis of $\delta^{18}O$ value of -3.0‰ to -1.5‰ (VPDB) obtained for the non-luminescent marine cements and on an assumed ambient seawater temperature of 10 °C owing to the paleosetting of the kess-kess mounds (paleolatitude of 35°S; water depth of 200-300 m). These values, together with the $\delta^{18}O$ of the microspar (-11,1‰ to –5,5‰), enable us to compute a minimal temperature range for the hydrothermal water between 31 and 56° C. These values constitute the low end member of a potential temperature range. Waters of higher salinity, like formation waters for instance, would give a higher precipitation temperature for the microspar.

Interpretation

Brachert's et al. (1992) interpretation

Based on their lithological and faunal analysis, Brachert *et al.* (1992) concluded that these mounds developed as "accumulations of more parautochthonous bioclastic sediments within the mounds, (...) caused by a self-sustaining system of hydrologic piling of sediment triggered by storms, preferred settlement of organisms upon these piles, producing bioclastic sediments and coeval biocementation of the growing mound flanks".

Belka's (1998) interpretation

Two main proposals were formulated by Belka (1998).

1) The mounds are spatially related to faults that served as conduits for hydrothermal fluids responsible for mound carbonate precipitation.

Based on structural analysis of the Hamar Laghdad massif (field measurements and aerial photo interpretation), Belka (1998) recognized three systems of faults (his Fig. 7, reproduced herein as Fig. 24) :

- a radial fault system of steeply dipping normal faults,
- a tangential fault system,
- a youngest fault system striking at N40°E and cutting across the Carboniferous.

The last is considered to be Variscan whereas the two others are Early Devonian. Belka's observation goes as follows : « The majority of mounds developed over cross-points of radial and tangential faults. These faults can easily be recognized within the intermound facies, where associated slumping phenomena attest to their synsedimentary character. Toward the mound, close to their bases, however, faults usually vanish within the mound carbonates and cannot be traced across the mounds. Because most faults continue generally on the opposite side of the mounds, their probable course under the mound structure can be inferred. It appears to correspond well with the elongation of mounds and the position of the growth centers. » ... « The network composed of radial and tangential faults resembles a system of thermally induced joints (...) known from laccolithic intrusions (...) and a fault pattern of domed strata above salt diapirs or uplifted intrusives » (p. 372).

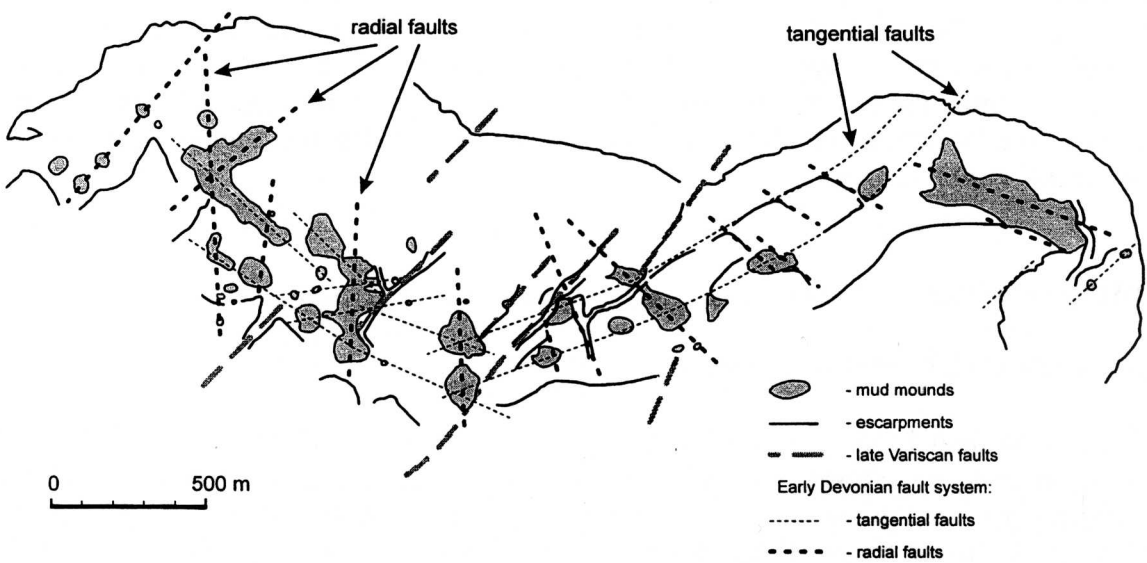

Figure 24 – Relationship of mounds and fault network at Hamar Laghdad, Tafilalt. *From Belka (1998, Fig. 7)*

Belka (1998) therefore concluded that the mounds « show a distinct trend in their spatial distribution, following a network of radial and tangential faults that were formed during Emsian times as a result of the doming caused by the underlying subvolcanic laccolithic intrusion » and that « the radial and tangential faults served as conduits for ascending hydrothermal fluids ... This hydrothermal activity persisted episodically until the Famennian, but only during the Emsian were the vents the sites of extensive carbonate production » (p. 376).

2) Mound carbonates were precipitated from fluids with a thermogenic methane component, involving aerobic bacterial oxidation of methane.

Based on the fact that « the bulk of samples from the mounds and the neptunian dikes are strongly depleted in ^{13}C » (his Fig. 11, reproduced herein as Fig. 25), Belka (1998) concluded that « thermogenic methane derived from the underlying basaltic intrusive » contributed, at least partly, to the fluids that precipitated the mound carbonates, and he therefore favored « aerobic bacterial oxidation of methane as a main process driving the carbonate precipitation and the rapid lithification of the mounds ».

Comments on Belka's (1998) isotope geochemistry.

Belka (1998) analyzed 29 samples for carbon and oxygen stable isotope ratios, from « mound and intermound facies, the calcite cements, and microspar matrix of dike infills. In sum, five Frasnian neptunian dikes and their host rocks were sampled ». From his Fig. 11 (herein Fig. 25), the breakdown is 5 samples from the mounds, 4 from the intermound, 2 from brachiopods, and 18 from (Frasnian ?) Neptunian dikes. Out of the 17 values depleted in ^{13}C (below -8‰), 11 are from the dikes.

Neptunian dikes of the Hamar Laghdad massif are all younger than the Emsian kess-kess mounds (Brachert *et al.*, 1992 ; Belka, 1998 ; Peckmann *et al.*, 1999). They are dated by mean of conodonts they contain. There is four groups of Neptunian dikes (Belka, 1998) : a) late Emsian-early Eifelian ; b) late Givetian – early Frasnian ; c) late Frasnian – middle Famennian (Upper *gigas* Zone – Upper *crepida* Zone) ; d) later Famennian (Lower *marginifera* Zone). We hardly found rationale behind using isotopic signature of dike material which is younger than the mounds and intermound to interpret origin of the mound bulk material.

Moreover, there is uncertainty as to the age of the mound material that has been analyzed. Clearly, Belka (1998) considered that all mounds at Hamar Laghdad, including the Hollard mound, formed during the Emsian. It is known however that at least one mound, the Hollard mound which is illustrated by Belka (1998, Fig. 9) and taken as an example in the text, is at least in part younger (Eifelian-Givetian) (Töneböhn, 1991 ; Brachert *et al.*, 1992 ; Peckmann *et al.*, 1999). Mounji *et al.*, (1998) and Peckmann *et al.* (1999) have shown the necessity to deal with the Hollard mound separately from the Emsian kess-kess mounds. For instance, among the 230 carbon and oxygen isotopic analyses we did on the Hamar Laghdad mounds (Mounji *et al.*, 1998 ; this guidebook,

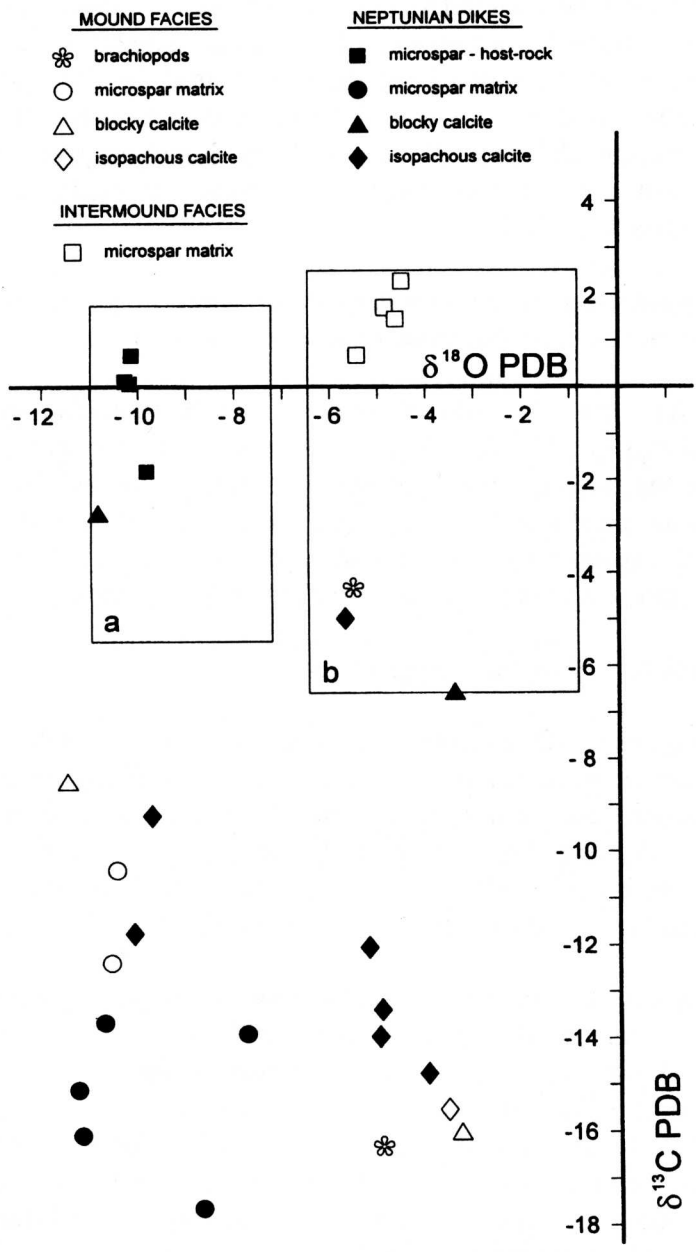

Figure 25 – Carbon and oxygen isotope values measured on calcite samples from the Hamar Laghdad. *Boxes indicate $\delta^{13}C$ and $\delta^{18}O$ ranges of finely crystalline carbonate matrix of the mounds (a) and of nonluminescent cements in crinoidal limestones underlying the mounds and in stromatactis cavities (b) as reported by Mounji et al (1996). Figure and citation from Belka (1998, Fig. 11).*

under Hollard mound), only samples from the core of the Hollard mound yielded values strongly depleted in ^{13}C. Obviously,more work is needed to evaluate this situation.

Therefore, we receive with circumspection Belka's conclusion as to the role of bacterial oxidation of methane with respect to the origin of all mounds at Hamar Laghdad.

Mounji, Bourque, Savard's (1998) interpretation

Our data lead us to propose a model that integrates the mound setting, their architecture, and their isotope composition.

On the architectural constraint side, we interpret that the potential builder organisms were too scarce to have controlled mound accretion, and, contrary to Brachert *et al.* (1992), that the steep-sided conical mound shape is very difficult to reconcile with a current or wave-driven accumulation of mud. We rather interpret the origin of the conical shape to be related to hydrothermal venting on the sea floor, although the slight asymetry of the cones may be due to persistent unidirectional currents during venting (Fig. 26). Early marine cementation of the mounds is indicated mainly by the presence of thick early marine cement crusts in all kinds of cavities, including collapse cavities formed locally with flat floors and more or less digitate roofs (stromatactis-like bodies), and to a lesser extent by synsedimentary fracturing of mound and intermound limestones (late Emsian Neptunian fractures). The hard cone and intermound surfaces are interpreted to have provided a suitable substrate for encrusting organisms, particularly the auloporids and other types of corals.

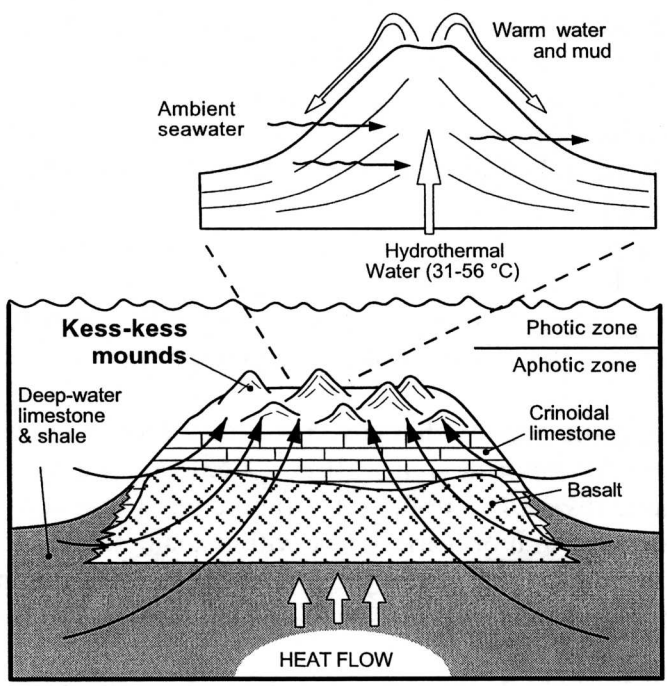

Figure 26 – Integrated model proposed to explain lithology, architecture, and geochemistry of kess-kess conical mounds of Hamar Laghdad massif, Tafilalt. *From Mounji et al. (1998).*

The isotopic signatures of the microspar, as compared to the early marine cements, suggests a sea-floor hydrothermal venting system. Such a system involved precipitation of mud from hydrothermal waters and progressive cementation of mound primary cavities in a deep-water marine environment during cone accretion. We postulate that seawater, or formation waters, infiltrated the sedimentary and volcanic rock pile, was heated and driven upward by thermal flux above the Hamar Lakhdad massif, and precipitated the bulk of the finely crystalline material that forms the mound and intermound limestones (Fig. 26).

Whereas this proposed hydrothermal model for the origin of the kess-kess mounds explains their architecture, setting, and isotope geochemistry, it raises other questions, particularly as to the biotic *vs* abiotic controls on carbonate precipitation, the origin of the thermal flux, and the nature of the plumbing system that brought the fluids to the sea floor.

Whether the carbonate precipitation from hydrothermal fluids was biogenically influenced is a difficult question to answer (*e.g.* Folk, 1994). Microbial communities are known to induce or trigger the $CaCO_3$ precipitation, and many studies of Paleozoic mounds (*e.g.* Monty *et al.*, 1995) have concluded to the determinant role of bacteria in mound genesis. Although a bacterially-mediated precipitation of $CaCO_3$ cannot be ruled out for the kess-kess mounds, we did not find evidence from which to infer such a control, like the typical pelletoidal texture of the mud (the microspar of both the mound and the intermound facies is uniform), or the presence of relics, molds, or forms that can be identified as bacteria, or at least suggest former bacteria. Unfortunately, the isotope geochemistry is of little help in that matter. If we know that carbon isotope fractionation can be influenced by microbial mediation (*e.g.*, Beauchamp and Savard, 1992; and many other papers dealing with chemosynthetic mounds in that special issue of Palaios), but not always (*e.g.*, Reitner *et al.*, 1997), we do not know any published example where oxygen isotope fractionation has been microbially changed. We therefore take for granted that calculation of the precipitation temperatures using $\delta^{18}O$ values can be done with reliability (O'Neil *et al.*, 1969), whether the precipitation was bacterially induced or not.

Although the magmatic activity that gave rise to the Hamar Lakhdad massif appear to be a prime candidate for the heat source, the low temperature hydrothermal convection system may well have resulted from the topographic relief on the sea floor related to the relative buoyancy of a column of warm water within a submarine topographic salient *vis-à-vis* a column of similar height where the top of the column comprises relatively cool sea water (*e.g.* Hartline and Lister, 1981; Noel and Hounslow, 1988).

If the mud cones were built by hydrothermal venting, there should be some sort of central conduit in each mound. Unfortunately, mound preservation is such that most of them are unbroken, without cross sections that expose their interior. Only a few are partly eroded. At best, the apices of several cones exhibit disturbed lime mudstone.

We believe that the kess-kess carbonate mounds are unique. On the basis of their shape, fauna, and isotope geochemistry, they do not resemble other Paleozoic mudmounds, such as the classical Carboniferous Waulsortian mounds (*e.g.*, Lees and Miller, 1985, 1995; Bourque *et al.*, 1995) or the red stromatactis mounds (*e.g.*, Bourque and Boulvain, 1993). They are structures totally different from modern and ancient chemosynthetic hydrothermal- or cold seep-related structures, such as the black smokers (*e.g.*, Rio *et al.*, 1992), the methane seeps of North Sea (Hovland, 1992), or the several examples of ancient chemosynthetic mounds (*e.g.*, Beauchamp and Savard, 1992; and many other papers in that special issue of Palaios). Although the general external shape of the Tepee Buttes described by Kauffman *et al.* (1996) and the kess-kess mounds seems to be the same as exposed today in outcrops, the internal morphology and microbiofacies zoning of the Tepee Buttes, and their low relief above sea floor (hardly higher than a few meters, as compared to tens of meters for the kess-kess) make them quite different from the kess-kess. An example that has some similarity to the Moroccan mounds is the modern nearshore coral reefs of Ambitle Island in the Tabar-Feni arc in New Guinea (Pichler and Dix, 1996) where distinct carbonate phases with marine and hydrothermal isotopic signals coexist.

Stop 2.1 The Boutchrafine section

Figures pertaining to this stop are Figs. 14, 27 and 28.

This quick stop will permit observation of the section laterally equivalent to the Hamar Laghdad section. We will focus on the limestone-poor Pragian-Emsian part of it, laterally equivalent to the Kess-Kess Formation (the crinoid sole, the mounds, and the intermound beds). The limestone ledge on top of the cliff corresponds to the Eifelian-Frasnian part of the section.

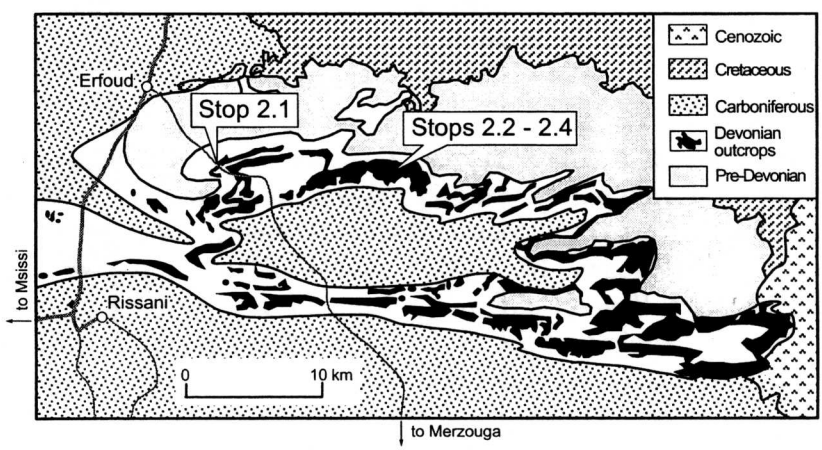

Figure 27 – Location map of stops 2.1 to 2.4. *See location on Figure 9.*

The microfacies of the Pragian limestones is typically a fine-grained crinoidal packstone, with accessory trilobite and brachiopod shells, tentaculitids and miscellaneous tiny shell debris. That of the calcareous Emsian limestones is a bioturbated tentaculitid wackestone to packstone, with a few trilobites, cephalopods and gastropods.

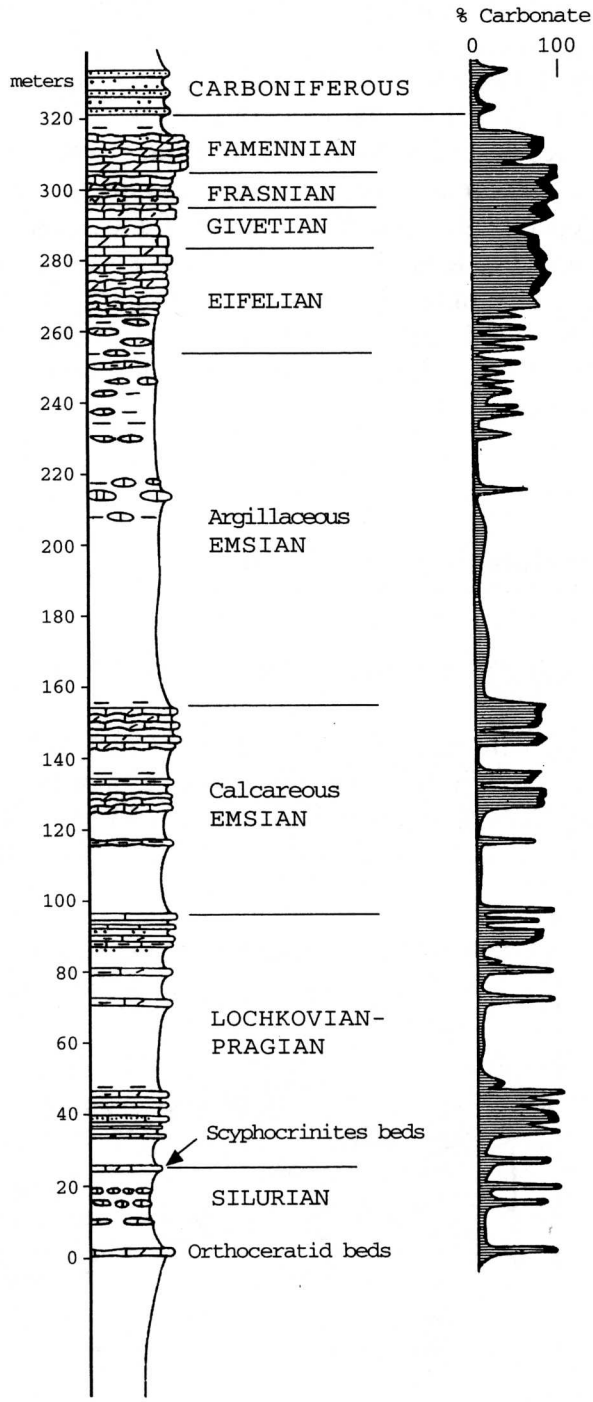

Figure 28 – Boutchrafine section lithological log, Stop 2.1. *Carbonate percent from Massa (1965).*

Stop 2.2 The crinoid sole

Figures pertaining to this stop are 13 and 29.

From the valley related to Hercynian faults that separates the eastern and western parts of the Hamar Laghdad massif (Fig. 13), we will walk up on a bedding plane to reach the contact between the volcanites and the limestones in the northern escarpment of the massif. The bed onto which we will walk up corresponds to the Orthoceratid condensed bed of Figure 29 section (23-26 m). Then, proceed up section to examine the best accessible section exhibiting the crinoid sole that developed on top of the volcanic piedestal and onto which mounds established. The uppermost part of the section, near the reg (plain) level, exposes the transition beds between the crinoid sole and the mound and intermound assemblage.

From the top of the cliff, you have a spectacular view on the kess-kess mounds and associated facies (see Fig. 16A).

Stop 2.3 The Kess-Kess mounds and the intermound beds

Figures pertaining to this stop are Figs. 13, 30, and 31.

Although all mounds at Hamar Laghdad are worth of observing and are likely to teach us something, we will focus on the central ones (Fig. 30) due to time constraints. Two itineraries are planned, both starting south of mound #1. Hopefully, we will have time to do both.

Path I

Along this itinerary, we will observe several features of the mounds and the inter-, infra-, and supramound beds, features that are likely to provoke lively discussions.

Point **a** : mound #1 is one of the few mounds where the core is exposed (Fig. 31A); the inner core is massive, whereas the outer core is bedded parallel to the mound outer surface. The auloporid wackestone with associated stromatactis-like spar bodies is particularly well exposed here. Note the angle between geopetal structures and bedding plane.

Point **b** : mound #7 exposes one type of transition between mound and intermound lithologies : massive thicker mound limestone passing laterally to well-bedded thinner intermound limestones (Fig. 19B).

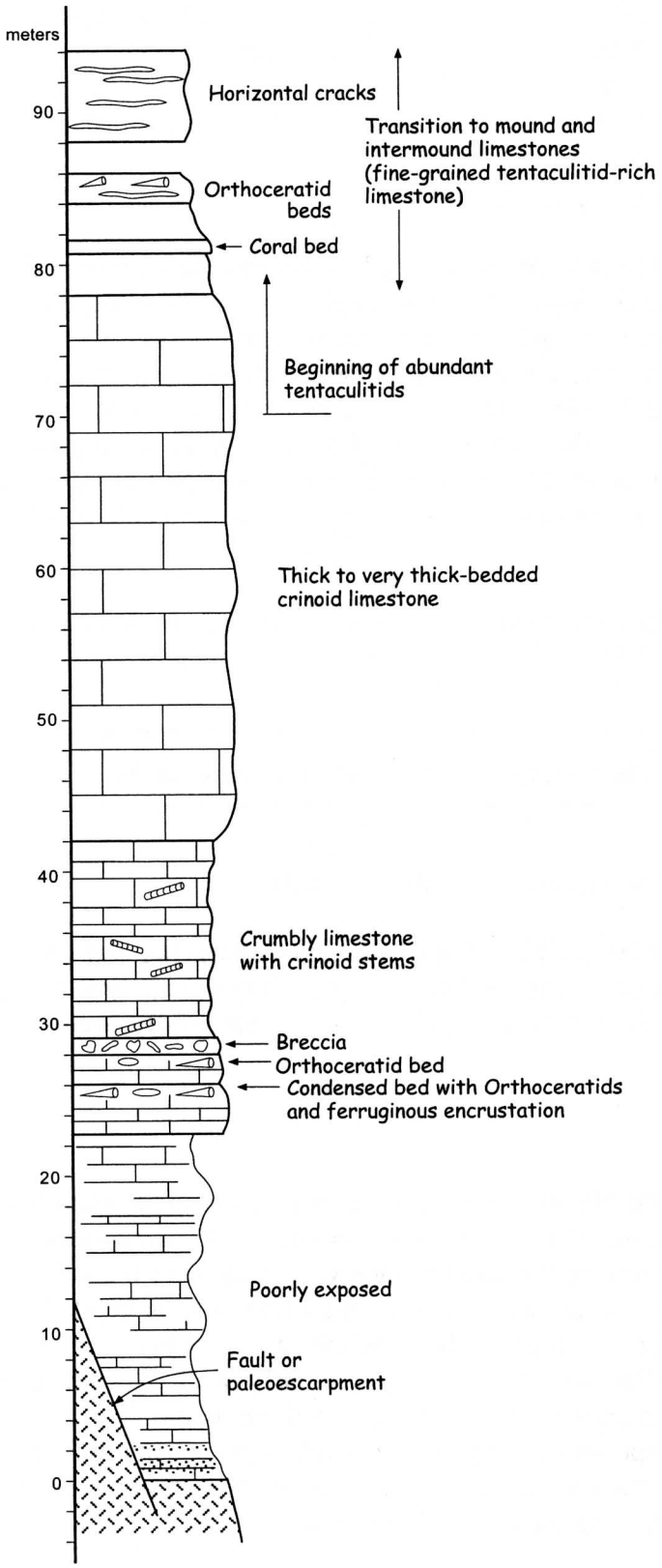

Figure 29 – Section through the crinoid sole at Stop 2.2.

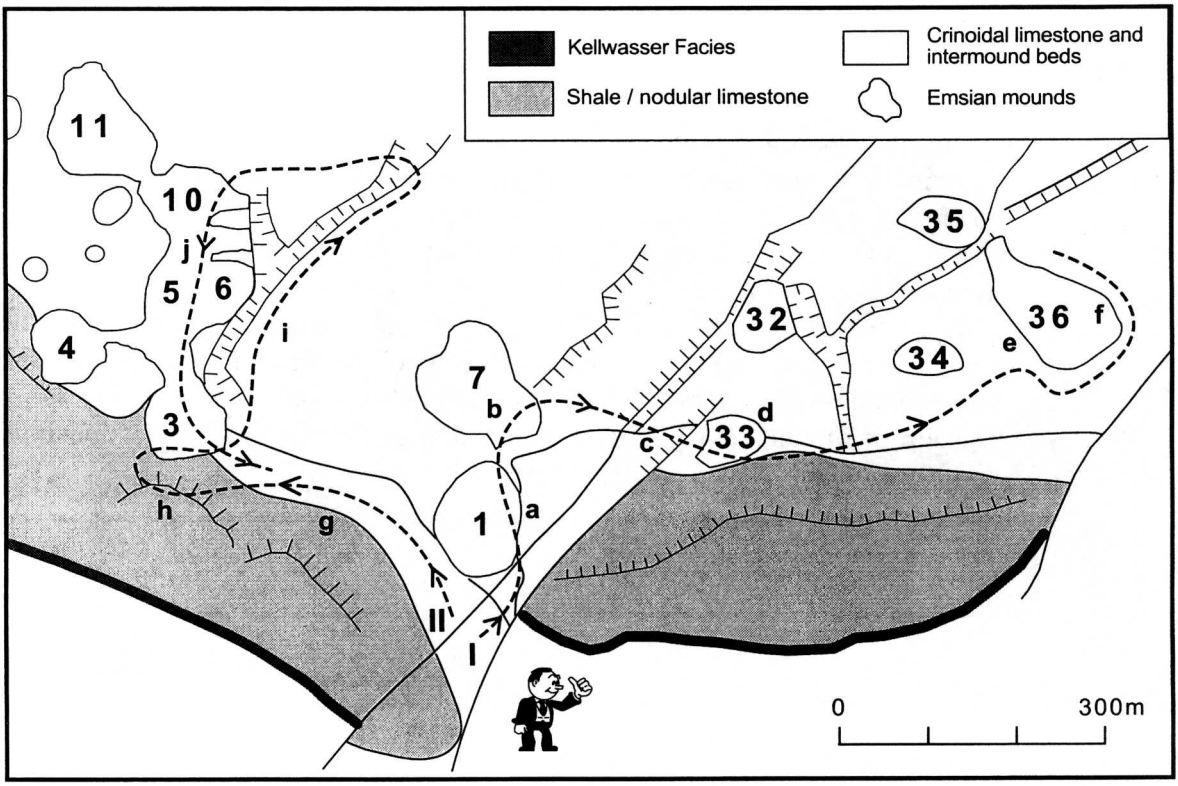

Figure 30 – Itineraries at Stop 2.3, Hamar Laghdad.

Point **c** : a vertical cut here exposes the relationships between the inframound beds, a small part of mound #33 core, and intermound beds. Note the relative massiveness of the core and its asymetry, as well as the onlapping intermound beds.

Point **d** : numerous Neptunian dikes can be observed on and around mound #33. Various types of material fill the dikes : black fibrous spar cement, light grey isopachous fibrous cement crusts, yellow spar, and various sediments (grey and red mud, bioclastic material). Is there an age relationship between each type of filling? Wide dikes (20-40 cm-wide) can be observed in the intermound area between mounds #33 and 36. Note the sinuosity and the frequent ramifications of the dikes.

Point **e** : Two wide dikes occur on soutwest flank of mound #36, with thin sheet-cracks parallel to the bedding plane and connecting with Neptunian dikes.
Note : we measured orientation of 34 vertical to subvertical Neptunian dikes around and between mounds #33 and 36. Polarisation is not strong, but roughly corresponds to radial and tangential fault systems described by Belka (1998).

Point **f** : the core of mound #36 is partly exposed, allowing to observe marked asymetry in flank geometry, as well as in bed thicknesses (Fig. 18A). Moreover, unconformity is visible within beds of the outer core on south flank of the mound (Fig. 31B).

Path II

Among features worth of pointing out along this itinerary are :

point **g** : on your left, you may observe the Eifelian-Frasnian shale/limestone that covers the mounds and the intermound beds.

Point **h** : climb on top of the Eifelian-Frasnian escarpement to obtain a nice view on mound #3 (Fig. 17A).

Point **i** : walk on the bedding plane east of a narrow gully; from this point, you will get a nice view on the western escarpment of the gully that exposes inframound beds, and mound and intermound bed relationships.

Point **j** : a group of mounds (#10, 5, 6) where lithology, geometry and relationships with the intermound beds can be observed.

Figure 31 - The kess-kess mounds of Hamar Laghdad. *(A) Mound #1; note internal bedding parallel to mound surface, and possible slump to the left. (B) Mound #36; note unconformity in lower left corner of photo. Person for scale (arrow).*

The Hollard Mound : an ongoing enigma

The Hollard mound, at the eastern extremity of the Hamar Laghdad massif (Fig. 13), sets apart of the other mounds, not only because of its age (Emsian to Givetian) that differs from that of the Emsian Kess-Kess, but also because of its geochemistry (Mounji *et al.*, 1998; Peckmann *et al.*, 1999). The following pages summarize the more recent work done on this peculiar mound which, in our opinion, remains enigmatic and needs further investigation.

The Hollard mound : signatures of hydrocarbon venting,

by Jörn Peckmann, Otto Heinrich Walliser, Walter Riegel and Joachim Reitner.

A recent study published by Peckmann *et al.* (1999) focussed on the Hollar mound. Key information from this study is reported here.

Geological Setting and Stratigraphy

The Hamar Laghdad is a small mountain range in the Tafilalt, 18 km ESE of Erfoud in SE Morocco (Fig. 13). In the Tafilalt, the Devonian sequences show features characteristic of a differentiated, relatively shallow, but vast epicontinental sea with prevailing hemipelagic to pelagic faunas and facies, respectively. When compared with that general pattern of the Tafilalt Devonian, the Hamar Laghdad shows an exceptional feature resulting from volcanic activity during the middle and late Lochkovian: Effusiva and a few sedimentary intercalations built a presumably N-S striking submarine ridge, at the Hamar Laghdad about 5.2 km wide and, after partial denudation, up to 100 m high. The volcanoclastic rise became settled by crinoids which produced up to 180 m of crinoidal limestone during the Pragian and Lower Emsian (Zlichovian). In the uppermost part of this so-called Kess-Kess Formation (Brachert *et al.*, 1992), mud mounds developed. Among them the cone-shaped mounds with their steep flanks, called Kess-Kess, are especially spectacular and have, therefore, been the subject of numerous investigations. The Hollard Mud Mound is situated near the eastern extent of the Hamar Laghdad immediately S of Kess-Kess 45 in Brachert *et al.* (1992: Fig. 4). The Hollard Mound is clearly younger than the Kess-Kess mounds (Fig. 32). According to our calculation, it started to develop about 3 million years later, at the very beginning of the Eifelian. The formation of the mud mound continued up to the uppermost Givetian and ended at the globally transgressive Givetian-Frasnian Boundary Event (Fig. 33). At the Hollard Mound a special situation exists with respect to neptunian dikes. In the core, from the base up to the top of the mound, a zone is exposed several meters wide consisting of dike fillings, vent deposits, and vent-influenced sediments as described below. This carbonate complex will be termed the core facies, in contrast to the off-mound sediments and the portions of the mound which are not vent-influenced.

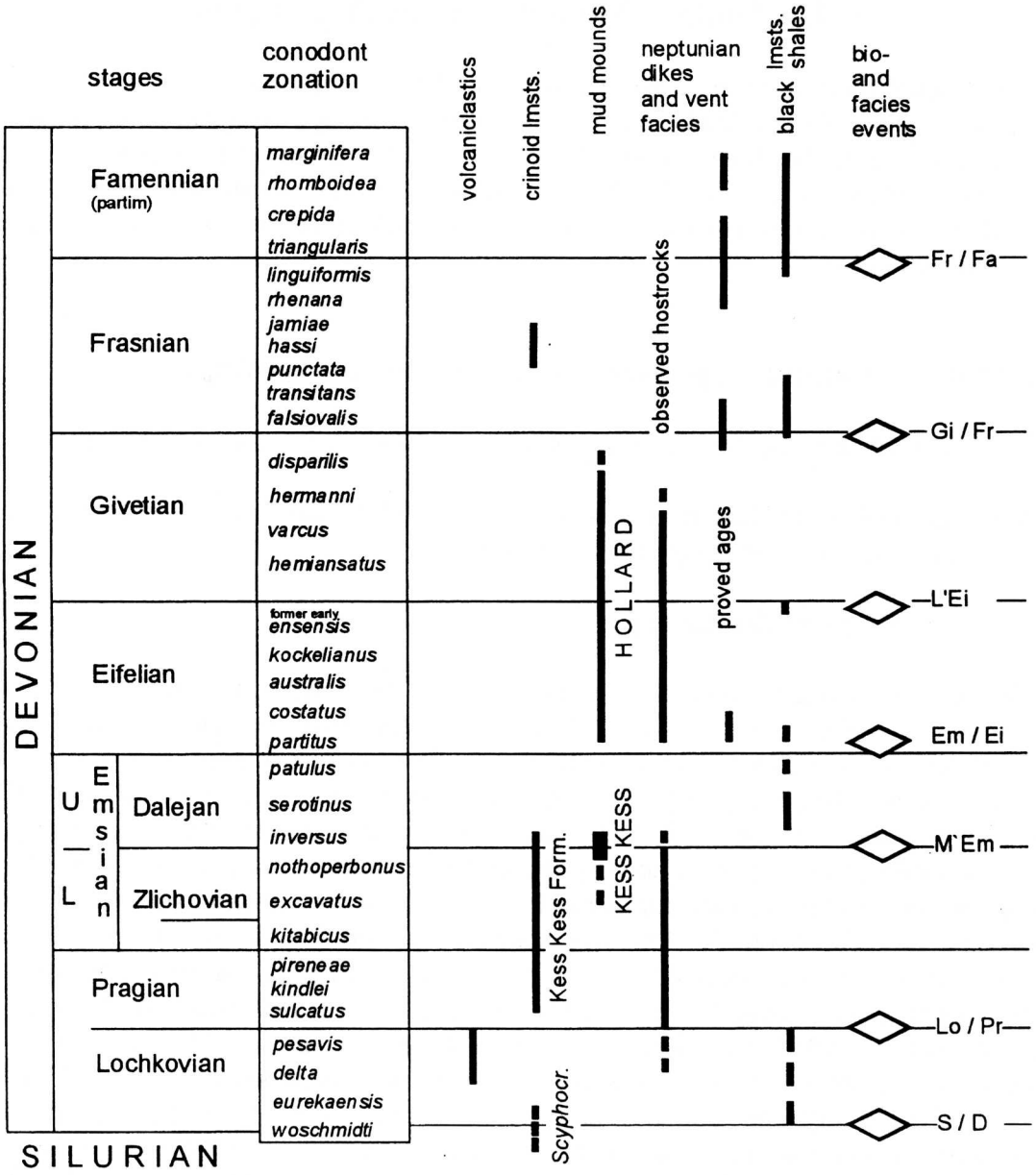

Figure 32 – Stratigraphic range of important features at the Hamar Laghdad *(from Brachert et al., 1992, Fig. 6; updated and revised). L : lower, M' : middle, U : upper, L' : late. From Peckmann et al. (1999, Fig. 3).*

Stable Isotopes

Vent carbonates show $\delta^{13}C$ values in the range of -11 to -20 ‰ PDB (Fig. 34). At the periphery of the vent site fossiliferous micrite of the surrounding facies has been affected by hydrocarbon venting, which is evident from its $\delta^{13}C$ values intermediate between the vent carbonates and the marine signatures of background carbonates. This is valid for both fossiliferous micrite directly adjacent to the vent deposits and for pieces of fossiliferous micrite that are embedded within hydrocarbon derived carbonate phases.

The $\delta^{18}O$ values from the carbonate of the Hollard Mound are exclusively negative and not compatible with precipitation in a normal marine environment as it is indicated by the associated fauna.

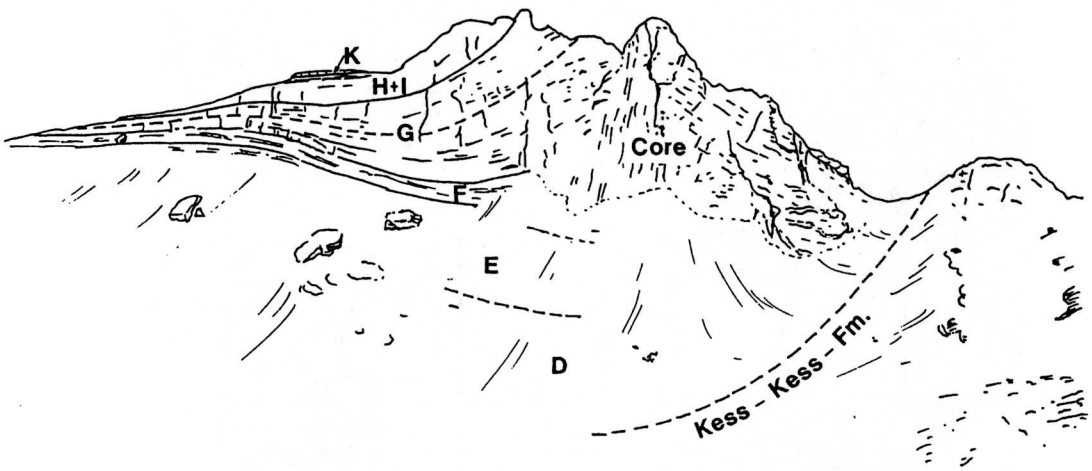

Figure 33 – The Hollard mound. *Letters indicate stratigraphic units, of which the Givetian ones significantly increase in thickness toward the core of the mound. (D + E: Upper Emsian; F: basal Eifelian Pinacites Limestone; F-H: Eifelian; I + K: Givetian, with Pharciceras Limestone at top). Dotted lines: supposed position of boundaries between stratigraphic units where boundaries are covered by debris. From Peckmann et al. (1999, Fig. 4)*

Palaeontology

The large bivalves included in the core facies and the immediately adjacent sediments represent at least two different taxa (Fig. 35). Cross sections (Fig. 36) indicate that they most probably do not belong to *Modiomorpha* as Töneböhn (1991) assumed, but rather to taxa of the Anomalodesmata, presumably to the Pholadomyoida. The bivalves of the core facies are almost exclusively articulated and represent an autochthonous assemblage. Bivalves of the adjacent sediments are disarticulated.

Petrography

In the core facies of the Hollard Mound deposition and precipitation of carbonate occurred in several phases. Dark-grey fossiliferous micrite represents the sediment of the normal marine Eifelian depositional environment and is the phase formed first. The phases which are postdating the formation of this micrite are a clotted micrite (cm on Fig. 36), a calcitic rim cement (rim cement B, rcB on Figs. 36 and 37), a cryptocrystalline carbonate with spheres (Fig. 38), an inclusion-rich calcitic cement (rim cement I, rcI on Fig. 37), rhombohedral calcite (rC on Fig. 37) and dolomite (listed in chronological order).

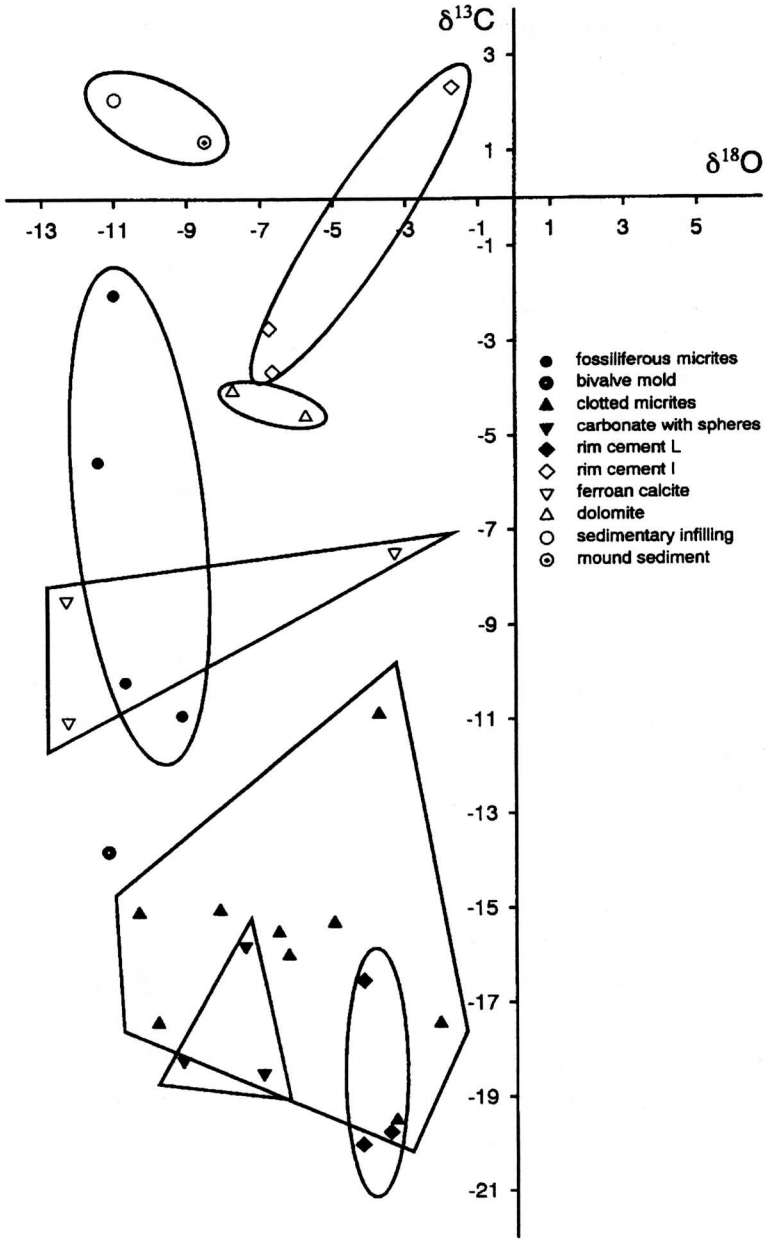

Figure 34 – $\delta^{13}C$ and $\delta^{18}O$ plot of carbonate phases in the Hollard mound. *From Peckmann et al. (1999, Fig. 5)*

Conclusions

The core facies of the Hollard Mound exhibits signatures of ancient hydrocarbon venting. $\delta^{13}C$ values of carbonates, carbonate phases similar to those reported from other vent sites, and dense clusters of articulated bivalves associated with these carbonate phases account for a vent origin of this facies.

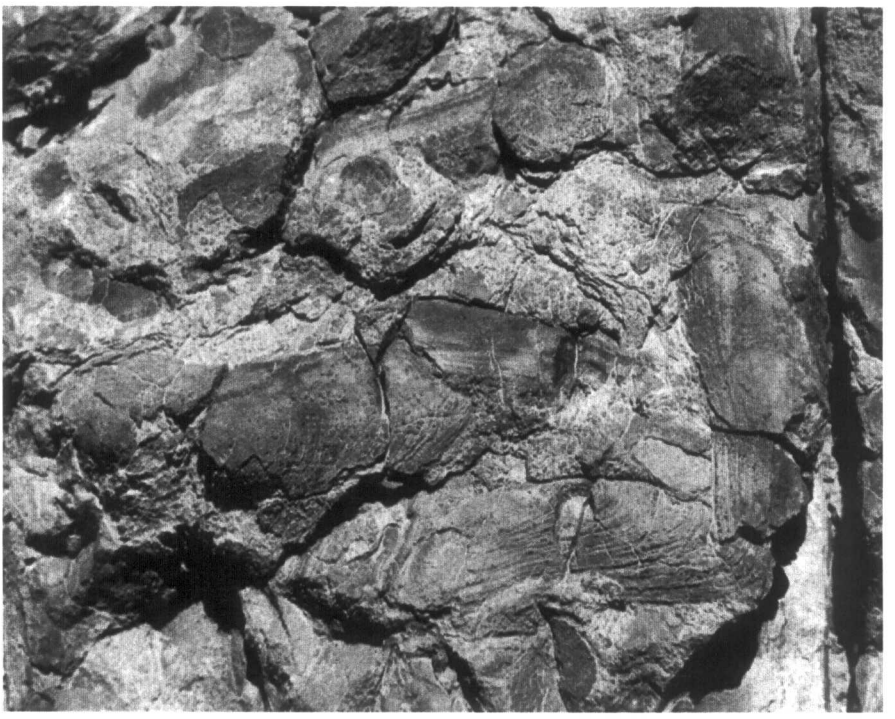

Figure 35 – Bivalves within vent-influenced sediments. *Field view is 17 cm-wide. From Peckmann et al. (1999, Pl. 47, Fig. 5)*

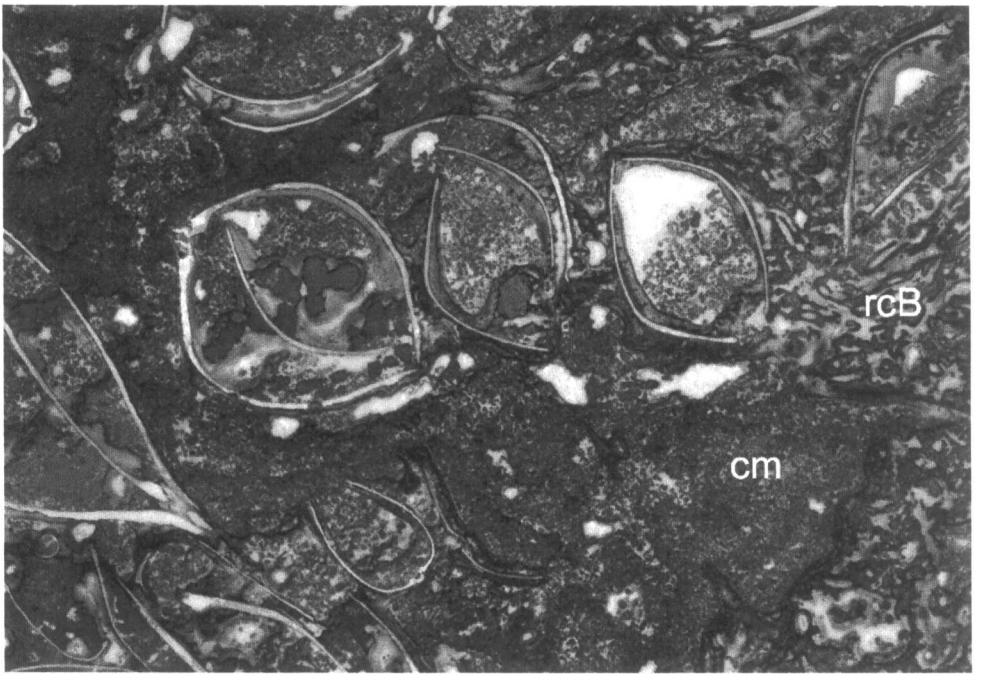

Figure 36 – Articulated bivalves embedded in vent carbonates *(scanned thin-section from the slab shown on Figure 35). Field view is 11 cm-wide. From Peckman et al. (1999, Pl. 47, Fig. 4).*

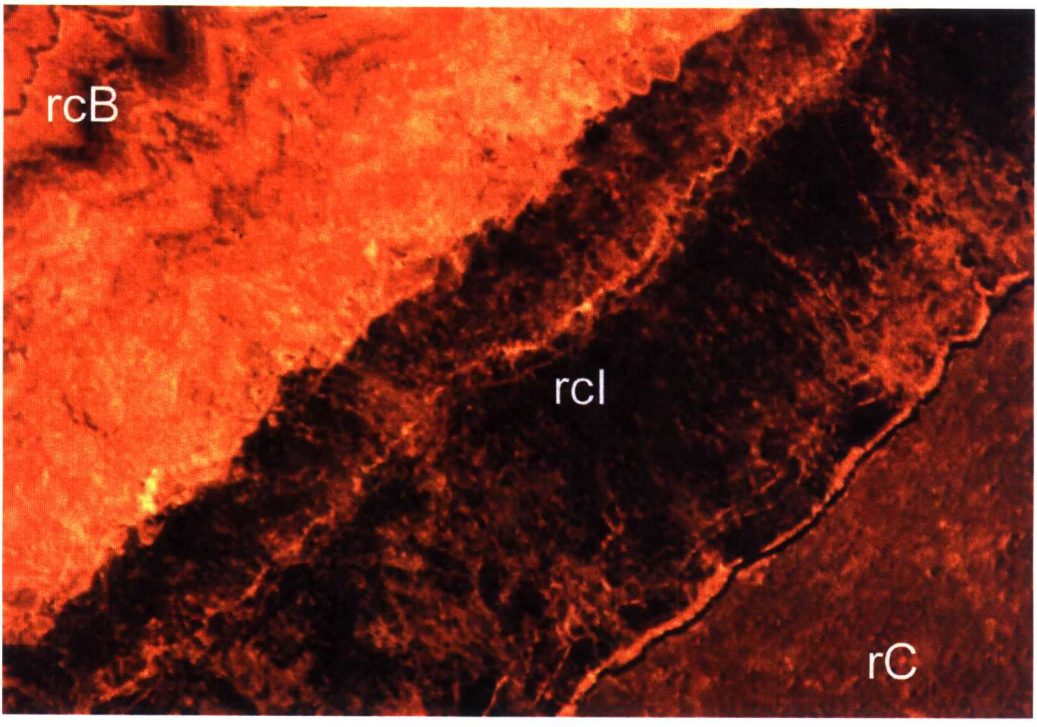

Figure 37 - Rim cement B, rim cement I and rhombohedral calcite *(from left to right). Two main growth zones within the rim cement I are evident, cathodoluminescence pattern. x 63. From Peckmann et al. (1999, Pl. 49, Fig. 2).*

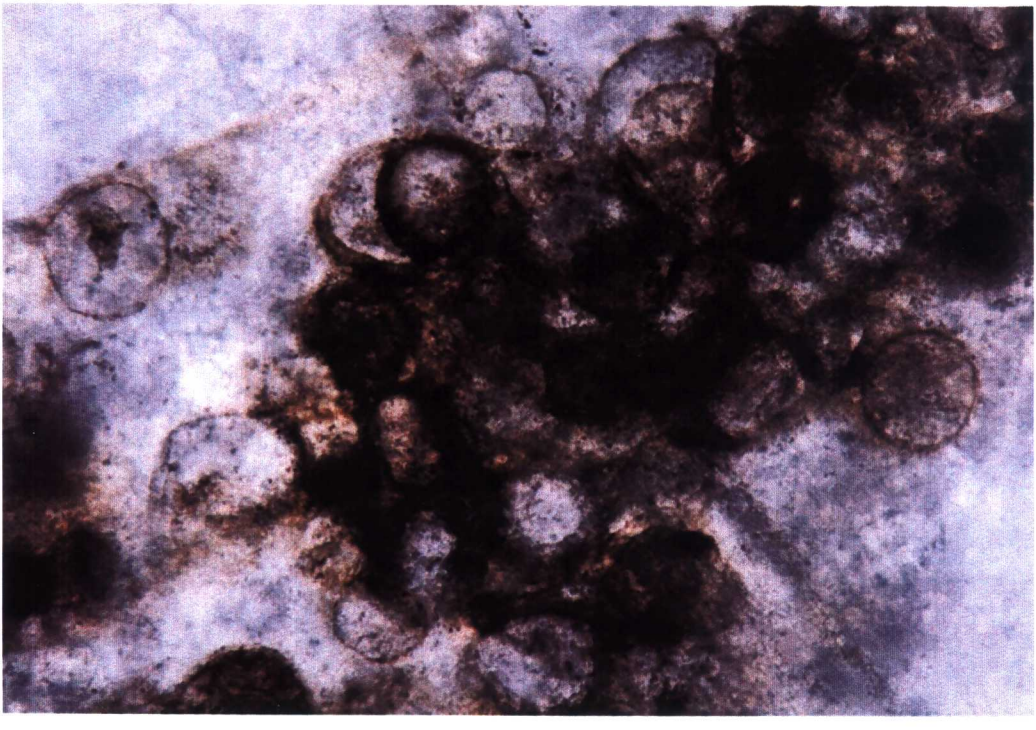

Figure 38 - Carbonate associated with spheres, plane polarized light. *x 77. From Peckmann et al. (1999, Pl. 48, Fig. 3).*

The carbonate phases which have been found to be related to hydrocarbon venting are clotted micrite, cryptocrystalline carbonate associated with spheres, and the rim cement B.

The bivalves of the core facies are arranged in clusters similar to the high abundance faunas of modern hydrocarbon-vents. Their abundance in the otherwise fossil-poor vent deposits accounts for a close relation to the ancient venting. It is likely that the Devonian bivalves were dependent on chemosynthetic pathways for their nourishment similar to the bivalves of modern vents and seeps.

The Hollard mound : complementary information,

by Mounji, D., Bourque, P.-A, and Savard, M.M.

Facies and architecture

For the purpose of description, the Hollard mound is divided into five units (Fig. 39). Unit 1 is a fractured limestone forming the massive core of the mound. Unit 2 is a thinly bedded limestone and shale unit, whereas units 3, 4 and 5 make three distinct thickly bedded limestone bodies in southern part of the mound. The mound core is affected by faulting and jointing giving the limestone its fractured state. Thickness of both units 3 and 4 increases significantly toward the mound core : from a thickness of 4 meters each at section E south of the mound, unit 3 expands to 28 meters, and unit 4 to 12 meters, for a combined thickness of 40 meters.

Relationship between the bedded unit 3 and the massive core (unit 1) is unclear. There is apparently a fault corresponding to the V-shaped erosion in center of the mound (Belka, 1998, Fig. 9), but wether or not there is significant displacement along it is most uncertain. Vague bedding in upper part of the mound northern peak (dotted lines on Fig. 39) suggests that at least part of unit 3 overlies the mound massive core. If the vertical displacement along the fault is unsignificant, the lower part of unit 3 is laterally equivalent to the core. Clarification of these relationships is essential to better constrain the isotope geochemistry (see below), and at this point more field work is needed.

Petrography and isotope geochemistry are based on samples taken along five sections in the mound and off-mound facies for a total of 54 samples (see Fig. 39 for distribution of samples).

Petrography

Unit 1. - The limestone of the core facies commonly has a dark color, although locally it is lighter grey. It is cross-cut by Neptunian dikes filled with isopachous fibrous-like cement crusts. At the thin-section level, two microfacies are distinguished, based on microspar and cavity types. **Microfacies 1a** corresponds to the light grey limestone. It has

a mudstone to wackestone texture and is composed of uniform microspar (4-20µm in crystal size) that contains variable proportions of Auloporid corals, tentaculitids, crinoids, trilobites, bivalves, gastropods, and brachiopods. The pore space is represented by stromatactis-type cavities that originated from collapse of uncemented material during early diagenesis. This microfacies is very similar to the microfacies of the Emsian kess-kess mounds. **Microfacies 1b**, that roughly corresponds to the dark limestone, is composed of a mixture of fossiliferous uniform microspar like that of microfacies 1a, and pelletoidal spar (spar cement with pellet-like microspar bodies). The pelletoidal spar is of two types : type A is made up of patches of usually spar-supported, poorly sorted, irregularly-shaped pelletoidal microspar bodies in a 100µm crystal size spar (Figs. 40A and 41A, B), and type B is clotted microspar made up of self-supported, well-sorted, sub-spherical microspar bodies in a 100µm crystal size spar, often occurring as geopetal fillings in cavities (Peckmann *et al.*, 1999, Pl. 47-4, and Fig. 36 herein; Fig. 41C, D). The first type seems to represent some sort of recrystallisation of the uniform microspar, whereas the second looks rather related to sediment infiltration, the pelletoidal texture being primary or inherited from sediment diagenesis. The cavities in microfacies 1b are seemingly solution cavities (Fig. 40A), contrary to those of microfacies 1a which are of stromatactis-type. Ghosts of tube-shaped (organic?) structures were observed in microfacies 1a (Fig. 40B). Microfacies 1b has been observed in mound core only (section C). It is not confined to specific parts of section C, but alternates with microfacies 1a along the section.

Unit 2. - This unit is thinly-bedded fine-grained limestone and shale, 6 meter-thick above Emsian shales. The limestone is a bioturbated tentaculitid-rich uniform microspar. Slumping has affected part of these beds.

Unit 3. - The limestone of this thick-bedded unit is an Auloporid and Thamnoporid mudstone to wackestone, with variable proportions of tiny skeletal elements of tentaculitids, crinoids, brachiopods, trilobites, sponge spicules, gastropods and bivalves. The « mud matrix » is a uniform microspar. Laminated « mud » locally occurs as internal sediment in cavities above first cement crusts.

Unit 4. - This unit is composed of the same fossiliferous mudstone-wackestone as unit 3. Between units 3 and 4, there is a 1 meter-thick argillaceous bed into which a limestone breccia, with clasts up to 40 cm, occurs at base of the steep mound flanks (Fig. 39). The clasts are composed of the same limestone as units 3 and 4. Further south, in flat lying limestone beds at base of unit 4, tepee-like structures occur at two levels one meter apart. Bed fragments are incorporated in argillaceous material in the core of these structures. No cements that usually are associated with true tepees were observed. This structure is more likely related to lateral sliding.

Unit 5. - This unit is composed of the same mudstone-wackestone as units 3 and 4.

Cover beds. - These cover beds correspond to a reddish finely crystalline limestone, referred to as *Pharciceras* Limestone by Peckmann *et al.* (1999).

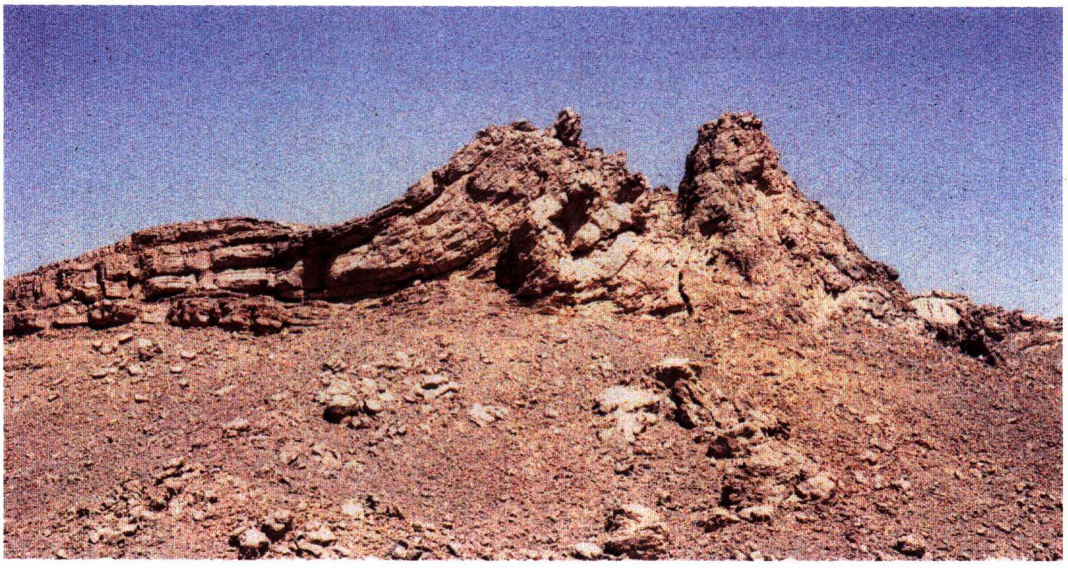

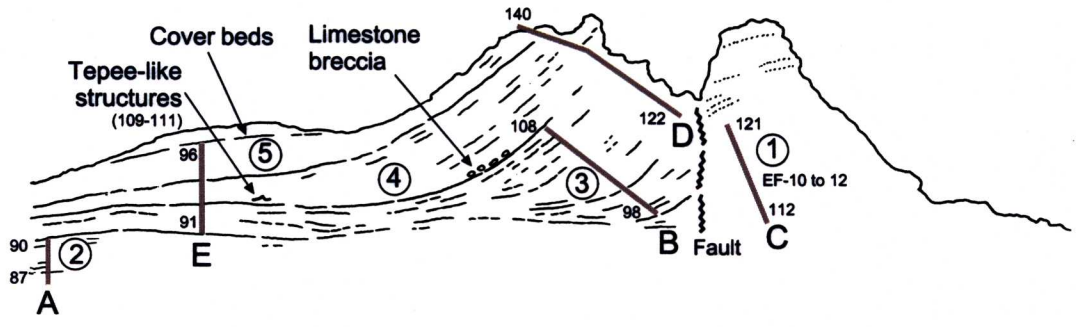

Figure 39 - The hollard mound at eastern end of Hamar Laghdad, Tafilalt, and lithological divisions. *A - E are studied sections. Encircled numbers are main divisions (see text). Small numbers are sample number suites.*

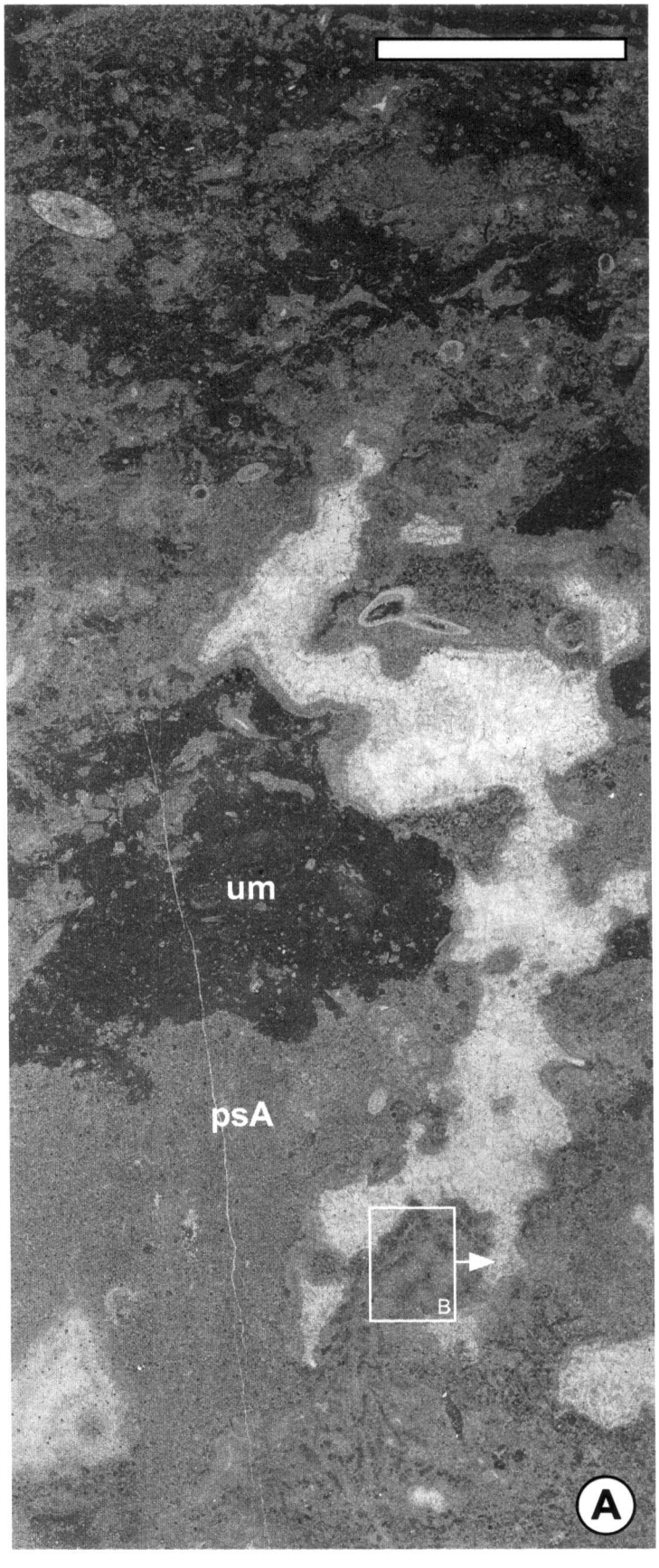

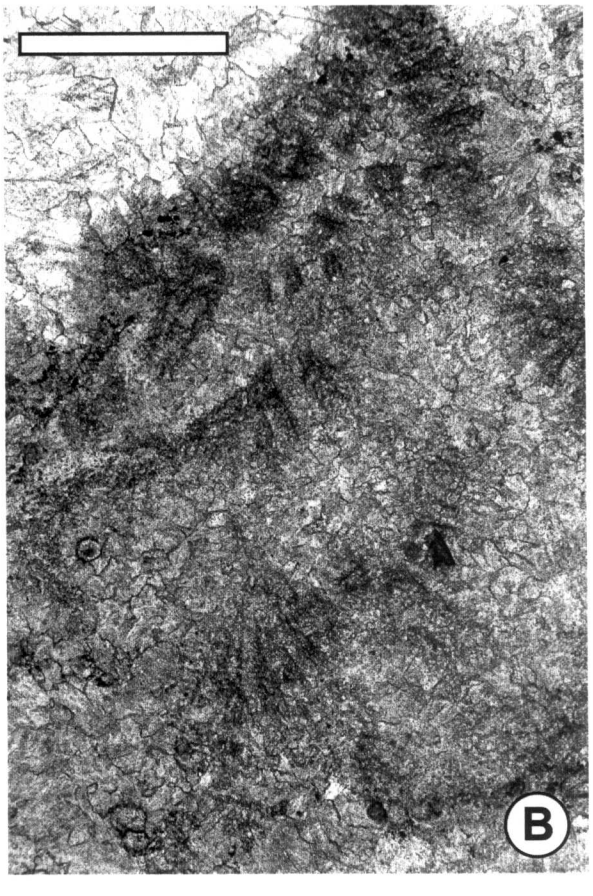

Figure 40 - Microfacies 1b of Hollard mound core facies.

(A) Mixture of uniform microspar (um) and type A pelletoidal spar (psA). Note irregular probable solution cavity. Scanned thin-section. Scale bar is 1 cm.

(B) Photomicrograph in plane-polarized light of a close-up of Figure A showing ghosts of tube-shaped structures. Scale bar is 1 mm.

Vertical thin-section, normally oriented.

Figure 41 – Microfacies 1b of Hollard mound core facies

(A) type A pelletoidal spar (psA) showing spar-supported pellet-like bodies, together with uniform microspar (um). Stained thin-section, bar scale is 1 mm. Sample 93HL-115.

(B) A closer view at type A pelletoidal spar. Unstained thin-section, bar scale is 1 mm. Sample 93HL-113.

(C) Type B pelletoidal spar showing clotted texture, together with uniform microspar in brachiopod. Stained thin-section, bar scale is 1 mm. Sample 92HL-115.

(D) Close-up of Figure C illustrating type B pelletoidal spar. Note that staining suggests that first cementation phase around pellet-like bodies was ferroan. Bar scale is 100μm.

All photomicrographs of vertical thin-sections, normally oriented.

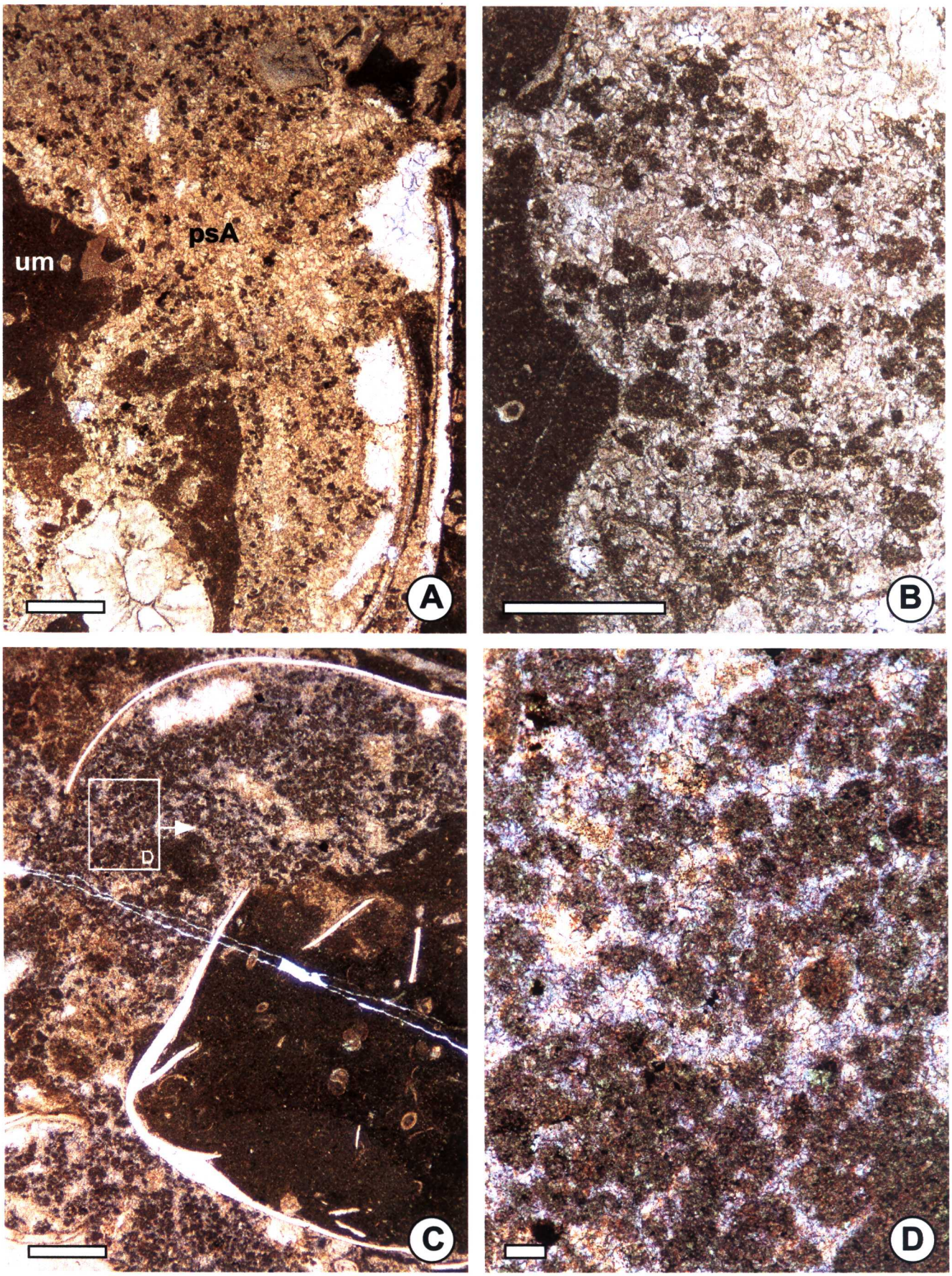
psA
um
A
B
D
C
D

Isotope geochemistry

Sampling for carbon and oxygen stable isotope content was done under CL control. Cement stratigraphy (defined on position in the succession, crystal shape, luminescence) of units 3, 4 and 5 (no cavities are large enough to permit sampling in unit 2) is the same as in Emsian kess-kess mounds (Fig. 21). Same cement designation (C1, C2 and C3) is therefore used. Cements of unit 1 (mound core) differ sufficiently from those of units 3 to 5 to use a different designation. They are referred to as cements G1 and G2. Under CL, cement G1 is distinctly thinly banded, dog tooth-shaped, crystals with alternating bright-luminescent and dull-luminescent bands with two zones of non-luminescent bands, one marking the end of the first fifth of G1, the other marking the end of it (Fig. 42). Cement G2 is a dull-luminescent sub-equant crystals. In places, solution features are observed between cements G1 and G2 (Fig. 42).

Five phases of the limestone were analyzed : cements C1, C3, G1 and G2, and microspar matrix. A total of 125 analyses from 52 rock samples distributed in the 5 sections were performed at the Delta lab of the Geological Survey of Canada in Québec City. Bulk results are shown on Figure 43 and present a rather complex distribution pattern. In an attempt to better understand this distribution, we have separated results from the mound core (unit 1) and those from the bedded units 2 to 5 (Fig. 44). The two resulting scattergrams exhibit two different worlds.

The distribution of C and O stable isotope values for units 2 to 5 are very similar to the one we obtained from the Emsian kess-kess (Fig. 22), and therefore the same interpretation is proposed : the precipitation of lime mud was influenced by hydrothermal venting on sea-floor. The isotope distribution for the mound core (unit 1) is much different. It presents two populations, both trending from a marine heavy $\delta^{13}C$ (near the zero axis) to a light end-member (down to –20,1‰), one along a « warm » $\delta^{18}O$ line at *circa* -11.0‰, and the other along a marine-like $\delta^{18}O$ line (*circa* -3.5‰). These two populations strongly suggest that at least two geochemical systems were acting simultaneously or in alternance on sea-floor during the building up of the Hollard mound : one resulting from high temperature waters (the same as the ones that precipitated the Emsian kess-kess and the Hollard mound unit 2 to 5 muds) interfering with a light carbon source (hydrocarbon), and the other derived from mixing of « cool » marine water and light carbon, feeding a bivalve chemosynthetic community as proposed by Peckmann *et al.* (1999), and responsible first for alteration and solution cavity production in the mudstone, and thereafter for precipitation of cements G1 and G2 in the cavities.

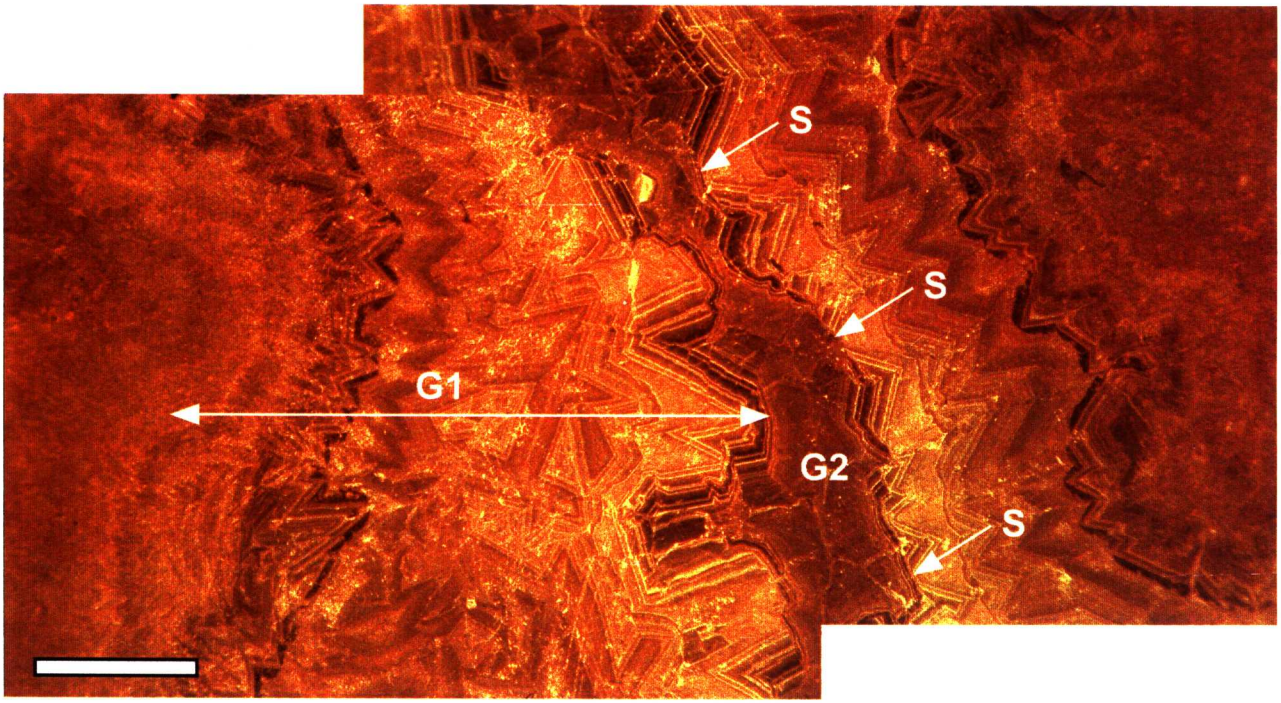

Figure 42 - Cathodoluminescence view of cement succession (G1 and G2) in cavities of Hollard mound core facies. *M : microspar, S : solution features. Scale bar is 500µm. Sample 93HL-116.*

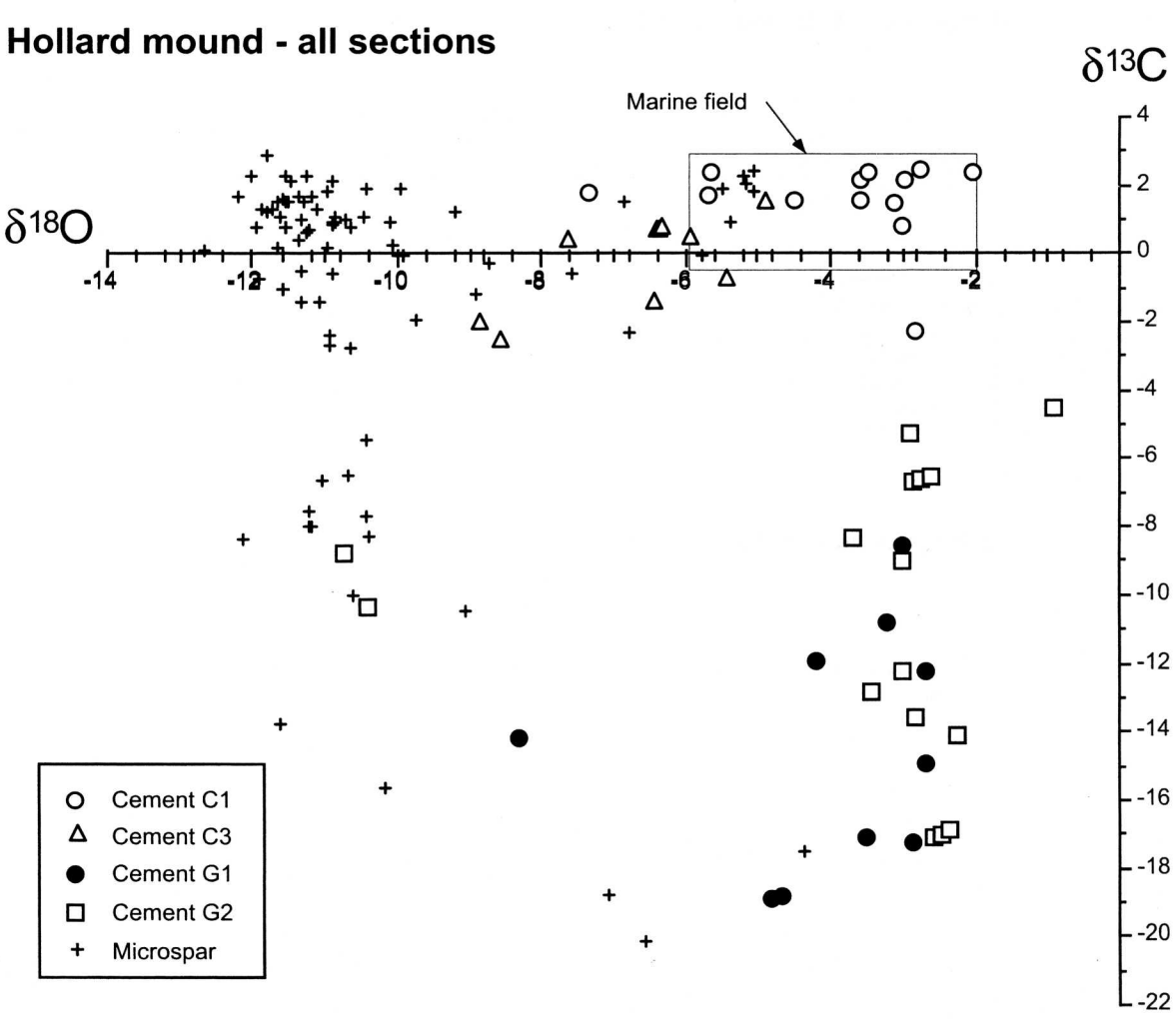

Figure 43 - Cross plot of $\delta^{18}O$ and $\delta^{13}C$ for cement phases C1, C3, G1, G2 and microspar of Hollard mound – all sections. *Early Devonian seawater field, based on brachiopod shells (Lohmann and Walker, 1989; Popp et al., 1986; Lavoie, 1993 ; Veizer et al., 1997). VPDB (Vienna Peedee belemnite standard) standard used.*

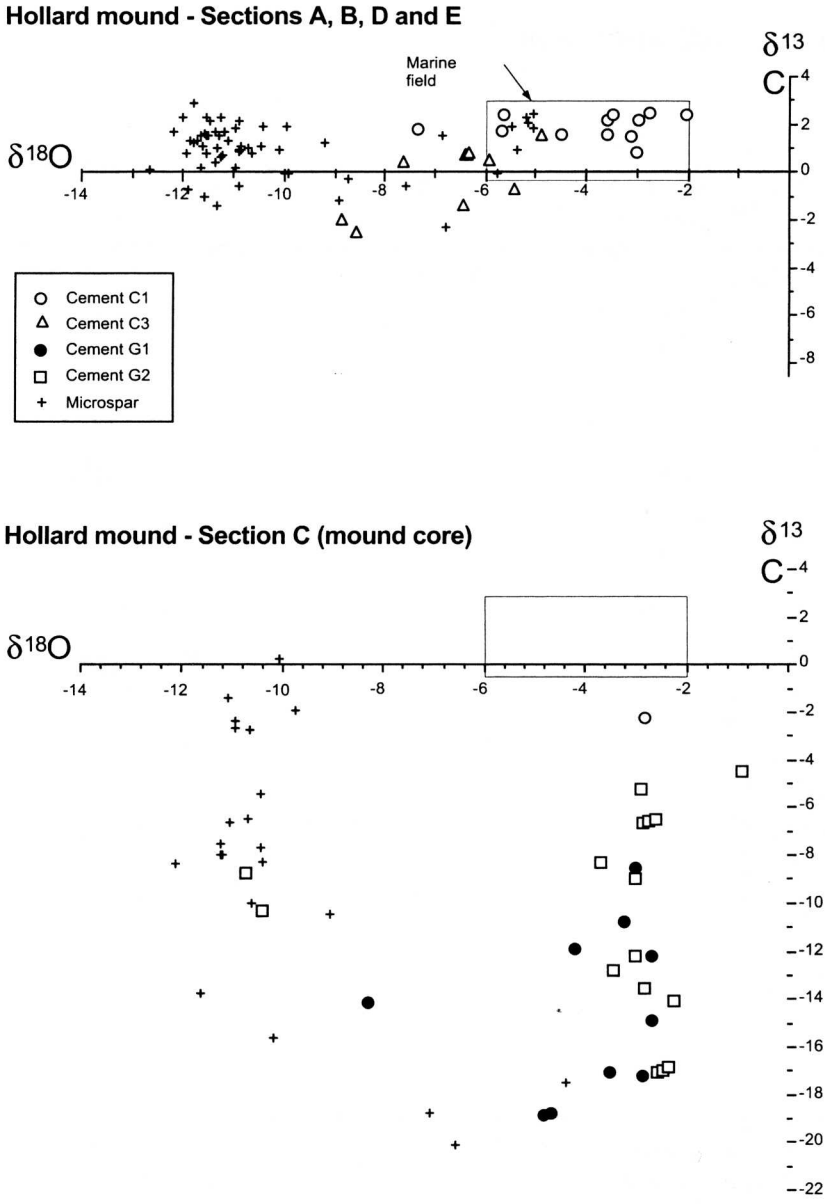

Figure 44 - Cross plot of $\delta^{18}O$ and $\delta^{13}C$ for cement phases C1, C3, G1, G2 and microspar of Hollard mound –Sections A, B, D, E, compared to section C (core). *Early Devonian seawater field, based on brachiopod shells (Lohmann and Walker, 1989; Popp et al., 1986; Lavoie, 1993 ; Veizer et al., 1997). VPDB (Vienna Peedee belemnite standard) standard used*

Stop 2.4 The Hollard mound

Figures pertaining to this stop are 13, 33, and 39.

Fist, climb on the hill facing the Hollard mound to the south-east in order to obtain a nice view and get your picture of the mound. This being done, climb toward the base of the mound to look first at the core, and thereafter at the southern flank with the breccia and the tepee-like structure.

Eilelian-Givetian Mounds of the Maïder

A few carbonate mounds outcrop in the southeastern part of the Maïder basin, in three areas : four mounds at Jbel el Otfal, one at Guelb el Mharch and one at Jbel el Mrakib areas (Fig. 45). They are all slightly younger than the Emsian kess-kess mounds of the Tafilalt (Eifelian-Givetian) (Fig. 12). Within the time frame of one day, only one mound can be visited, the Aferdou el Mrakib at Jbel el Mrakib. A brief description and illustration of the other mounds is nevertheless presented here.

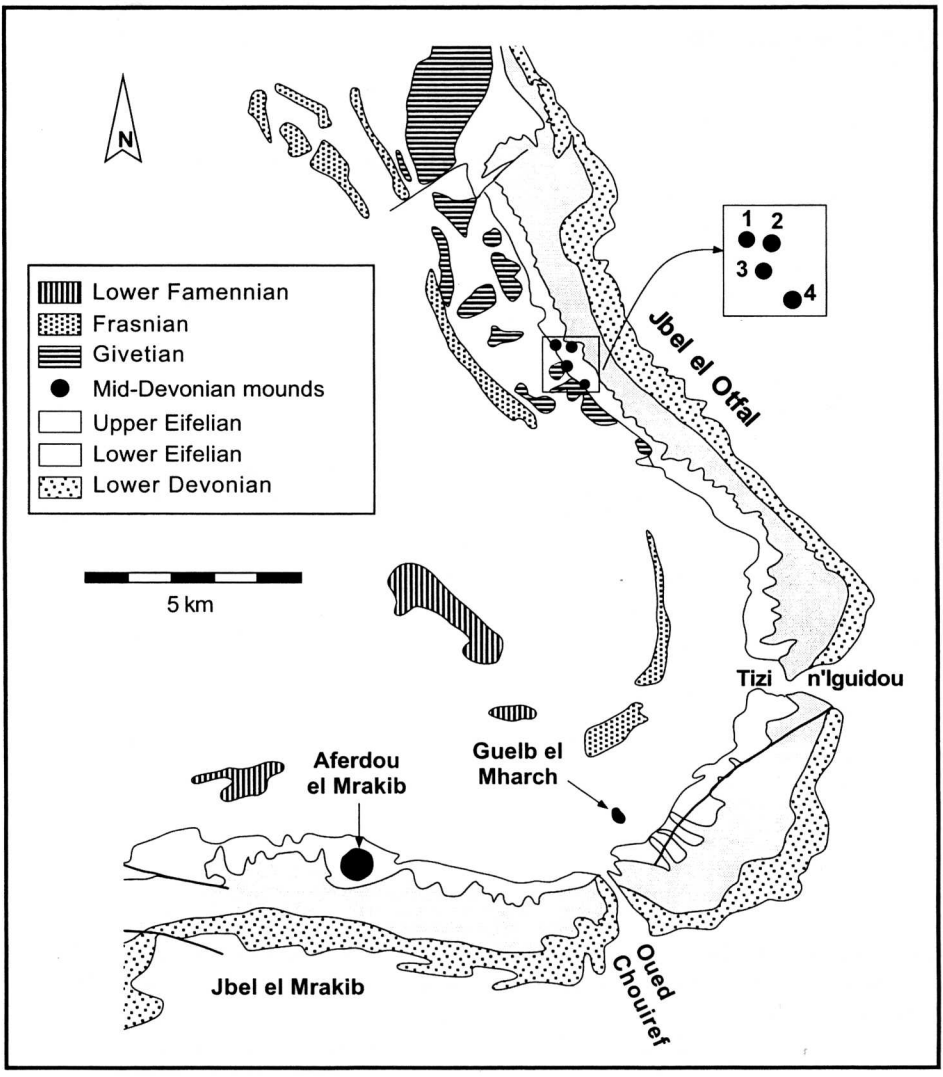

Figure 45 – Geological map of southeastern Maïder, and location of Devonian carbonate mounds. *From Wendt, 1993.*

Jbel el Otfal Mounds

Four mounds outcrop at Jbel el Otfal. They were labeled mounds #1 to 4 by Wendt (1993). One only is exposed entirely (mound #2), the three others exhibiting only their sommital part. The four mounds are Eifelian in age (Kaufmann, 1996; Belka *et al.*, 1997) : mounds #1, 2 and 3 belong to the Lower *costatus* zone, whereas mound #2 was dated as *kockelianus* zone (Fig. 12). The following description is based on mound #4 where underlying and flank beds are exposed and where erosion has partly exposed the mound core (Fig. 46A). It is the largest of the four mounds. It has an elongated, slightly asymetrical, conical shape, ~200 m-long, ~100 m-wide, and ~25 m-high.

The underlying succession is made up of 55 m of Lower Eifelian, thin to medium-bedded, argillaceous bioclastic crinoidal limestone with the trace fossil *Zoophycos*, overlied by a 2 m-thick unit of crinoidal limestone that forms the sole of the mound (Fig. 46A, 48A). The actual mound is composed of some of the facies recognized at the Aferdou el Mrakib mound (see under description of this mound for a more detail account on these facies); the mound succession is the following, upsection (Fig. 47) :

- the mound core, made up of a lense of bedded shale and bioclastic limestone; these are mostly hidden under present day talus debris, nevertheless observable provided one makes some digging;
- facies AM-4 : a 4 m-thick crinoidal packstone-grainstone;
- facies AM-6 : a 8 m-thick Auloporid-rich mudstone (Fig. 48B);
- facies AM-8 : a 2 m-thick stromatactis and sponge spicule wackestone-mudstone;
- a 50 cm-thick summit bed made up of a Rugose coral (*Pinacophyllum sp.*) boundstone composed of 15 to 20% of corals in lime mudstone, with accessory crinoids, brachiopods and ostracodes; this facies is unknown at Aferdou el Mrakib and Guelb el Maharch;

At foot of the mound (Fig. 47), the mound limestone passes laterally to a 5 m-thick bedded bioclastic limestone and shale succession overlying the crinoidal sole bed and topped with 50 cm of a distinctive Orthoceratid and Goniatitid limestone dated as Lower *costatus* zone (same age as the mound itself). Above the cephalopod limestone, is a bedded shale/bioclastic limestone succession, deformed by slumping (Fig. 46B).

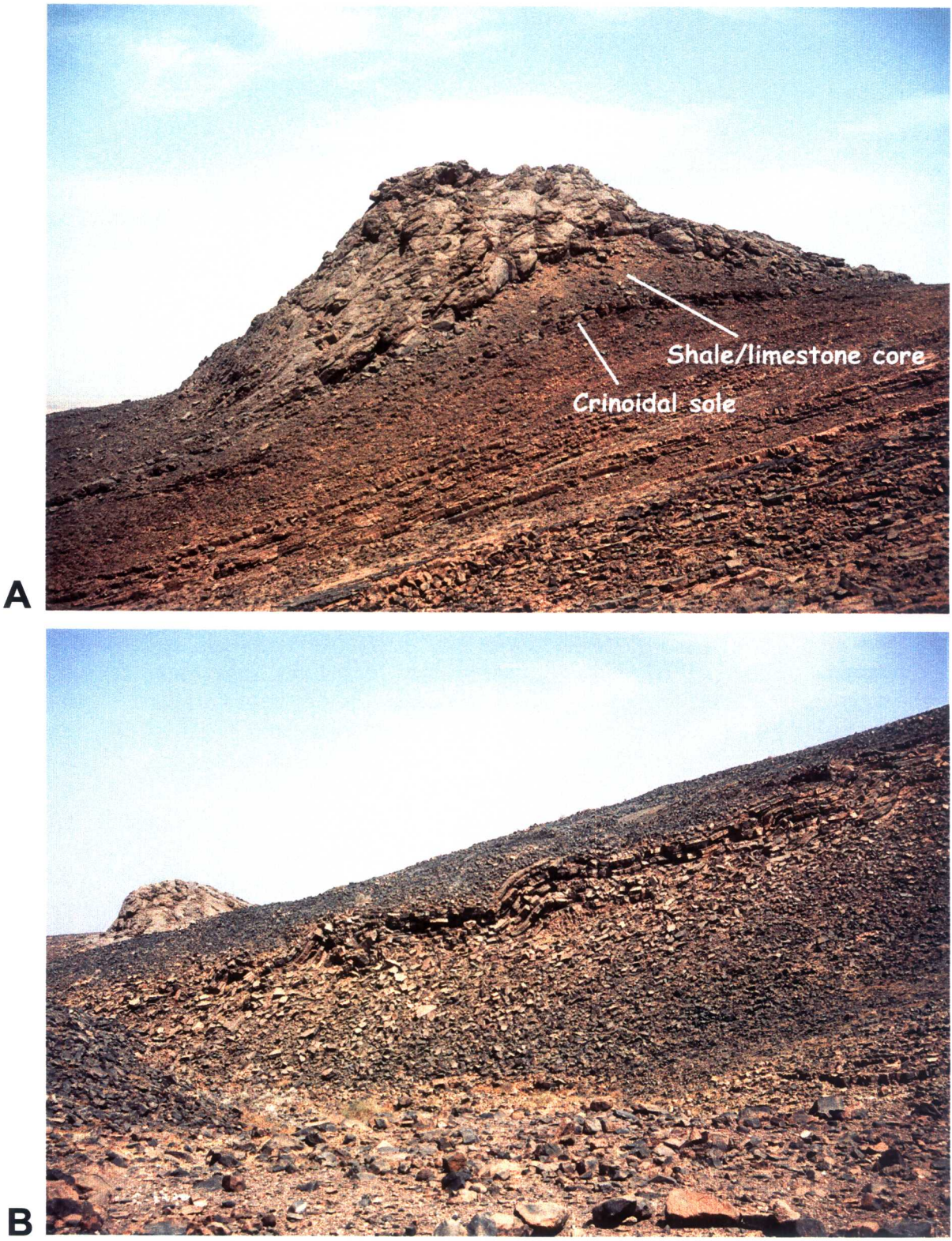

Figure 46 - Jbel el Otfal mounds and slumped cover beds. (A) Mound #2. (B) Slumped beds covering mound #2, with mound #1 in the background.

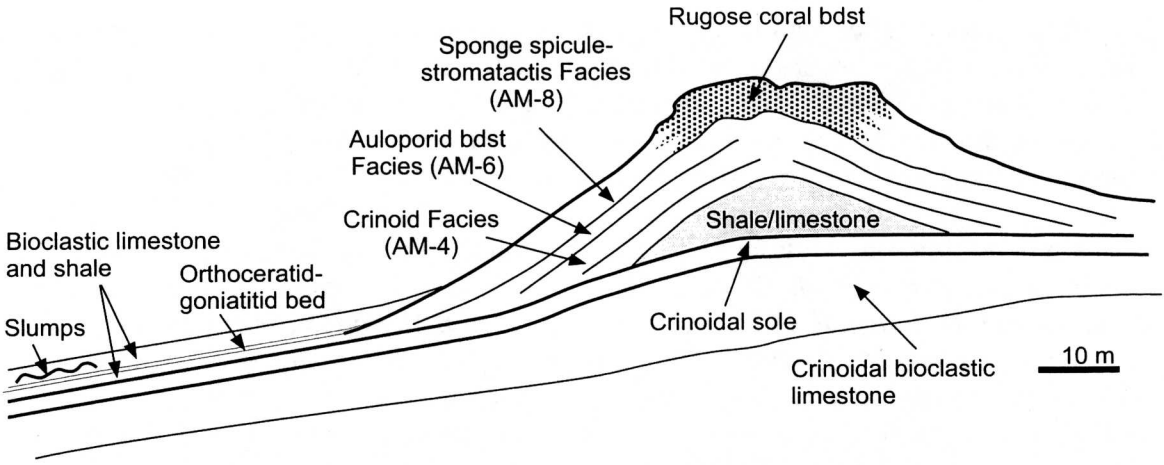

Figure 47 – Sketch of Jbel el Otfal mound #2 showing facies distribution and relationships. *See under Aferdou el Mrakib mound (below) for signification of AM-4, AM-6 and AM-8.*

Guelb el Mharch Mound

Only the summit part of the Guelb el Mharch mound is exposed in the Oued Chouiref plain (Fig. 49). It forms a 45 m-high cone, 200 m in diameter, with 30 to 45° dipping flanks . This summit is younger than the Jbel el Otfal mounds; it has been dated as the Lower *varcus* zone (Belka *et al.*, 1997; Kaufmann, 1998). Three of the Aferdou el Mrakib mound facies were recognized here, upsection : crinoidal packstone-grainstone (AM-4), Auloporid mudstone (AM-6), and stromatactis and sponge spicule wackestone-mudstone (AM-8). These limestones are cross-cut by Neptunian dikes. A dolomitisation corridor crosses accross the mound (Fig. 49).

Aferdou el Mrakib Mound

Among the Maïder mounds, the Aferdou el Mrakib mound is the largest and the one that presents the greatest diversity of facies. It was studied by Hollard (1974), and more recently by Wendt (1993), Kaufmann (1996, 1997, 1998) and Mounji (1999). It occurs on top of a gently northerly dipping (6°) homoclinal Emsian-Eifelian succession of well-bedded tentaculitid limestones and shales becoming rich in crinoid debris upsection. The mound and off-mound beds are dated Givetian (*hemiansathus* and Lower *varcus* zones) (Belka *et al.*, 1997; Kaufmann, 1998).

Architecture and geometry

The Aferdou el Mrakib mound is sub-circular in plan view, *circa* 1200 x 1000 m, and 130 m-high, with steeply dipping flanks at 25 to 55° (Fig. 50).The relationship between the mound and the off-mound facies is not readily observed. In an off-mound position, coral-stromatoporoid breccia forms distinctive units. Kaufmann (1998) placed one of these units below the mound and considered that the overlying well-bedded limestones were time equivalent and therefore interbedded with the mound limestones (Fig. 51). Our

field observations rather lead us to conclude that these coral-stromatoporoid breccias, to which dark *Zoophycos*-bearing calcilutites and calcarenites are associated, are onlapping the mound flanks (Figs 52, and 58A under Stop 2.5). This Givetian assemblage of dark *Zoophycos* limestones and coral-stromatoporoid breccias does not significantly differ from the one known at several other localities in the Tafilalt-Maider (see above).

The mound lithology is described by Kaufmann (1996, p. 27) as « *rather uniform and consisting of indistinctly thick-bedded, stromatactoid boundstones (purely descriptive : wackestones and floatstones). No distinction between flank- and core-facies can be made. (...) The beds dip away from the center suggesting that the mound grew concentrically, both expanding laterally and vertically. Unfortunately, no informations about eventual ecological succession within the mound can be obtained, because the Aferdou mound is not cut by erosion and therefore does not exhibit its internal structure* ». Our survey of the mound rather shew us that the mound itself is composed of a succession of facies that more likely reflects ecological succession (see description below and section under Stop 2. 5).

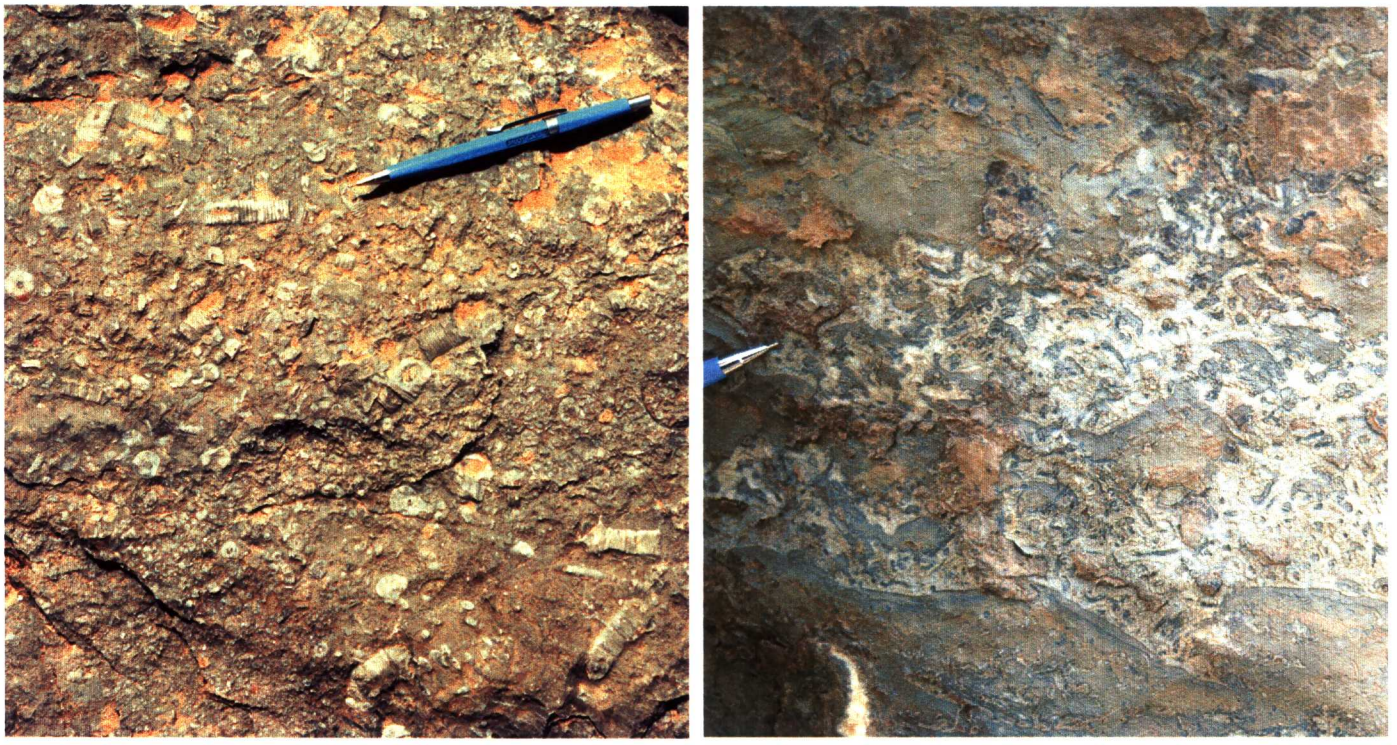

A

B

Figure 48 - Field photography of (A) the crinoidal sole limestone, and (B) the Auloporid boundstone facies with local large cement patches likely related to mud collapse in the Auloporid network.

Figure 49 - The Guelb el Mharch mound in the Oued Chouiref plain. *Note the dolomitization corridor across the mound (reddish material).*

A

B

Figure 50 - The magnificent Aferdou el Mrakib mound. (A) Viewed from the north. (B) Viewed from the southeast. *Width of mound is ~1200 meters, and height ~130 meters.*

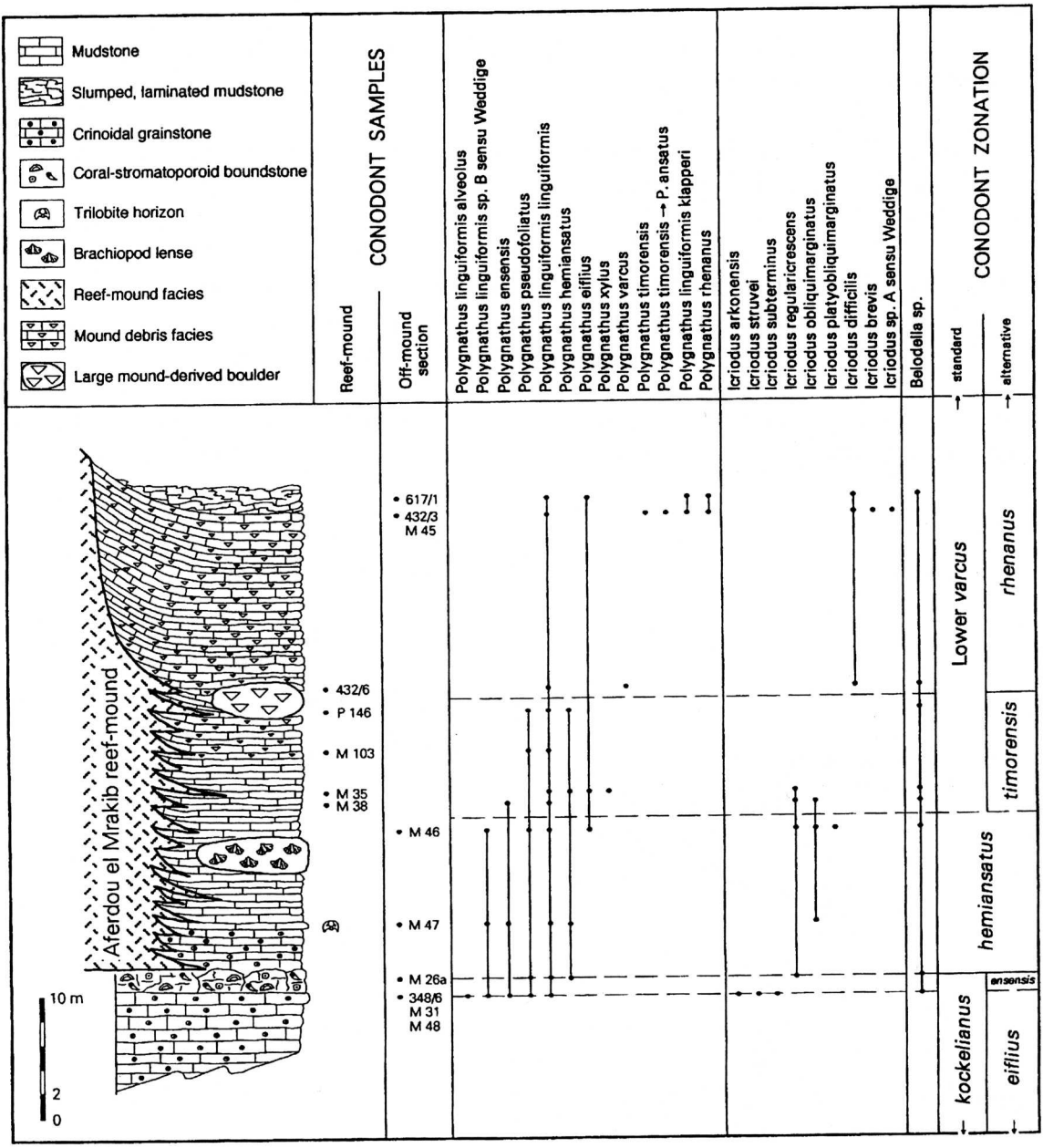

Figure 51 – Lithology of Aferdou el Mrakib off-mound section with conodont distribution. *Alternative conodont zonation after Belka et al. (1997). From Kaufmann (1996).*

Facies mosaic and Petrography

The distribution of facies at Aferdou el Mrakib mound is given on Figure 52. The succession underlying the mound is composed of three facies noted as AM-1 to AM-3.

Facies AM-1 : Tentaculitid fine-grained limestone and shale. The limestone is a tentaculitid-crinoid wackestone-packstone with accessory trilobites, bivalves and ostracodes.

Facies AM-2 : Phacopid beds. This constitutes a marker unit in the Jbel el Mrakib succession. It is a 1,5 m-thick packstone rich in the large phacopid trilobite *Drotops megalonamicus* which is found on fossil markets worldwide.

Facies AM-3 : Pentamerid beds. It is a 3 m-thick unit of tentaculitid packstone, similar to that of facies AM-1, very rich in articulated shells of the Gypidulid brachiopod *Ivdelinia sp.*

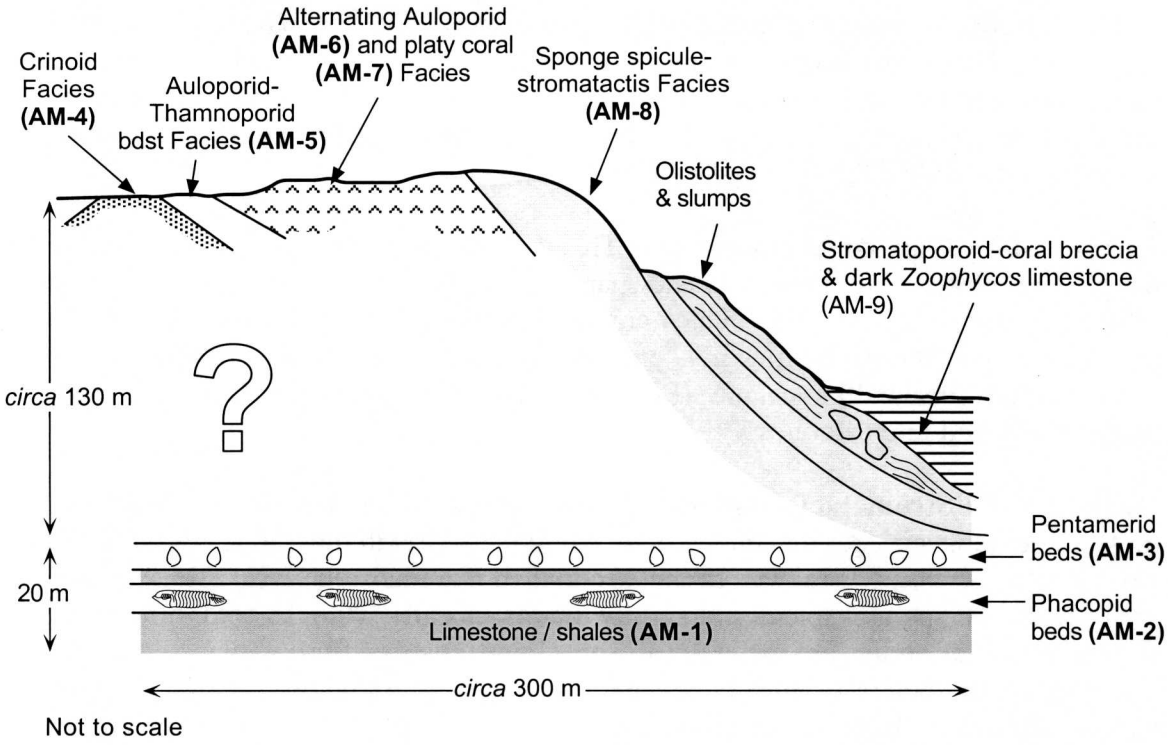

Figure 52 – Sketch showing facies distribution and relationships at Aferdou el Mrakib mound, Maïder basin.

The mound itself is composed of five facies, noted as AM-4 to AM-8, at least for the exposed part of the mound. The facies succession was observed on top of the mound, starting from the oldest exposed bed (see section under Stop 2.5). It is noteworthy that the core of the mound, below facies AM-4, is not exposed.

Facies AM-4 : crinoidal limestone. It is a calcarenite-calcirudite outcropping in 20 cm to 1 m-thick beds. The microfacies is a disarticulated crinoid ossicle-rich (20-30%) packstone-grainstone with accessory trilobites, brachiopod, bivalve, ostracode, and fenestrate and Fistuliporid bryozoan bioclasts. The lime mud matrix is uniform and often occur as infiltration in the grainstone; it makes up 25% of the facies. Auloporid boundstone occurs locally within this facies.

Facies AM-5 : Auloporid-Thamnoporid boundstone. This facies is made up of thick beds (1 m and up) of coral limestone alternating with crinoidal limestone beds identical to facies AM-4. The coral limestone is composed of delicate Auloporid (up to 30% in places) and Thamnoporid (10 to 15 %) tabulate corals (Fig. 53A), and a few Rugosan corals, with accessory (<5%) crinoid, trilobite, brachiopod, bivalve and ostracode bioclasts. The coral network has been infiltrated by uniform lime mud (10 to 20%) and cemented by isopachous crusts of fibrous-like calcite.

Facies AM-6 : Auloporid boundstone. This limestone is composed of a delicate network of 10 to 20% of unbroken Auloporid corals comprised in a lime mud matrix. It exhibits decimeter-sized stromatactis-like spar bodies with flat base and digitated top (Fig. 53B). These spar bodies originated more likely from early marine cementation of cavities created by local collapses of the mud within the coral network. The spar bodies are made up of isopachous crusts of fibrous-like calcite cement around the corals and other bioclasts (Fig. 53C).

Facies AM-7 : Platy coral boundstone. This thick bedded facies is mainly composed of the platy coral *Alveolites* (10-15%) and spar cement (up to 60%), with a lesser volume of infiltrated mud. The *Alveolites* plates are forming a very open framework with shelter cavities partly infiltrated by lime mud and subsequently cemented by isopachous crusts of early marine fibrous-like calcite (Fig. 54). Accessory bioclasts (5%) are crinoids, brachiopods, and rare trilobites.

Facies AM-8 : Stromatactis and sponge spicule limestone. This facies corresponds to most of the flank surfaces that envelop the Aferdou el Mrakib mound. It is a thick-bedded stromatactis calcilutite (Fig. 55). In thin sections, it is a mudstone-wackestone containing up to 10% of sponge spicules and tiny debris, locally with crinoid bioclasts. The stromatactis spar bodies are made up of isopachous crusts of fibrous-like calcite cement. The uppermost meters of this facies are deformed by slumping and locally contains meter-sized olistoliths of the same composition.

→

Figure 53 – Auloporid, and Auloporid-Thamnoporid boundstone facies (AM-5 and 6).

(A) Scanned thin-section showing coral frame infiltrated by microbioclastic mud (perched) and cemented by fibrous-like calcite crusts. Note the thin dark lining between generations of cement crusts. Bar scale is 1 cm. Sample 96AM-101.

(B) Field photography of Auloporid boundstone facies showing large cement patches likely related to mud collapse in the Auloporid network

(C) Scanned thin-section showing an Auloporid frame infiltrated by lime mud and cemented by fibrous-like isopachous calcite crusts. Note geopetal and perched mud. Bar scale is 1 cm. Sample 96AM-104.

B

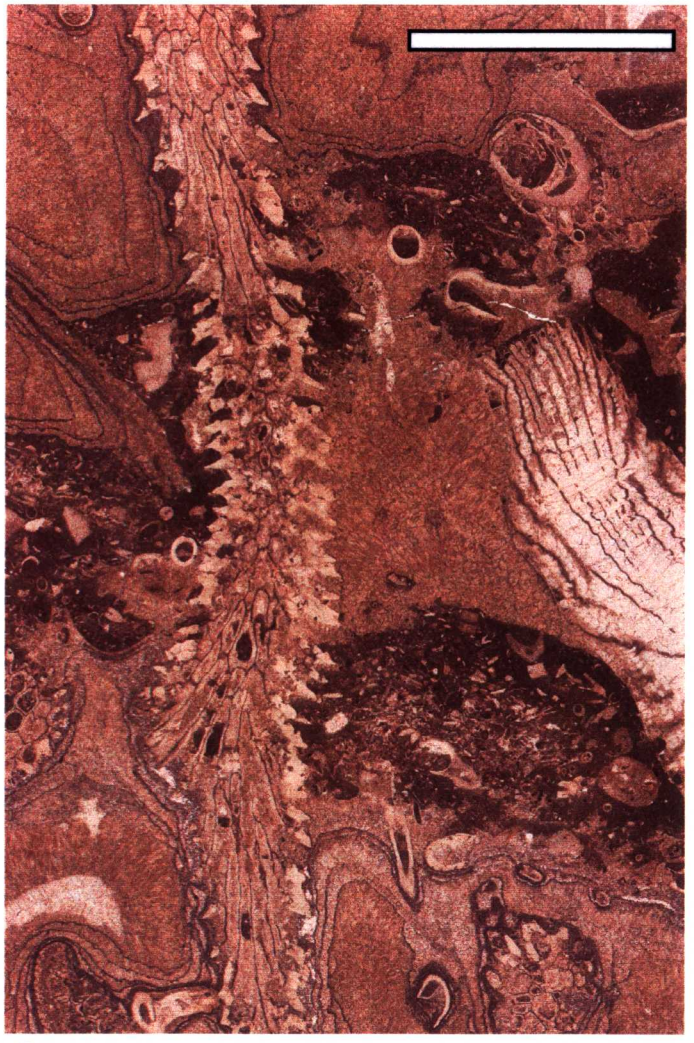

A

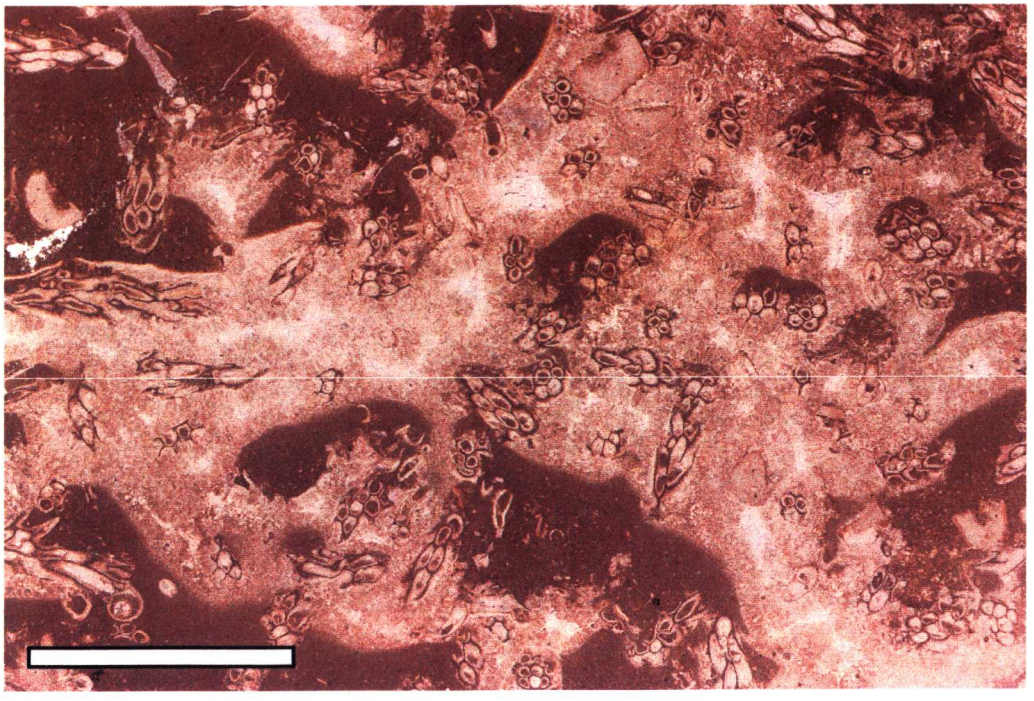

C

Auloporid, and Auloporid-
Thamnoporid bdst facies (AM-5 & 6)

Figure 54- Platy coral facies (AM-7).

(A) Field photography of the platy coral facies. The three components of this facies are readily observed here : platy corals (PC), isopachous fibrous-like cement (CM) below coral plates, and lime mud (LM).

(B) Scanned thin-section showing platy coral,cement and lime mud. Bar scale is 1 cm. Sample 96AM-114.

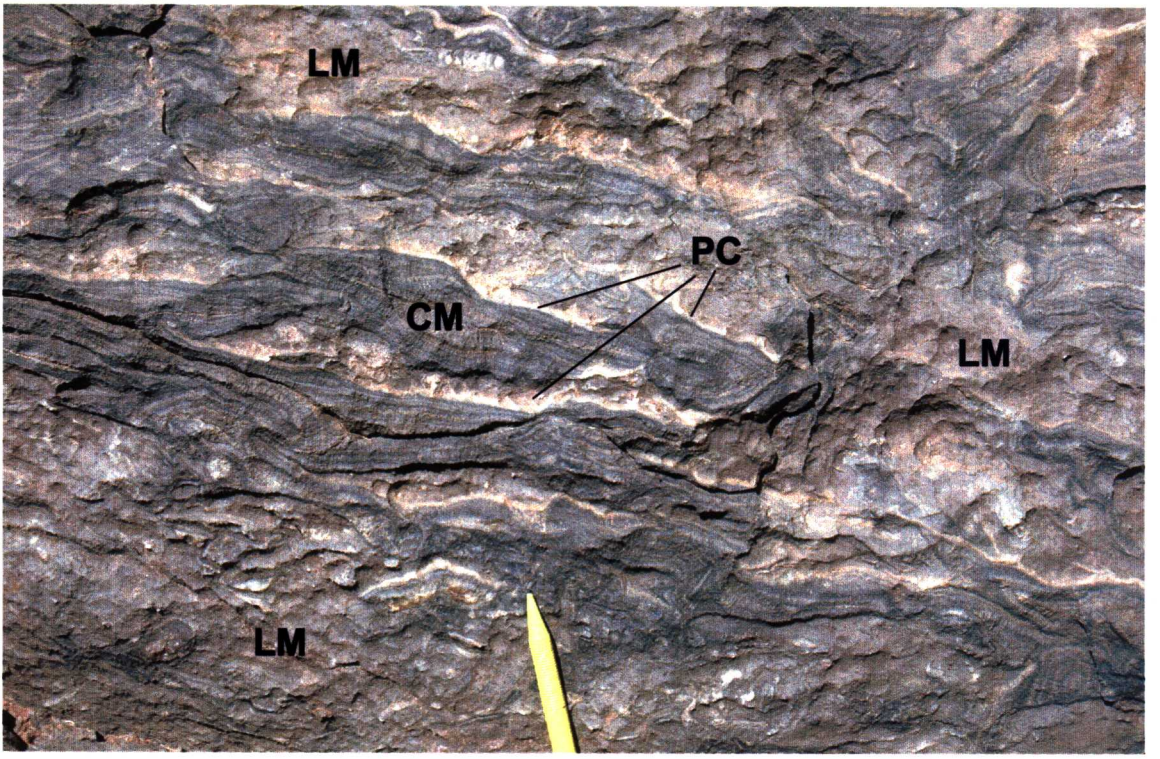

A

Platy coral bdst facies (AM-7)

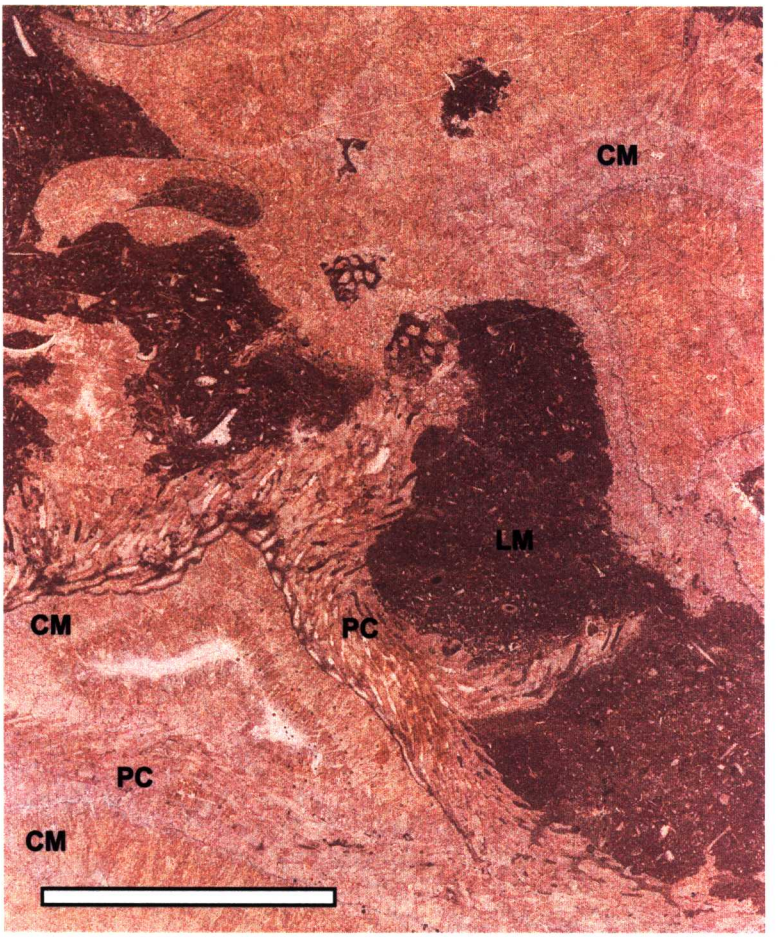

B

Figure 55 – Sponge spicule and stromatactis facies (AM-8).

(A) Field photography illustrating the stromatactis mudstone.

(B) Scanned thin-section showing the microbioclastic mudstone (polymud texture). Bar scale is 1 cm. Sample 96AM-123.

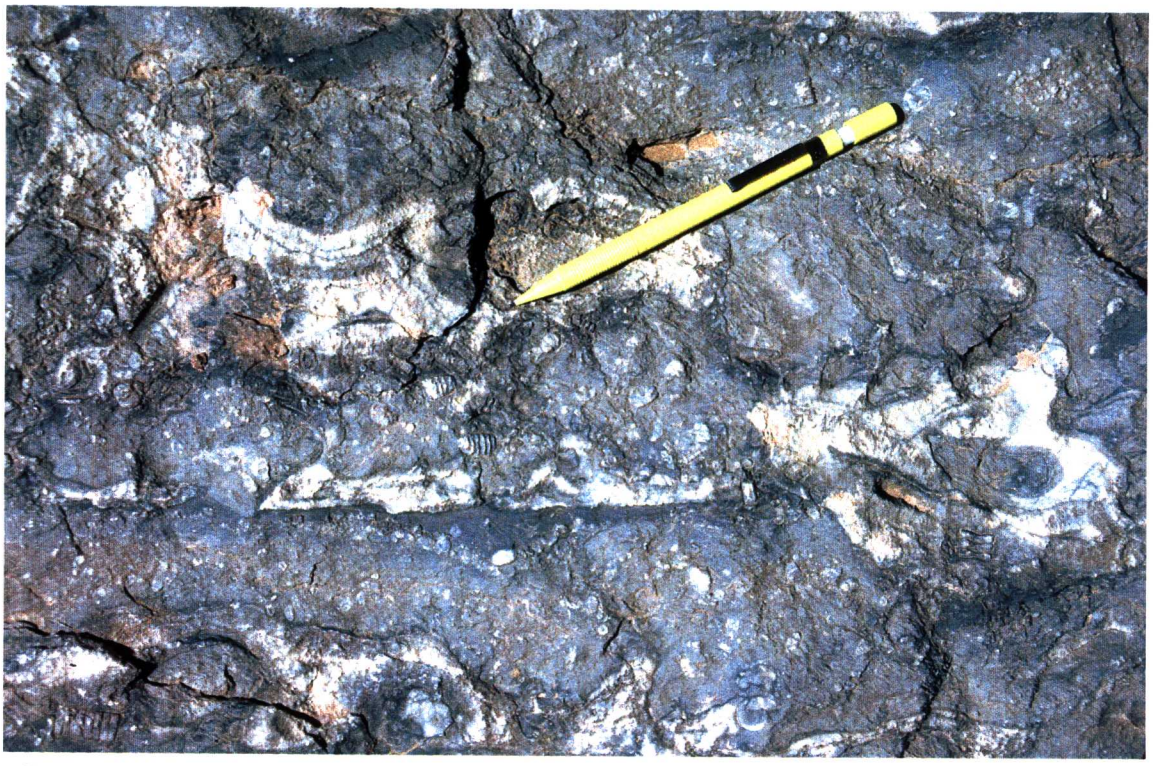

A

Sponge spicule - stromatactis mudst facies (AM-8)

B

The succession that onlaps the mound is composed of one facies, noted as AM-9.

Facies AM-9 : dark *Zoophycos* limestone with coral-stromatoporoid breccia. This Givetian dark limestone with local *Zoophycos* that contains beds of coral-stromatoporoid breccia is the same that occurs in several sections of the Tafilalt-Maïder (see above).

The mound facies are locally cross-cut by Neptunian dikes filled either by crusts of fibrous-like calcite cements or fine-grained sands « *comparable with that of the Lower Carboniferous deltaic facies that overlies the Devonian sequence in the eastern Anti-Atlas* » (Wendt, 1993, p.80). Dolomitization also has affected part of the mound limestones. A SW-NE trending corridor of dolomitization cross-cuts the southwestern mound flanks up to the core where, on top of the mound, nearly 70% of the limestone has been dolomitized (see Fig. 58B under stop 2.5 below).

Isotope geochemistry and significance

Cement stratigraphy of the Maïder mounds, performed under cathodoluminoscopy, is rather simple. Three cement phases, very similar to C1, C2 and C3 recognized in the Emsian kess-kess mounds of the Tafilalt, were distinguished and therefore also noted as C1, C2 and C3. We analyzed 79 samples for C and O stable isotope ratios from cements C1 and C3 (the C2 was too thin to be separated mechanically), and the microspar forming the bulk of the mounds. Distribution of analyses is the following : 44 samples from Aferdou el Mrakib mound, 18 samples from Guelb el Mharch, and 17 samples from Jbel el Otfal mound #2. An additional 3 samples from non-luminescent layers of brachiopod shells were also analyzed (Aferdou el Mrakib). Results are given on Fig. 56. These results are consistent with those published by Kaufmann (1997).

As in the case of the Tafilalt mounds, we analyzed also splits of 20 samples weighing from 2 to 4 mg for their $^{87}Sr/^{86}Sr$ ratios in cements C1 and C3, and the microspar. Results are given on Fig. 57.

Taken separately or all together, the results of C and O isotopic analyses can be grouped in three fields.

Field 1, at the one end of the spectrum, is made up of cement C1 and brachiopod values. In the three mounds, it presents values fairly well grouped within the range of $\delta^{18}O_{VPDB}$ = -5,0 to –2,3‰ and $\delta^{13}C_{VPDB}$ = +1,4 and +3,1‰. It is interpreted to indicate marine cementation because the values are in agreement with published values for Lower Devonian carbonates that are thought to have been in equilibrium with their respective seawater (Lohmann and Walker, 1989; Popp *et al.*, 1986; Lavoie, 1993 ; Veizer *et al.*, 1997). The $^{87}Sr/^{86}Sr$ ratios of cement C1 are also consistent with a marine origin (Burk *et al.*, 1982 ; Veizer, 1989).

Field 3, at the other end of the spectrum, corresponds to cement C3 values. These values are not as well grouped as those of field 1, but they nevertheless show a significant depletion in both ^{18}O and ^{13}C (a shift in $\delta^{18}O$ of 3,7‰ in average for the Aferdou el Mrakib mound, of 5,4‰ for the Guelb el Mharch mound, and of 4,5‰ for the Jbel el Otfal mound #2 ; and a shift in $\delta^{13}C$ of 0,8‰ in average for the Aferdou el

Mrakib mound, of 0,4‰ for the Guelb el Mharch mound, and of 0,4‰ for the Jbel el Otfal mound #2). We agree with Kaufmann's (1997) argumentation that these values are consistent with precipitation in the burial diagenetic environment. The latter evaluated the burial depth at 420-670 m, based on a pre-orogenic geothermal gradient of 50° C/km (Belka, 1991).

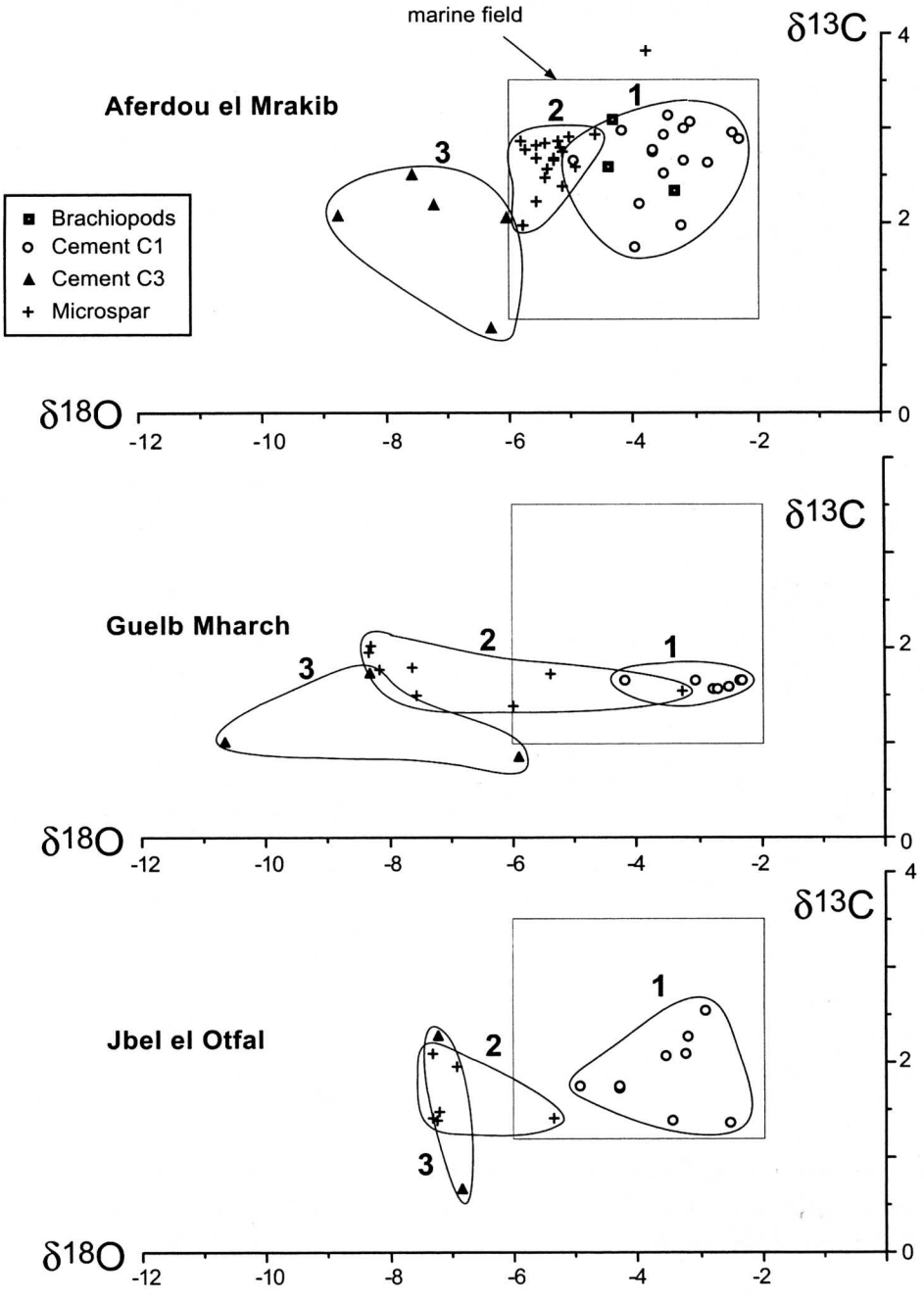

Figure 56 - Cross plot of $\delta^{18}O$ and $\delta^{13}C$ for cement phases C1, C3, microspar, and a few brachiopod samples of the Maïder mounds. *Marine water field, based on brachiopod shells (Lohmann and Walker, 1989; Popp et al., 1986; Lavoie, 1993 ; Veizer et al., 1997). VPDB (Vienna Peedee belemnite standard) standard used.*

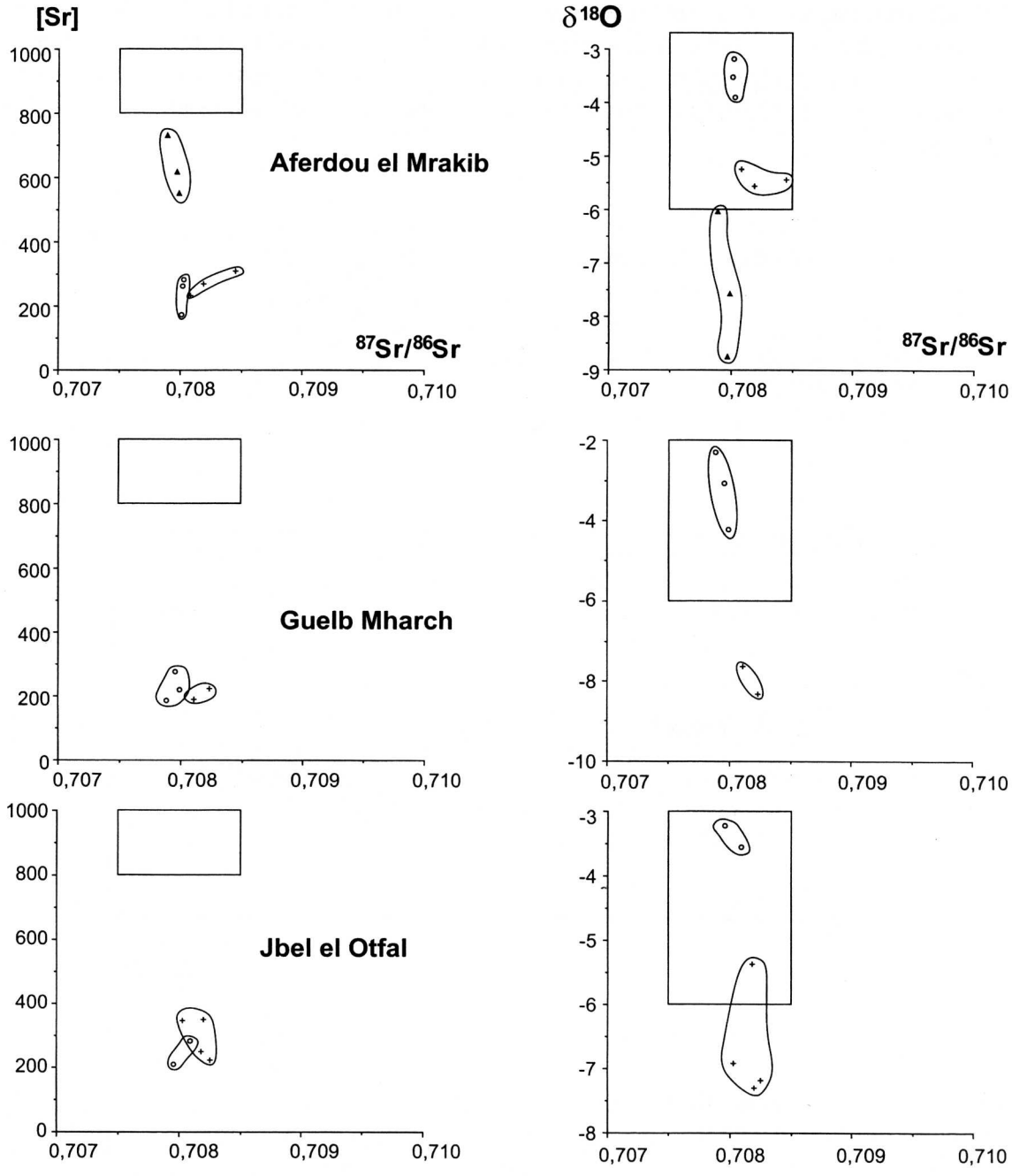

Figure 57 – Cross plot of $^{87}Sr/^{86}Sr$ and $\delta^{18}O$ for cement phases C1 and C3, and microspar, from split samples for C and O isotopic analyses, for the Maïder mounds. *Marine range is from Burke et al. (1982). VPDB is Vienna Peedee belemnite standard. Symbols are same as in Figure 56.*

Field 2, corresponding to the microspar values, has practically the same $\delta^{13}C$ average values as field 1, but yields in between field 1 and 3 as to the $\delta^{18}O$ values. This is particularly obvious for the Aferdou el Mrakib mound where the $\delta^{18}O$ shift is 1.8‰ in average. This can be translated into an increase of ~9° C in pore water fluid temperature compared to marine waters. If this increase in temperature is related to burial, the burial

depth can be estimated at ~180 m, based on a geothermal gradient of 50° C/km cited above. Kaufmann (1997) concluded that the depletion in ^{18}O of the microspar is related to a one-step neomorphism of a calcite micrite precursor (in opposition to an aragonite precursor) in the burial diagenetic, a conclusion to which we concur for the same reasons (low Sr content and presence of tiny micrite flakes observed under SEM). An alternative hypothesis would be to consider that cementation of the primary micrite occurred at *circa* 180 m of burial depth. Such cementation has been invoked by Bourrouilh *et al.* (1998) and Bourque *et al.* (1998) for Devonian mounds in Montagne Noire where cementation of the mud occurred at *circa* 150 m. However, the key observations that lead these workers to conclude to mud cementation at such a burial depth were not found here.

The $^{87}Sr/^{86}Sr$ ratios of microspar are consistent with a marine-derived fluids for the precipitation of the microspar (Fig. 57).

Speculative hypothesis on Maïder mound origin

A puzzling observation we made on the mound limestones at the Jbel el Otfal mound #2 is that geopetal surfaces in skeletal cavities or at base of stromatactis are parallel to accretionary surfaces (bedding planes), suggesting that sea-floor was sub-horizontal during deposition. The presence of a shale core which structure is not actually observable (horizontally bedded, deformed, chaotic?) adds to the puzzle. Together with occurrence of slumps in the beds capping the mound, these puzzling observations suggest that the mound shape may have been acquired, after limestone deposition, by deformation related for instance to slumping.

Very similar observations were made at Aferdou el Mrakib mound. The geopetal surfaces, either under the shelter cavities made by the *Alveolites* plates, or at base of stromatactis, also are parallel to bedding planes, a feature also noted by Kaufmann (1997). Moreover, we did not observe any ecological zonation from base to top of the mound along the enveloping facies AM-8 unit (Fig. 52). If the present day relief of the mound roughly represents relief during time of deposition (130 m minimum), it is surprising that no vertical ecological zonation developed in a 130 m of water depth range.

>>> For the sake of discussion. Can we rule out the possibility that the present day mound structure with steeply dipping flanks is a kind of pop-up structure created during Givetian time, just before deposition of the coral-stromatoporoid breccias and *Zoophycos* dark limestone (facies AM-9) (Mounji and Bourque, 1998; Mounji, 1999; Fig. 59 herein)? If so, the observed zonation, from muddy delicate coral facies to sponge spicules-stromatactis mudstone facies, and finally to the coral-stromatoporoid breccias and *Zoophycos* dark limestone, would represent an overall deepening trend.

Kaufmann (1997) proposed that « *the primary fine-grained carbonate originated from autochthonous precipitation by nonpreserved microbial (cyanobacteria/bacterial) communities. This hypothesis is supported by high accumulation rates (10-20 times higher than for the off-mound facies), purity of mound carbonates (>95%), and homogeneaous calcite mineralogy* (p. 947) ». We found no evidence supporting mud

production by microbial communities. Attributes of the volumetrically important coral facies (AM-5, 6 and 7) suggest that the coral played a significant role in baffling the mud (no matter how it was produced) and that very early cementation on the sea floor was a very active process leading to effective and rapid « mound » accretion. As to the overlying sponge spicule-stromatactis mudstone, it is very similar to the well known stromatactis mound facies of the Paleozoic, and is interpreted the same way (*e.g.*, Bourque and Boulvain, 1993).

Stage 1: Development of a vertically zoned biostromal structure, from delicate coral muddy facies to sponge spicule-rich stromatactis mudstone facies (AM-4 to 8).

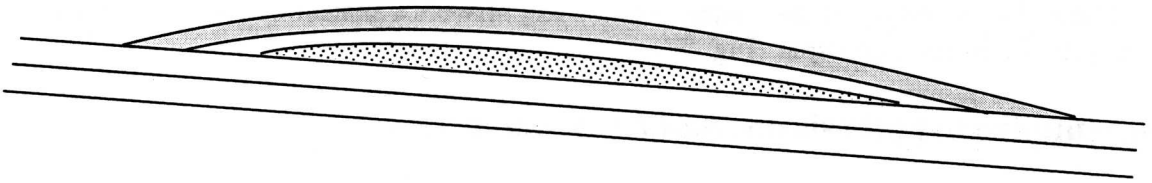

Stage 2: Sliding and pop-up. Olistholite and slump formation on mound flanks.

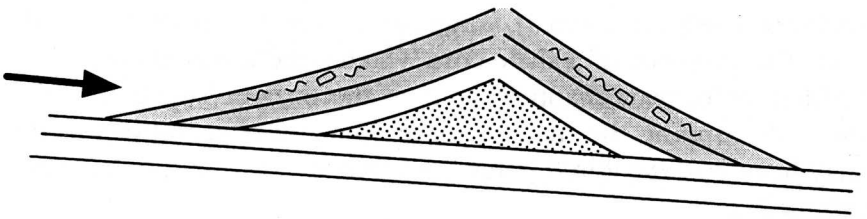

Stage 3: Progressive burial under coral-stromatoporoid breccias and dark *Zoophycos* limestones (AM-9).

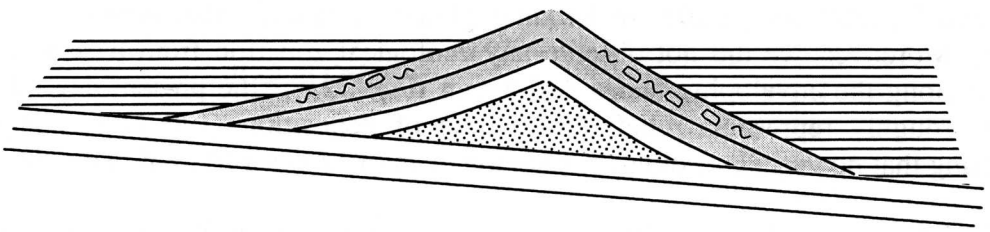

Figure 58 – Possible development sequence of the Aferdou el Mrakib mound, Maïder. *After Mounji and Bourque (1998) and Mounji (1999).*

Stop 2.5 Aferdou el Mrakib mound

Figures pertaining to this stop are Figures 45, 52, 59, and 60.

Be prepared for a long day. We will arrive from the north and will climb on top of the mound (Fig. 59B) to observe the more complete section of this mound (Fig. 60). While getting down, we will look at relationships between the mound and off-mound facies.

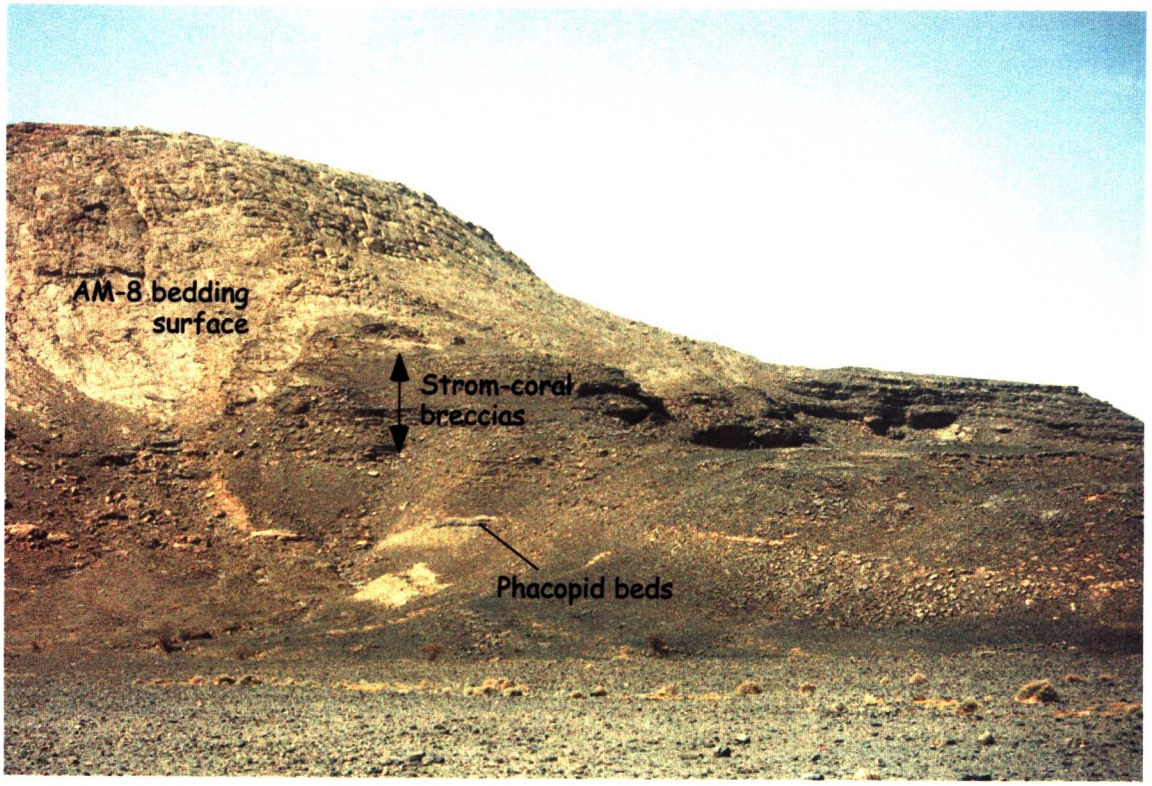

A

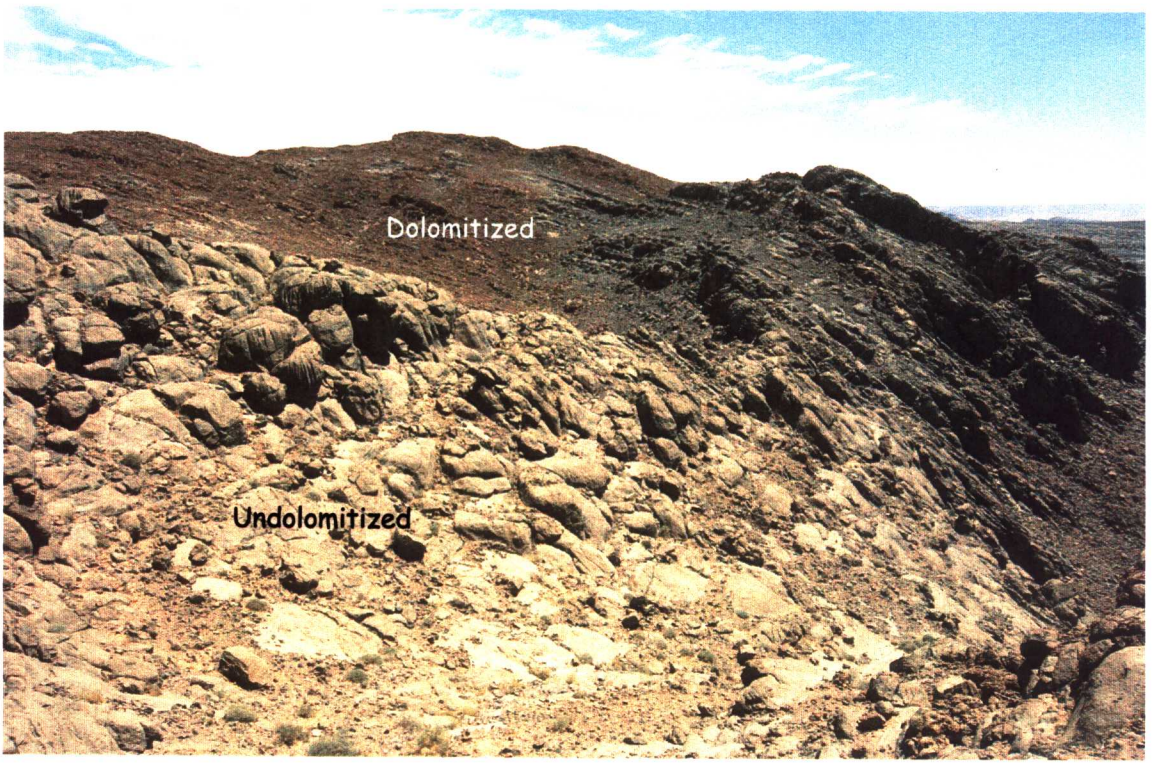

B

Figure 59 - The Aferdou el Mrakib mound, Maïder. *(A) The stromatoporoid-coral breccia units onlapping facies AM-8 forming the mound outer surface. (B) Part of the section on top of the mound (Stop 2.5).*

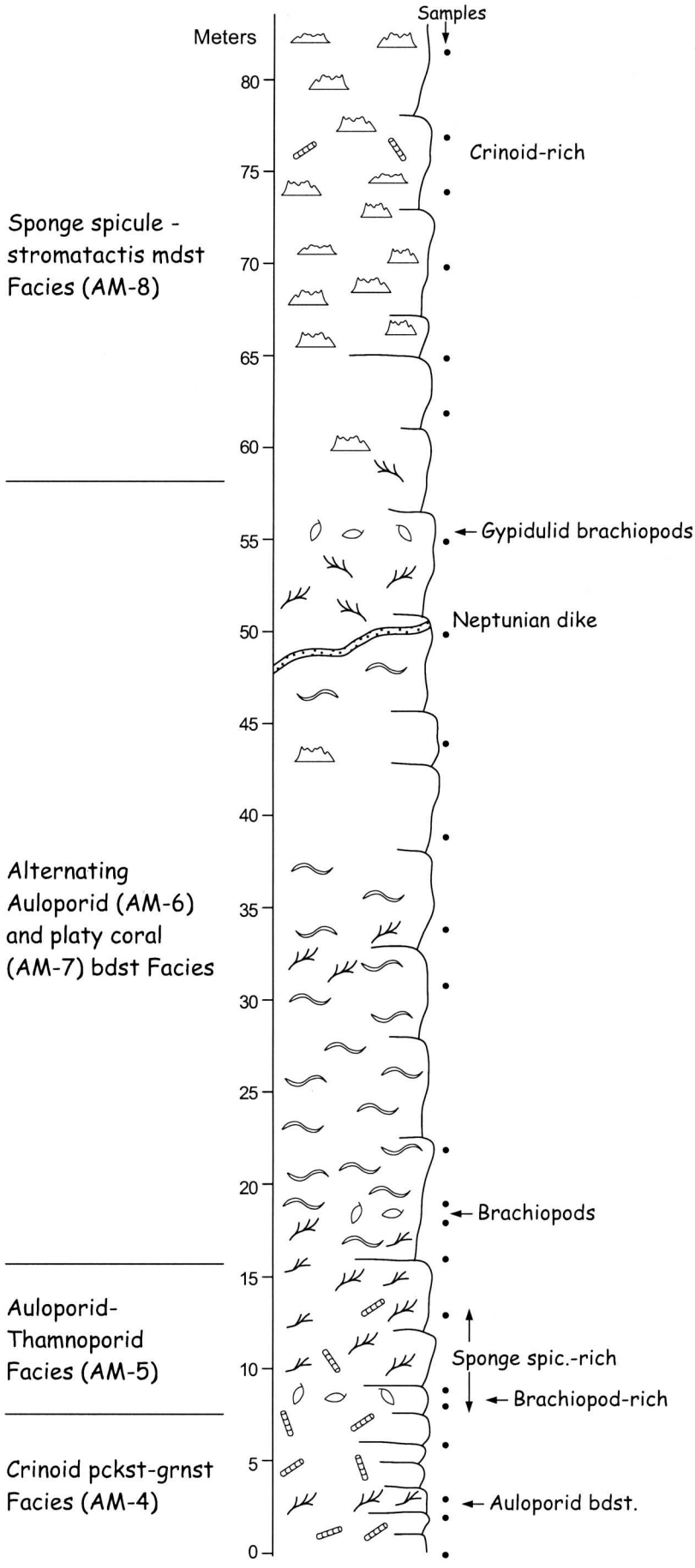

Figure 60 - Facies succession on top of Aferdou el Mrakib mound, Stop 2.5.

References cited

Alem, A. and **Gendrot, C.,** 1968, Étude sur l'Hamar Lakhdad (Tafilalt), Rapport interne du Bureau de recherches et de participation minières, Département Pétrole, Maroc.

Bathurst, R.C.G.,1958, Diagenetic frabrics in some Dinantian limestones: Liverpool Manchester Geological Journal, v. 2, p. 11-36.

Bathurst, R.C.G.,1975, Carbonate sediments and their diagenesis: Elsevier Scientific Publishing Company, Amsterdam, Oxford, New York, 658 p.

Beauchamp, B., and **Savard, M.M.**, 1992. Cretaceous Chemosynthetic Carbonate Mounds in the Canadian Arctic. Palaios, v. 7, p. 434-450.

Becker, R. T., and **House, M. R.**, 1991, Eifelian to Early Givetian goniatites at Boutchrafine and Jbel Amelane, Tafilalt (Anti-Atlas, S. Morocco). Field meeting of the Subcommission on Devonian Stratigraphy I.U.G.S., 28, Guidebook. p. 59- 73.

Becker, R. T., and **House, M. R.**, 1994a, International Devonian goniatite zonation, Emsian to Givetian, with new records from Morocco. Cour. Forsch. -Inst. Senckenberg, v. 169, p. 79- 135.

Becker, R. T., and **House, M. R.**, 1994b, Kellwasser events and goniatites successions in the Devonian of the Montagne Noire with comments on possible causations. Cour. Forsch. -Inst. Senckenberg, v. 169, p. 45-77.

Belka, Z., 1991, Conodont colour alteration patterns in Devonian rocks of the eastern Anti-Atlas, Morocco. Jour. African Earth Sci., v. 12, p. 417-428.

Belka, Z., 1998, Early Devonian Kess-Kess carbonate mud mounds of the eastern Anti-Atlas (Morocco), and their relation to submarine hydrothermal venting. Jour. Sedimentary Research, v.. 68, p. 368-377.

Belka, Z., **Kaufmann, B.**, and **Bultynck, P.**, 1997, Conodont-based quantitative biostratigraphy for the Eifelian of the eastern Anti-Atlas, Morocco. Geol. Soc. America Bull., v. 109, p. 643-651.

Bensaid, M., 1974, Étude sur des goniatites à la limite du Dévonien moyen et supérieur du Sud marocain. Notes et Mémoires du Service Géologique du Maroc, no. 264, p. 81-140.

Bensaid, M., **Bultynck, P.**, **Sartenaer, P.**, **Walliser, O.H.** and **Ziegler, W.**, 1985, The Givetian-Frasnian Boundary in pre-Sahara Morocco. Cour. Forsch.-inst. Senckenberg, v. 75, p. 287-300.

Bourrouilh, R., **Bourque, P.-A., Dansereau**, P., **Bourrouilh, F.**, and **Weyant, P.** 1998. Sea-level variations on a Paleozoic carbonate platform margin: A Devonian Montagne Noire example. Sedimentary Geology, v. 118, p. 95-118.

Bourque, P.-A., and **Boulvain, F.**, 1993, A model for the origin and petrogenesis of the red stromatactis limestone of Paleozoic carbonate mounds. Jour. Sed. Petrology, v. 63, p. 607-619.

Bourque, P.-A., **Dansereau, P.**, and **Bourrouilh, R.** 1998. Early cementation of mud-rich mounds: how early? GAC-MAC-APGGQ Annual meeting, Québec, Abstracts with Program, v. 23, p. A22-23.

Bourque, P.-A., **Madi, A.**, and **Mamet, B. L.**, 1995, Waulsortian-type bioherm development and response to sea-level fluctuations: Upper Visean of Bechar basin, Western Algeria. Jour. Sed. Research, v. 65, p. 80-95.

Bourque, P.-A., and **Raymond, L.**, 1994, Diagenetic alteration of early cement of Upper Silurian stromatactis. Sedimentology, v. 41, p. 255-269.

Brachert, T.C., **Buggish, W.**, **Flügel, E.**, **Hüssner, H.M.**, **Joachimski, M.M.**, **Tourneur, F.** et **Walliser, O.H.**, 1992, Controls of mud mound formation: the Early Devonian Kess-Kess Carbonates of Hamar Laghdad, Anti-Atlas, Morocco. Geologische Rundshau v. 81, p. 15-44.

Bultynck, P., 1985, Lower Devonian (Emsian)- Middle Devonian (Eifelian lowermost Givetian) conodont successions from the Ma'der and the Tafilalt, southern Morocco. Cour. Forsch.-inst. Senckenberg, v. 75, p. 261-286.

Bultynck, P., 1987, Pelagic and neritic conodont successions from the Givetian of Pre-Sahara Morocco and the Ardennes. Bull. Institut Royal des Sciences Naturelles de Belgique, Sciences de la Terre, v. 57, p. 149-181.

Bultynck, P., 1989, Conodonts from a potential Eifelian-Givetian Global Boundary Stratotype at Jbel Oudriss, Southern Ma'der, Morocco. Bull. Institut Royal des Sciences Naturelles de Belgique, Sciences de la Terre, v. 59, p. 95-103.

Bultynck, P., and **Hollard, H.**, 1980, Distribution comparée de conodontes et goniatites dévoniennes des plaines du Dra, du Ma'der et du Tafilalt (Maroc). Aardkundige Mededelingen, v. 1, 73 p.

Bultynck, P., and **Jacobs, L.**, 1981, Conodontes et sédimentologie des couches de passage du Givetien au Frasnien dans le Tafilalt et dans le Ma'der (Maroc présaharien). Bull. Institut Royal des Sciences Naturelles de Belgique, Sciences de la Terre, v.. 53, p. 1-34.

Burgess, C.J., and **Lee, C.W.**, 1978, The development of a Lower Jurassic carbonate tidal flat, Central High Atlas, Morocco. 1: Sedimentary history.- Jour. Sed. Petrol., v. 48, p. 777-794.

Burke, W. H., **Denison, R. E.**, **Hetherington, E. A.**, **Koepnick, R. B.**, **Nelson, H. F.**, and **Otto, J. B.**, 1982, Variations of seawater $^{87}Sr/^{86}Sr$ throughout Phanerozoic time. Geology, v. 10, p. 516-519.

Choubert, G., 1948, Sur la géologie des plaines de Dra et le Tazout. Comptes Rendus sommaires de la Société Géologique de France, v. 5, p. 99-101.

Choubert, G., 1952, Histoire géologique du domaine de l'Anti-Atlas. *In* Géologie du Maroc, Fasc. 1, Notes et Mémoires du Service Géologique du Maroc, no. 100., Rabat.

Choubert, F., **Clariond, L.**, and **Hindermayer, J.**, 1952, Anti-Atlas central et oriental. XIX Cong. Géol. Internat., Alger, Livret-guide, Excursion C 36, Ser. Maroc, no. 100, p. 77-194, Rabat.

Clariond, L., 1934, La série Paléozoïque des territoires du Tafilalt (Maroc). Comptes Rendus, Académie des Sciences de Paris, v. 198, p. 2270-2272.

Clariond, L., 1935, Etude stratigraphique sur les terrains du sud marocain. La série Primaire du Saghro, du Maïder et du Tafilalet. Publ. Ass. Et. géol. Méditerr. occid., v. 5, Part 1, no 12.

Clariond, L., and **Hindermayer, J.**, 1952, Anti-Atlas Central et Oriental. Excursion C 36, Livret Guide 19e Congr. géol. int., Alger, sér. Maroc. No. 11, Rabat.

Dresnay, R. du, 1971, Extension et développement des phénomènes récifaux jurassiques dans le domaine atlasique marocain, particulièrement au Lias moyen. Bull. Soc. géol. France, v. 13, p. 46-56.

présaharien). Comptes Rendus sommaires de la Société Géologique de France, 1962, p. 175-177.

Hollard, H., 1963, Un tableau stratigraphique du Dévonien du Sud de l'Anti-Atlas. Notes Serv. Géol. Maroc, no. 172, p. 105-109.

Hollard, H., 1965, Précisions sur la stratigraphie et la répartition de quelques espèces importantes du Silurien supérieur et de l'Éodévonien du Maroc présaharien. Notes et Mémoires Service Géologique du Maroc, no. 183, p. 23-32.

Hollard, H., 1967, Le Dévonien du Maroc et du Sahara nord-Occidental. *In* Symp. Devonian Syst., Calgary, 1967, Alberta. Canadian Soc. Petr. Geol., v. 1, p. 203-244.

Hollard, H., 1974, Recherches sur la stratigraphie des formations du Dévonien moyen, de l'Emsien supérieur au Frasnien, dans le Sud du Tafilalt et dans le Maïder (Anti-Atlas oriental). Notes Mém. Serv. Géol. Maroc, N°. 264, p. 7-68.

Hollard, H. 1977. Le domaine de l'Anti-Atlas au Maroc. The Anti-Atlas area in The silurian-devonian Boundary. IUGS Series A, N°. 5, p. 168-194.

Hollard, H. 1981. Principaux Caractères des formations dévoniennes de l'Anti-Atlas. Notes et Mémoires du Service Géologique du Maroc, no. 308, p.15-21.

Hopkins, J.C., and **Aitken, S. A.**, 1993, Porosity developpement in Devonian carbonates, Tafilalt Basin. Office Nationale de Recherches et d'Explorations Petrolières du Maroc (ONAREP), Internal Report.

Hovland, M., 1992, Hydrocarbon seeps in northern marine waters - their occurence and effects. Palaios, v. 7, p. 376-382.

Jacobshagen, V., **Görler, K.**, and **Giese, P.**, 1988, Geodynamic evolution of the Atlas System (Morocco) in post-Palaeozoic times. In: Jacobshagen, V. (ed.) The Atlas System of Morocco. Lect. Notes Earth Sciences, v. 15, p. 481-499.

James, N.P., and **Bourque, P.-A.** I992. Reefs and Mounds, *In* Walker, R., and James, N.P. (eds.), Facies Models, Response to Sea-Level change. Geological Association of Canada, p. 323-347.

Jenkyns, H.C., 1988, The Early Toarcian (Jurassic) anoxic event: Stratigraphic, sedimentary, and geochemical evidence. American Journal of Science, v. 288, p. 101-151.

Kaufmann, B., 1996, Facies, Stratigraphy and Diagenesis of Middle Devonian reef and mud-mounds in the Mader (eastern Anti-Atlas, Morocco). Unpublished Ph.D. thesis, Tübingen University, 70 p.

Kaufmann, B., 1997, Diagenesis of Middle Devonian carbonate mounds of the Mader Basin (eastern Anti-Atlas, Morocco). Jour. Sed. Research., v.. 67, p. 945-956.

Kaufmann, B., 1998, Facies, Stratigraphy and Diagenesis of Middle Devonian reef and mud-mounds in the Mader (eastern Anti-Atlas, Morocco). Acta Geologica Polonica, v. 48, p. 43-106.

Kaufmann, E. G., **Arthur, M. A.**, **Howe, B.**, and **Scholle**, P. A., 1996, Widespread venting of methane rich fluids in Late Cretaceous (Campanian) submarine springs (Tepee Buttes), Western Interior seaway, U.S.A. Geology, v. 24, p. 799-802.

Lasemi, Z., and **Sandberg, P.A.,** 1984, Transformation of aragonite dominated lime muds to microcrystalline limestones. Geology, v. 12, p. 420-423.

Lasemi, Z., **Sandberg, P.A.**, and **Boardman, M.R.**, 1990, New microtextural criterion for differentiation of compaction and early cementation in fine-grained limestones. Geology, v. 18, p. 370-373.

Lavoie, D., 1993, Early Devonian marine isotopic signatures: Brachiopods from the upper Gaspé Limestones, Gaspé Peninsula, Québec, Canada. Jour. Sed. Pet., v. 63, p. 620-627.

Lees, A., and **Miller, J.**, 1985, Facies variation in waulsortian buildups, Part 2; Mid-Dinantien buildups from Europe and North America. Geological Journal, v. 20, p. 159-180.

Lees, A., and **Miller, J.**, 1995, Waulsortian banks. *In* Monty, C. L. V., Bosence, D. W. J., Bridges, P. H., and Pratt, B. R. (eds), 1995, Carbonate Mud-Mounds, Their Origin and Evolution. Internat.. Ass. Sed., Spécial Publication, p. 191-271.

LeMaître, D., 1947a, Le récif coralligène de Ouihlane. Notes et Mémoires du Service Géologique du Maroc, N° 8, p. 1-113.

LeMaître, D. 1947b. Contribution à l'étude du Dévonien du Tafilalet. II- Le récif corralligène de Ouihlane. Protectorat de la république Française au Maroc. Direction de la production industrielle et des mines. Division des mines et de la géologie. Service géologique, Notes et mémoires, no. 67, 115 p.

Little, C.T.S., and **Benton, M.J.**, 1995, Early Jurassic mass extinction: A global long-term event. Geology, v. 23, p. 495-498.

Lohmann, K. C., and **Walker, C. G.**, 1989, The $\delta^{18}O$ record of Phanerozoic abiotic marine calcite cements. Geophysical Research Letters, v. 16, p. 319-322.

Manspeizer, W., 1988, Triassic-Jurassic rifting and opening of the atlantic: an overview. In: Manspeizer, W. (ed.), Triassic-Jurassic Rifting. Dev. Geotectonics, v. **22**, part A, p. 41-79.

Manspeizer, W., Puffer, J.H., and **Cousminer, H.L.**, 1978, Separation of Morocco and eastern North America: A Triassic-Liassic stratigraphic record. Geol. Soc. Am. Bull., v. 89, p. 901-920.

Massa, A., 1965, Observations sur les Séries Siluro-Dévoniennes des Confins Algéro-Marocains du Sud. Compagnie Française des Pétroles, Notes et Mémoires, no. 8.

Mattis, A.F., 1977, Nonmarine Triassic sedimentation, Central High Atlas Mountains, Morocco.- Jour. Sed. Petrol., v. 47, p. 107-119.

Mehdi, M., 1995, Stratigraphie intergrée, analyse séquentielle et micropaléontologie du Jurassique et du Crétacé inférieur de l'avant-pays Rifain oriental (Maroc). Unpublished D.Sc. thesis, Université Mohamed I, Faculté des Sciences, Oujda, 345 p.

Menchikoff, N., 1933, La série Primaire de la Saoura et des chaînes d'Ougarta. Bull. Serv. Géol. Algérie, 2nd Ser., Fasc. II, p. 109-123.

Menchikoff, N., 1936. Etudes géologiques sur les confins algéro-marocains du Sud. Bull. Soc. Géol. France-Paris, 5th Ser., Tome-6.

Michard, A., 1976, Éléments de Géologie Marocaine. Notes et Mémoires du Service Géologique du Maroc, v. 252, 408 p.

Montenat, C., **Baidder**, L., **Barrier**, P., **Hilali**, A., **Lachkhem**, H., **Mennig**, J. 1996. Contrôle tectonique de l'édification des monticules biosédimentaires dévoniens du Hmar Lakhdad d'Erfoud (Anti-Atlas oriental, Maroc). Comptes Rendus de l'Academie des Sciences, Serie II. Sciences de la Terre et des Planètes, v. 323 (4), p. 297-304.

Monty, C. L. V., **Bosence, D. W. J.**, **Bridges, P. H.**, and **Pratt, B. R.** (eds), 1995, Carbonate Mud-Mounds, Their Origin and Evolution. Internat.. Ass. Sed., Spécial Publication, no. 23, 537p.

Mounji, D., 1995, Pétrogenèse des monticules kess-kess dévoniens de Hamar-Lakhdad, Tafilalt, Anti-Atlas Oriental, Maroc. Unpublished M.Sc. thesis, Université Laval, Québec, 91 p.

Mounji, D., 1999, Les plates-formes carbonatées d/voniennes du Tafilalt-Maïder, Anti-Atlas oriental, Maroc : sédimentologie, diagenèse et potentiel pétrolifère. Unpublished Ph.D. thesis, Université Laval, Québec. 307 p.

Mounji, D., and **Bourque, P.-A.** 1998. The Devonian mound-like structures of the Maider Basin, Moroccan Sahara: mud mounds or pop-up structures? GAC-MAC-APGGQ Annual meeting, Québec, Abstracts with Program, v. 23, p. A129.

Mounji, D., **Bourque P.-A.**, and **Savard, M. M.**, 1996, Architecture and isotopic constraints on origin of Lower Devonian conical mounds (Kess-Kess) of Tafilalt, Anti-Atlas, Morocco. Internat. Assoc. Sed., 17th African-European Meeting, Sfax, Tunisia, Abstracts, p. 192-193.

Mounji, D., **Bourque P.-A.**, and **Savard, M. M.**, 1998, Hydrothermal origin of Devonian conical mounds (kess-kess) of Hamar-Lakhdad Ridge, Anti-Atlas, Morocco. Geology, v. 26, p. 1123-1126.

Munnecke, A., **Westphal, H.**, **Reijmer, J.J.G.**, and **Samtleben, C.**, 1997, Microspar development during early marine burial diagenesis: a comparison of Pliocene carbonates from the Bahamas with Silurian limestones from Gotland (Sweden). Sedimentology, v. 44, p. 977-990.

Neuweiler, F., and **Mehdi, M.**, (In prep.), Liassic mud mounds and related sedimentary facies (Central High Atlas, Morocco). Facies.

Noel, M., and **Hounslow, M. W.**, 1988, Heat flow evidence for hydrothermal convection in Cretaceous crust of Madeira Abyssal Plain. Earth and Planetary Science Letters, v. 90, p. 77-86.

ONAREP, 1998, Paleozoic Depositional System: Geology & Play Concept : Internal Report: Second Seminar on Petroleum Exploration in Morocco, Rabat, November 24-25), 32p.

O'Neil, J. R., **Clayton, R. N.**, and **Mayeda, T. K.**, 1969, Oxygen isotope fractionation in divalent metal carbonates. Jour. Chemical Physics, v. 12, p. 5547-5558.

Peckmann, J., **Walliser, O. H.**, **Riegel, W.**, and **Reitner, J.** 1999. Signatures of hydrocarbon venting in a Middle Devonian Carbonate mound (Hollard Mound) at the Hamar Laghdad (Anti-Atlas, Morocco). Facies, v. 40, p. 281-296.

Pichler, T., and **Dix, G. R.**, 1996, Hydrothermal venting within a coral reef ecosystem, Ambitle Island, Papua New Guinea. Geology, v. 24, p. 435-438.

Piqué, A., and **Michard, A.**, 1989, Moroccan Hercynides: A synopsis. The Paleozoic Sedimentary and Tectonic Evolution at the Northern Margin of West Africa. American Journal of Science, v. 289, p. 286-330.

Popp, B. N., **Anderson, T. F.**, and **Sandberg, P. A.**, 1986, Brachiopods as indicators of original isotopic composition in some Paleozoic limestones. Bull. Geological Society of America, v. 97, p. 1261-1269.

Reitner, J., **Arp, G.**, **Theil, V.**, **Gautret, P.**, **Galling, U.**, and **Michaelis, W.**, 1997, Organic matter in Great Salt Lake Ooids (Utah, USA)-First approach to a formation via organic matrices. Facies, v.. 36, p. 210-219.

Rio, M., **Roux, M.**, **Renard, M.**, and **Schein, E.**, 1992, Chemical and isotopic features of present day bivalve shells from hydrothermal vents or cold seeps. Palaios, v. 7, p. 351-360.

Robertson's Research Limited Inc., 1993, The Geology and Hydrocarbon Potential of the South Atlas Region of Morocco. ONAREP/ exploration, internal report by Robertson Research International Limited (United Kingdom).

Roch, E., 1934, Sur des phénomènes remarquables observés dans la région d'Erfoud (confins algéro-marocains du Sud). Publ. Ass. Et. Géol. Méditeranée occidentale, v. 5, p. 1-10.

Schwarz, G., and **Wigger, P.J.**, 1988, Geophysical studies of the earth's crust and upper mantle in the Atlas system of Morocco. *In* Jacobshagen, V. (ed.), The Atlas System of Morocco. Lect. Notes Earth Sciences, v. 15, p. 339-357.

Septfontaine, M., 1986, Milieux de dépots et foraminifères (Lituolidés) de la plate-forme carbonatée du Lias Moyen au Maroc. Revue de Micropaléontologie, v. 28, p. 265-289.

Töneböhn, R., 1991, Bildungsbedingungen epikontinentaler Cephalopodenkalke (Devon, SE-Marokko). Göttinger Arbeiten zur Geologie und Paläontologie, Göttingen, v. 47, 114 p.

Veizer, J., Bruckschen, P., Pawellek, F., Diener, A., Podlaha, O. G., Garden, G. A. F., Jasper, T., Korte, C., Strauss, H., Azmy, K., and **Ala, D.**, 1997, Oxygen isotope evolution of Phanerozoic seawater. Palaeogeography, Palaeoclimatology, Palaeoecology, vl. 132, p. 159-172.

Walliser, O. H. (ed.) 1991. Morocco field meeting of the subcomission on Devonian stratigraphy. I.U.G.S. Nov. 28- Dec. 5 (Guide book), p. 1-79.

Walliser, O. H., Bultynck, P., Weddige, K., Becker, R. T., and **House, M. R.**, 1995, Definition of the Eifelian-Givetian Stage boundary. Episodes, v. 18, p. 107-115.

Warme, J.E., 1988, Jurassic carbonate facies of the Central and Eastern High Atlas rift, Morocco. *In* Jacobshagen, V. (ed.), The Atlas System of Morocco. Lect. Notes Earth Sciences, v. 15, p. 169-199.

Warme, J.E. (ed.), 1989, Evolution of the Jurassic High Atlas rift, Morocco: Transtension, structural and eustatic controls on carbonate facies, tectonic inversion. Guidebook, Am. Assoc. Petr. Geol. Field seminar, 24 September to 1 October 1989, Publ. No. 9, Exploration Geosciences Institute, Colorado School of Mines, Colorado, U.S.A., 332 p.

Wendt, J., 1988, Facies pattern and paleogeography of the Middle and Late Devonian in the eastern Anti-Atlas (Morocco). *In* McMillan, N.J., Embry, A.F. & Glass, D.G. (eds). Devonian of theWorld, Canadian Soc. Petrol. Geol. Memoir 14, v. I, p. 467-480.

Wendt, J., 1993, Steep-Sided carbonate mud mounds in the Middle Devonian of the eastern Anti-Atlas, Morocco. Geological Magazine, v. 130, p. 69-83.

Wendt, J., and **Aigner, T.**, 1985, Facies patterns and depositional environments of Paleozoic cephalopod limestones. Sedimentary Geology, v. 44, p. 263-300.

Wendt, J., Aigner, T., and **Neugebauer, J.**, 1984, Cephalopod limestone deposition on a shallow pelagic ridge: The Tafilalt-Platform (Upper Devonian, Eastern Anti-Atlas, Morocco). Sedimentology, v. 31, p. 601-625.

Wendt, J., and **Belka, Z.**, 1991, Age and depositional environment of Upper Devonian (Early Frasnian to Early Famennian) black shales and limestones (Kellwasser Facies) in the Eastern Anti-Atlas, Morocco. Facies, v. 25, p. 51-90.

Oral Session

-Abstracts-

Cretaceous methane-derived carbonate mounds in the Canadian Arctic: end-member of the chemosynthetic-photosynthetic reef continuum

***Benoit Beauchamp**, Geological Survey of Canada, Calgary, Canada, bbeauchamp@gsc.nrcan.gc.ca*

Sea-floor hydrocarbon seepage and/or hydrothermal fluid venting is a common phenomenon in many modern sedimentary basins, occurring in a variety of low to high latitude settings, from the shallowest water areas to abyssal depths. This phenomenon is invariably associated with the bacterial oxidation of some of the seeping/venting chemical compounds, sometimes accompanied by the development of unique biological and geological features, such as chemosynthetic "life oasis", "black smokers", or methane-derived carbonates. The best preserved of such features, and least equivocal in terms of their chemosynthetic origin, invariably occur in truly inhospitable areas characterized by deep, cold and dark conditions. The scarcity of easily recognizable vent- and seep-related geological products in shallow, warm and bright settings is not an indication that the bacterial transformation of reduced compounds does not take place in hospitable settings, but rather that chemosynthesis, whenever and wherever it occurs, interferes with other processes operating on the sea floor resulting in hybrid geological products, the chemosynthetic components of which are difficult, and sometimes impossible, to decipher.

Accordingly, sedimentologists are just starting to appreciate to what extent the venting and seepage of gas and fluid has contributed to both the initiation and subsequent growth of carbonate reefs, modern or ancient. Rapidly accumulating evidence portrays a continuum of biological and geological reef products. At one end of the spectrum are the reefs, mounds, buildups, etc. that formed entirely as a result of chemosynthesis in response to fluid/gas venting and/or seepage. It is hard to envision such products as forming anywhere but in the darkest, coldest, and deepest water environments. At the other end of the spectrum are the reefs, mounds, buildups, etc. that formed entirely as a result of photosynthesis, that is in a wide variety of more hospitable areas where venting and seepage does not occur.

Ten years after they were first documented, the Cretaceous methane-derived carbonate mounds of the Canadian Arctic remain some of the world's finest, and truly unequivocal examples of ancient chemosynthetic mounds. Four carbonate mounds, interpreted as cold-seep communities, were fed by methane, and perhaps higher hydrocarbons, that seeped along syn-sedimentary fault systems associated with a graben and a salt diapir. These mounds represent the end-member of the chemosynthetic-photosynthetic reef continuum as they formed in a deep, cold, high latitude, and clastic-dominated environment, a setting totally inhospitable for photosynthetic reef growth. The kind of geological products that would have resulted if the hydrocarbon seepage had occurred at a time or at a place favourable to photosynthetic reef growth is anyone's guess. However, it is not hard to envision that the hard substrate generated through chemosynthesis would have been rapidly colonized by *bona fide* reef-forming organisms resulting in a sizable mound or buildup, the chemosynthetic signature (biota, cement, isotope, etc.) of which would have been greatly diluted, or confined, within a classic reef construction.

Pockets of *in situ* bivalve accumulations associated with warm-temperature marine cement within an otherwise classic phylloid algal reef of Carboniferous age in the Sverdrup Basin is a fine example of such an hybrid reef resulting from a combination of chemosynthetic and photosynthetic processes. Such products are probably very common in the rock record.

Belgian Frasnian mud mounds

***Frédéric Boulvain**, Géologie-Pétrologie-Géochimie, B20, Université de Liège, Sart Tilman B-4000 Liège, Belgium. fboulvain@ulg.ac.be; http://www.ulg.ac.be/geolsed*

The Belgian Frasnian mud mounds occur in three stratigraphic levels (Arche Membre, Lion Membre and Petit-Mont Membre) in an overall backstepping (transgressive) succession. Petit-Mont and Arche Membres form the famous red and grey "marble" exploited for ornamental building stone since Roman times. Belgian mud mounds have been studied for more than a century by many authors. According to their fabric, biota, stable isotopes (Boulvain *et al.*, 1992), these buildups are not seepage-related (cf. Peckmann *et al.*, 1998).

The evolution and distribution of the facies in the mounds is thought to be associated with ecologic evolution and relative sea-level fluctuations (Boulvain, 1993; Bourque & Boulvain, 1993; Boulvain & Herbosch, 1996).

A composite facies sequence starting from below the photic and storm wave base zones and progressing toward subexposed environments is defined (Boulvain, 1993; Boulvain & Herbosch, 1996). The sequence consists of red spiculitic wackestones with stromatactis (facies 3), becoming progressively enriched in crinoids and corals (facies 4), then in peloids and cyanobacteria (5). The sequence is then continued with gray stromatoporoid and stromatactis floatstones and rudstones (6); algal-peloids wackestones and packstones with Codiaceae-Udoteaceae and thick algal coatings (7); algal and cryptalgal bindstones (8); branching stromatoporoids rudstones (10) and loferites (11). The transition from aphotic to cyanobacteria photic zone is reflected by facies sequence 4-5; the transition from cyanobacteria to green algae photic zone, by sequence 6-7. The storm wave base is reached with facies (5) and fair-weather wave base with facies (7).

The first three facies of the Petit-Mont Membre mounds (stromatactis-sponges, corals-crinoids-stromatactis, corals-crinoids-bryozoans-cyanobacteria) show a very nice red color, due to a dispersed thin oligist pigment. This pigment originates from degradation of iron-bacteria, probably from the *Sphaerotilus-Leptothrix* group (threads) and Siderocapsaceae (coccoids). As deduced from the sedimentological reconstruction, these organisms are thought to be microaerophilic, living in a moderately reducing environment. In some cavities (neptunian dykes, zebra,...) iron-bacteria, together with other microorganisms, erect small (mm-sized) endostromatolites, called "microstromatolites". Complex microbial communities may have contributed to mound accretion as primary builders and/or mud producers.

The 30 to 40 m thick "Les Bulants" bioherms (Petit-Mont Membre) are catch-up buildups displaying only a vertical facies succession (3-4-5-7-8) and a low relief. The 60 to 80 m "Les Wayons" mounds (Petit-Mont Membre) possess a relatively high relief with steep flanks and bioclastic talus (9). These catch-up-give-up mounds present the same sequence as the former, but their relief is responsible for a marked lateral differentiation. "St-Rémy" mounds (Petit-Mont Membre) are smaller buildups growing in deeper parts of the ramp: they are almost totally constituted by (3) and (4). "Lion" type mounds (Lion Membre) are 150 m thick buildups developing in a relatively shallower environment, forming a keep-up (6), followed by a catch-up-give-up sequence (7-8-10-11-6).

The fore-mound facies of the Lion type mounds and the Arche Membre mounds are now sedimentologically investigated, to complete the model. The Lion fore-mound facies show large scale interdigitations between "normal" mound facies (6-7-8-10) and various types of flank deposits.

One of the most puzzling problem concerns the time relationship between the mounds and the off-mound facies (bedded limestones, shales, nodular limestones). Until now, these off-mound facies have never been the subject of detailed sedimentological analyses. To elucidate this problem, new attempts are made (together with more classical sedimentological and stratigraphical methods) with the study of palynologic content (Vanguestaine *et al.,* 1999) and total magnetic susceptibility (Devleeschouwer & Boulvain, in progress).

References:

Boulvain, F., 1993. Sédimentologie et diagenèse des monticules micritiques "F2j" du Frasnien de l'Ardenne. *Serv. Géol. Belgique Prof. Papers*, 1993 (2), **260**, 427 pp.

Boulvain, F. & Herbosch, A., 1996. Anatomie des monticules micritiques du Frasnien belge et contexte eustatique. *Bull. Soc. Géol. France*, **167** (3), 391-398.

Boulvain, F., Herbosch, A. & Keppens, E, 1992. Diagenèse des monticules micritiques de la partie supérieure du Frasnien du Synclinorium de Dinant (Belgique). *C.R. Acad. Sc. Paris,* **315** (II), 551-558.

Bourque, P.A. & Boulvain, F., 1993. A model for the origin and petrogenesis of the red stromatactis limestone of Paleozoic carbonate mounds. *J. of Sedimentary Petrology*, **63** (4), 607-619.

Peckmann, J., Reitner, J. & Neuweiler, F., 1998. Seepage related or not? Comparative analyses of Phanerozoic deep-water carbonates. *Unesco Intergovernmental Oceanographic Commission, workshop report* **143**, 18-19.

Vanguestaine, M., Pardo-Trujillo, A., Coen-Aubert, M., Roche, M. & Boulvain, F., 1999. Evolution of organic debris and palynomorphs preservation in two sections of Late Middle Frasnian age (Southern Dinant Synclinorium border, Belgium), in press.

Duration of cementation in some Minervois Devonian stromatactis mud-mounds, southern France.

***Robert Bourrouilh**, Laboratoire CIBAMAR, Université de Bordeaux I, 33405 Talence, France. r.bourrouilh@cibamar.u-bordeaux.fr*

Cementation of carbonate buildups commonly called mud mounds is generally considered to have been early, based mainly on the carbon and oxygen stable isotope signature of their stromatactid cavity and Neptunian fracture cements.

However, previous work (Bourque *et al.*, 1998) on mud-rich stromatactis mounds in Caunes-Minervois, (Montagne Noire, France), lead to the conclusion that the cementation of stromatactids cavities and Neptunian cracks tooks place while the mound facies was still soft, or at least plastic, and that the bulk of the mound was cemented later, in a very shallow burial environment (less than 150m deep), under strong fresh water influence.

New data are brought on dating of the Neptunian dikes of three Minervois mud-mounds.

- **In the Rocamat quarry**, the mud-mound contains Upper Emsian (*serotinus*) conodonts. Two main types of Neptunian dikes occur. The first one is related to distension that occurred during the mound growth or very early after its development. Some of them were passageway for undercurrents which formed large (up to 1,5 to 2 cm in diameter) pisoids, some having crinoid ossicles as nuclei. Some pisoids also entered into the open stromatactid cavities. It was not possible to date precisely these pisoids, but the mound is capped by Eifelian (conodonts) crinoidal grainstones, indicating a decrease in water depth. It is possible that the stromatactis cavities were still open during Eifelian, and then filled by pisoids.

A second type of dikes is sedimentary multifilled. These dikes cross-cut the pisoid-filled dikes. They are observable in the three main mud-mounds.

- **In the Villerambert mound**, one of these multifilled dikes contains tentaculitids, bryozoans, crinoidal grainstones and packstones in which a Givetian conodont fauna has been isolated.

- **In the Cyrnos Caunes-Minervois quarry**, one dike contains colonial corals, and crinoidal grainstones and packstones. The sedimentary filling is also multiple and is made up of grainstones and packstones with tentaculitids, bryozoan, and crinoidal ossicles. Some samples of the dike contain a Givetian fauna, while others, an Upper Frasnian conodont fauna. The dike sharply cuts the stromatactis mound. It was also the passageway for a manganese mineralization that cross-cuts Famennian strata which therefore predate the Mn-mineralization.

An interesting point is that this post-Famennian mineralization enters the stromatactis network, an indication that the network was not then completely filled with calcitic cements.

Therefore, even if the bulk of the mound formed during upper Emsian (*serotinus* zone), it seems that the stromatactis network was not completely cemented until, at least, the Famennian. How early was the calcitic cementation of the Minervois stromatactis mud-mounds? We can now say that the cementation went on from the Emsian (about 390 Ma) to the Famennian (about 350 Ma), *i.e.* for more than 40 Ma.

Reference

Bourque, P.-A., Dansereau, P. et Bourrouilh, R. 1998. Early cementation of mud-rich mounds: how early? GAC-MAC-APGGQ Annual meeting, Québec, Abstracts with Program, v. 23, p. A22-23.

Internal flow and cementation in mounds

A. Conrad Neumann *and* ***Thomas Shay****, Marine Science Dept., University of North Carolina, Chapel Hill, NC, 27599-3300*

Elongate, asymmetric mounds, 100's of meters long and up to 50m high, occur 500 to 600 m's deep in the NE Straits of Florida, onto the Blake Plateau and up on the Florida-Hatteras slope. They have been designated, "Lithoherms" (from "lithified bioherms") because of the pervasive occurrence of early cements. The cements occupy inter- and intraskeletal voids as well as microscopic solution cavities. The cements are Mg-calcites of about 16 mole percent $MgCO_3$. A textural sequence is observed that seems to first favor the rapid precipitation of fine, multinucleate micrite ("paste"). This grades into a clotted "structure grumeleuse", which in turns grades into a common peloidal phase. The sequence ends with microspar coatings on peloids and cavity walls or even the infilling of the remaining cavity with microspar.

The mounds appear to accrete from the trapping, binding and baffling effect of attached filtering organisms, which are zoned according to position on the mound relative to current flow. Ahermatypic, cold water corals occupy the accreting nose of the mound that faces into the current. Large zooanthid fans occupy the crest of the mounds where currents are strongest. The down-current end of the mounds is covered with comatulid crinoids, often in rows.

Bottom currents no more than a few tenths of a knot (5 to 10 cm/sec) increase to flows as strong as 2 to 3 knots at the crest as a result of the effect of the compression of streamlines over the mounds. The pressure gradient associated with this acceleration (low pressure at the crest of the mound, high pressure at the leading and trailing edges) may be sufficient to force an interstitial flow into and upward through the porous mound. Over a long period of time of steady bottom current flow this internal pressure driven flow could well be enough to draw water through the complex of cavities and provide the obvious and voluminous internal cement. Over time the process is self-limiting because the cavities close as cementation fills the voids and restricts the flow. The evidence for this comes from the cementation sequence that starts with rapidly precipitated forms in the open voids and ends with the slow growth of druse and infilling microspar closing the voids. In some rocks certain phases dominate, such as the peloids.

The expected flowlines over the mound and interstitial flow within the mounds is sketched in the cross section cartoon below.

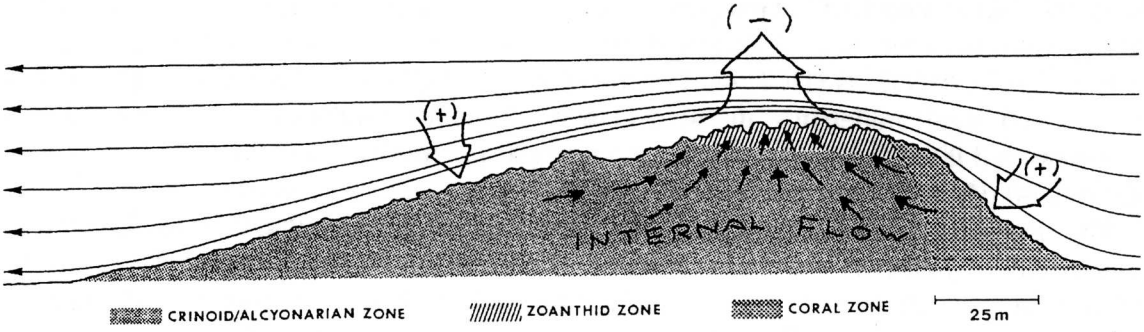

Schematic diagram of lithoherm biozonation showing conceptual compression of stream lines that produces rapid flow over crest. Maximum velocities recorded over crests (area of greatest compression) exceed 100 cm/sec.; velocities recorded over sediment-covered areas between mounds are 2-7 cm/sec.

Comparative analysis of refractory organic matter from ancient polymuds and related spar cements using time-resolved laser fluorescence spectroscopy (TRLFS)

***Fritz Neuweiler**, IMGP, Univ. Goettingen, Germany & Institute for Petrology and Geochemistry, Univ. Liège, Belgium*
***Andreas Reimer**, IMGP, Univ. Goettingen, Germany*
***Gerhard Geipel**, **Margret Rutsch**, and **Karl-Heinz Heise**, Institute for Radiochemistry, Research Center Rossendorf/Dresden, Germany*

Polymuds represent a succession of polygenetic carbonate muds accumulating to form a composite microcrystalline fabric. Polymuds are typical features of Waulsortian and Mesozoic carbonate mud mounds. A well preserved example of a polymud rock was sampled from an Upper Albian sequence of the S margin of the Sierra d'Aralar, Province Navarra, N Spain. The boundstone consists of a primary frame of microsolenid corals, encrusting foraminifera, encrusting bryozoans, and coralline sponges. As a secondary frame there are lithistid and hexactinellid sponges associated with a large volume of polymuds. Late internal sediment is a red algae biodetritus. Isopachous marine cements and late diagenetic drusy spar cement closed residual pore space.

Total organic carbon contents range from 0.3 to 0.7 weight-%. Fluorescence microscopy (excitation 395-440 nm, emission > 470 nm) revealed that fluorescent compounds include authigenic micrites, geopetal allomicrite (pars), skeletal material from coralline sponges and red algae, and isopacheous rim cement (weak fluorescence). The spar mosaic and most of the skeletal debris is non-fluorescent as well as those parts of microcrystalline sediment which had become recrystallized towards microspar. What type of compounds cause this fluorescence and where are the loci of those compounds,

extra- or intracrystalline? Applying differential extraction methods, we were able to differentiate between two extracrystalline fractions (NaOH, 1-10 and >10 kD) and two intracrystalline fractions (HCl > 1kD and NaOH > 1 kD) of authigenic micrite, allogenic micrite, red algal biodetritus and spar cement. Aqueous solutions were measured using time-resolved laser fluorescence spectroscopy (50 ps intervals, 430-610 nm, excitation at 400 nm, 60 µJ, laser pulse < 130 fs).

The overall nature of the organic compounds bearing molecular sites of fluorescence (chromophores) corresponds to the fraction of marine humic and fulvic acids. Authigenic micrite shows high relative amounts of intracrystalline humic compounds, whereas it is *vice versa* in the case of allomicrite. Red algal biodetritus shows intermediate values in the intracrystalline fractions and a dominant portion in the extracrystalline fraction > 10 kD. Results obtained from spar cements are close to detection limits with slightly elevated portions in the extracrystalline fraction > 10 kD.

What concerns the understanding of authigenic mineralisation and allomicritic phases in mud mounds, our results indicate a) that mineralisation preserves the early stages of organic matter diagenesis within these crystals, b) that these compounds already had passed through biodegradation and were at the stage of oxic recondensation reactions, and c) that allomicrite has a potential contribution via bioerosion and sediment feeding, causing the accumulation of refractory organic matter upon grain surfaces during ingestion and re-ingestion.

A possible example of modern mud mound province, the Bay of Florida (U.S.A.), anatomy and controls : meteorological, chemical and physical

*N. **Paysan**, and **F.G. Bourrouilh-Le Jan**, Laboratoire CIBAMAR, Université Bordeaux 1, Avenue des Facultés, 33405 Talence Cédex, France*
*L. **Doyle**, The Center of Nearshore Marine Science of the University of South Florida, 140 Seventh Avenue South, St. Petersburg, Florida 33701, USA*
*R. **Bourrouilh**, Laboratoire CIBAMAR, Université Bordeaux 1, Avenue des Facultés, 33405 Talence Cédex, France*

An overall study of the shallow water carbonate sedimentation of the Bay of Florida is presented. Until now, this model has been the object of only fragmentary and dispersed works. The interest and innovation of this study consist in the fact that the parameters controlling the shallow water sedimentation of the Florida Bay, are very different from those of other models, as the Arabo-Persian Gulf or the Great Bahama Bank.

The Bay of Florida is an environment which is protected from the direct influences of the ocean by the Pleistocene emerged Florida Keys. It is contiguous to the Everglades from which it receives fresh waters. Florida Bay is different from other models by its underwater karst-derived geomorphology which is particular and presents large basins, 3 m deep, separated by underwater muddy sills; different also by its fluctuating salinity, by the high oxygenation rate of its waters due to the presence of continuously submerged

meadows of calcareous green algae and sea grass, and by its geographical position along hurricane tracks of the tropical north Atlantic Ocean.

The influences of hurricanes are marked by the transport of bioclasts on several tens of km towards the Everglades, and by periodical (3 to 5 years, according to hurricane frequency) low salinity water stagnation, while, in fact, the Bay of Florida is being on the process of hypersalinity under the influences of man and of human settlements, endangering the relict fauna that the Bay of Florida has sheltered until now, as manatees, horse shoe crabs and reptiles.

The Bay of Florida is thus an area of shallow water carbonate sedimentation with foraminifera and molluscs (a foramol province), but limited to micro-platforms dispersed in the whole bay. The micro-platforms resemble bioherms or mud mounds with a central core of wackestones surrounded by grainstones and packstones.

The sedimentary piles roughly present sequences of growing-upward energy for 2000 years. The diagenesis is primarily calcitic with dissolution of aragonite located deeply down in cores.

A discussion of Florida Bay mud mounds is presented.

Key words : carbonates, Florida, hurricane, salinity, oxygene, sedimentary sequences, ^{14}C.

Fossilized biofilms of methanotrophic bacteria in a Miocene cold seep carbonate

J. Peckmann, *Institut und Museum für Geologie und Paläontologie, Georg-August-Universität, Goldschmidtstrasse 3, D-37077 Göttingen, Germany.*
jpeckma@gwdg.de
V. Thiel, *and* ***W. Michaelis***, *Institut für Biogeochemie und Meereschemie, Universität Hamburg, Bundesstrasse 55, D-20146 Hamburg, Germany*
J. Reitner, *Institut und Museum für Geologie und Paläontologie, Georg-August-Universität, Goldschmidtstrasse 3, D-37077 Göttingen, Germany*

Two types of methane-derived carbonates have been described from the Marmorito locality in the Italian Apennines, the '*Lucina* limestone' and the 'Marmorito limestone'(Clari *et al.*, 1994). Here we report on the 'Marmorito limestone', which exhibits a microcrystalline dolomitic matrix crosscut by calcitic veins. The dolomite ($\delta^{13}C$: -40.2 to –38.9‰) and the calcite cement ($\delta^{13}C$: -28.5 to –17.3) are strongly depleted in ^{13}C indicating that they derived from the oxidation of methane.

The fracturing of the matrix is caused by an in situ brecciation of the seep deposit. The resulting clasts are overgrown by coatings with a cloudy appearance. The thickness of these overgrowths varies from 10 to 1000 µm. They also consist of dolomite. In contrast to the dolomitic matrix they exhibit an intense autofluorescence. Most intense fluorescence halos are observed as particular globules. Remains of the fluorescent

overgrowths within the matrix indicate that these organic-rich residues were enclosed during ongoing dolomite aggregation.

FE-SEM analyses of the overgrowths show that they are formed of peculiar crystal aggregates. These are (i) crusts composed of hemispheres, (ii) rod-shaped crystal aggregates with rounded, brush-like terminations, and (iii) dumbbells that occur in the center of rod-shaped crystal aggregates. All these precipitate varieties have been found to be induced by bacterial activity in laboratory experiments (Buczynski and Chafetz, 1991).

Biomarker analyses yielded evidence for the presence of methanotrophic bacteria during carbonate formation. Sterols and hopanols carrying an extra methyl group at C-4 and C-3 were extracted from the carbonate. Likely biological precursors of the chemofossils were identified in methanotrophs (Neunlist and Rohmer, 1985).

The dolomitic overgrowths observed in the 'Marmorito limestone' derive from the microbial oxidation of methane, exhibit an intense fluorescence, and consist of crystal aggregates typical for a bacterial mediation. We interpret the overgrowths as fossilized biofilms of methanotrophic bacteria, which is corroborated by biomarker data (Peckmann *et al.*, 1999). Additional indications for bacterial activity at the ancient Marmorito seep were observed by Cavagna *et al.* (1999).

References

Buczynski C., and Chafetz H.S., 1991, Habit of bacterially induced precipitates of calcium carbonate and the influence of medium viscosity on mineralogy. Journal of Sedimentary Petrology, v. 61, p. 226-233.

Cavagna S., Clari P., and Martire L., 1999, The role of bacteria in the formation of cold seep carbonates: geological evidence from Monferrato (Tertiary, NW Italy). Sedimentary Geology, v. 126, p. 253-270.

Clari P., Fornara L., Ricci B., and Zuppi G.M., 1994, Methane-derived carbonates and chemosynthetic communities of Piedmont (Miocene, northern Italy): an update. Geo-Marine Letters, v. 14, p. 201-209.

Peckmann J., Thiel V., Michaelis W., Clari P., Gaillard C., Martire L., and Reitner J., 1999, Cold seep deposits of Beauvoisin (Oxfordian; southeastern France) and Marmorito (Miocene; northern Italy): microbially induced authigenic carbonates. International Journal of Earth Sciences, v. 88, p. 60-75.

Neunlist S., and Rohmer M., 1985, Novel hopanoids from the methyotrophic bacteria *Methylococcus capsulatus* and *Metylomonas methanica*. Biochemical Journal, v. 231, p. 635-639.

Upper Devonian (Frasnian) Mudmound Reefs, Mount Hawk Formation, Canadian Rocky Mountains

***Brian R. Pratt**, Department of Geological Sciences, University of Saskatchewan, Saskatoon, Saskatchewan S7N 5E2, Canada*

The Mount Hawk Formation (Upper Devonian, Frasnian) in various locations in the Rocky Mountains contains deep-water, mudmound-style reefs that accreted on the gently inclined ramps adjacent to shallow-water carbonate platforms. Normally dolomitized, several of the larger examples that crop out north of Jasper, Alberta, are still limestone. Two were sampled in detail and preliminary observations are presented.

The reefs are each about 35 m thick, and exposed widths at their bases are respectively 45 m and 60 m. They present a striking domical geometry, although the southern margin of the southern reef is nearly vertical. They are flanked by thin- and nodular-bedded, dark-coloured lime mudstones, wackestones and rare grainstones. The lower inter-reefal beds interfinger abruptly with the reefal margins, whereas the upper ones onlap them, preserving some 15 m of synoptic relief. These beds contain atrypoid brachiopods, *Thamnopora* branching tabulate corals, and *Disphyllum* branching rugose corals, robust monaxon sponge spicules, ostracodes, gastropods, tentaculitids, encrusting calcareous worm? tubes, foraminifers (*Nanicella*, *Evlania*?) and echinoid ossicles. Many gastropod and brachiopod bioclasts are broken; some coral and stromatoporoid fragments are bioeroded. In some beds the biota represents an *in situ* community, whereas in others most of the bioclasts are probably derived from the reefs.

The reefs are composed of packed to sparse biomicrite, micrite and indistinctly clotted micrite with abundant stromatactis and fenestrae. Sponge spicules are common and exhibit two distinct size groupings: large monaxons and tetraenes, and small monaxons and multi-rayed forms; dense accumulations of small monaxons are present locally in the micrite matrix. Bioclasts include abundant ostracodes, and variably common whole and disarticulated brachiopods, *Thamnopora*, laminar stromatoporoids, *Amphipora* branching stromatoporoids, foraminifers (*Nanicella*, *Evlania*? and irregular, single-chambered forms), echinoid ossicles, *Rothpletzella* (=*Sphaerocodium*) microbial? encrustations and *Girvanella* filament bundles and tangles that grade into dense micrite clasts that recall *Tubiphytes*. Bryozoans, worm? tubes, fish plates and gastropods are rarer elements. Algal microborings are absent, but larger borings which may be from worms or sponges occur in some Thamnopora. Much of the larger brachiopod material is fragmental, suggesting the presence of soft-bodied predators. In some areas gastropod aragonite has been leached and the molds filled by fibrous calcite cement.

Stromatactis is irregular in the cores and laminoid at the flanks; these laminoid forms are laterally discontinuous and do not appear to be cavities from dilation and separation of sediment layers. The larger stromatactis contain fibrous calcite locally with several generations separated by peloids, microbial micrite laminae or sponge spicule networks with a micrite matrix. Some contain unusual micrite peloids of fine-sand size. Inclusion zoning of the cement is present in some cavities but has not yet been investigated geochemically. Smaller fenestrae and interparticle pores are cemented by blocky calcite. Synsedimentary fracturation has not been observed.

As with other mudmounds, microbial biofilms or mats are thought to have stabilized the lime mud and bioclasts and induced the clotted micrite and fenestral fabric. The community shows photosynthetic elements and at present there is no biotic evidence to suggest a role for chemosynthesis. Unlike the Devonian mudmounds of Belgium, Poland and perhaps North Africa, these reefs seem to lack a structural control on their location, although it is possible that minor faulting did occur during growth.